Green synthesis of silver nanoparticles from Indian Hawthorn (*Rhaphiolepis indica*) and the investigation of their antimicrobial, antioxidant and cytotoxic effects

Aurelie Ngalula Nsumpi

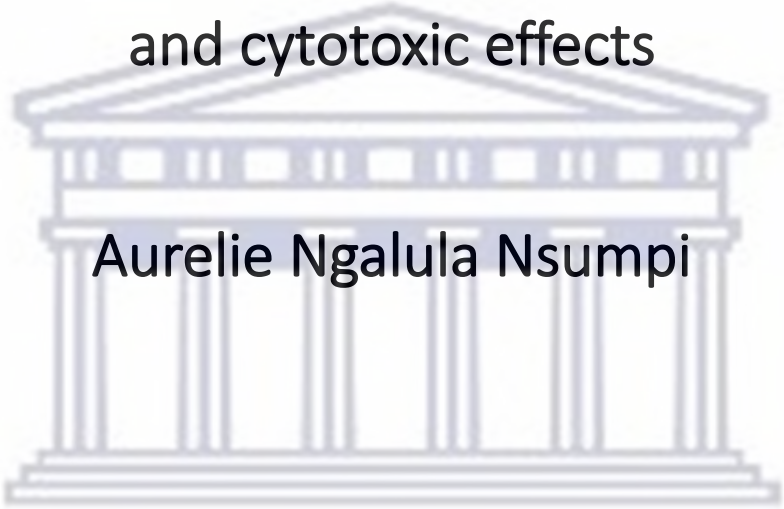

A thesis submitted in fulfilment of the requirements for the degree of Magister Scientiae in the Department of Biotechnology, University of the Western Cape.

Supervisor: Prof. Abram Madiehe

Co-supervisor: Dr. Nicole Sibuyi

8th January 2024

KEYWORDS

Silver nanoparticles

Rhaphiolepis indica

Indian Hawthorn

Nanotechnology

Green synthesis

Antimicrobial agents

Antimicrobial resistance

Antioxidant

Cytotoxicity

ABSTRACT

The global health concern pertaining the rapid spread of antimicrobial resistance (AMR) has led to a rise in mortality rate caused by infectious diseases that have become difficult to treat due to the misuse and lack of novel antibiotics. Nanotechnology is one innovative approach that has the potential to eradicate the burden of AMR with silver nanoparticles (AgNPs) well known for their antibacterial properties. Currently, AgNPs can be synthesised using a greener approach which makes use of the phytoconstituents in plants providing more advantages over the conventional chemical synthesis methods (i.e rapid, cost-effective, safer for the environment and sustainable) also enhancing the antioxidant properties of AgNPs for the treatment of degenerative diseases caused by oxidative stress. Indian Hawthorn (*Rhaphiolepis indica*) berries have been used to treat cardiovascular diseases, high blood pressure and heart failure and are known to have high content of polyphenols which are involved in bioreduction of metal-based NPs (MNPs) with enhanced bio-activities.

In the current study, silver nanoparticles (AgNPs) were synthesised using Indian Hawthorn fruit extract (IHFE). Different parameters were optimised to obtain the optimum conditions for synthesis. The biosynthesised AgNPs (IHFE-AgNPs) were characterised using UV-Vis spectroscopy (UV-Vis), dynamic light scattering (DLS), Fourier-transform Infrared (FTIR) and High transmission electron microscopy (HR-TEM). The stability of IHFE-AgNPs was assessed in different biological such as dH_2O, ddH_2O, Phosphate buffered saline (PBS), Mueller-Hinton broth (MHB), DMEM complete and incomplete. Antibacterial activities of IHFE and IHFE-AgNPs were performed on *S. aureus,* MRSA, *K. pneumoniae*, *A. baumannii*, *P. aeruginosa*, *E. Cloacae*, and *E. coli* using agar well diffusion and micro-dilution assays. Furthermore, antioxidants studies of IHFE and IHFE-AgNPs were assessed using assays such as 2,2-diphenyl-1-picrylhydrazyl (DPPH), 2,2'-azino-di-(3-ethylbenzthiazoline sulfonic acid (ABTS) and Ferric reducing antioxidant power (FRAP). Additionally, cell viability was assessed following a 24 hrs exposure to increasing concentrations of IHFE and IHFE-AgNPs (0.78- 100 µg/ml).

The synthesis of IHFE-AgNPs was confirmed by colour change and surface plasmon resonance (SPR) at 406 nm. The hydrodynamic size was 123.6 nm with a polydispersity index (PDi) of 0.311 and a ζ-potential of -11.2 ± 4.38 mV, indicating monodispersed and moderately stable IHFE-AgNPs. The IHFE-AgNPs were spherical with average core size of 8.61 nm. The IHFE-AgNPs exhibited antibacterial against both Gram-positive and Gram-negative bacteria with *E. cloacae* and *P. aeruginosa* being the most susceptible Gram-negative strains. Furthermore, the results confirmed that IHFE-AgNPs has antioxidant scavenging abilities against free radicals and were non-toxic to KMST-6 cells at concentrations below 100 µg/ml. The results concluded that IHFE-AgNPs have a potential to eradicate AMR and treat diseases caused by oxidative stress. Future investigations should be performed to learn about the antibacterial mechanism of action of the IHFE-AgNPs such as ROS production. Based on the antioxidant scavenging abilities of IHFE-ANPs, wound-healing potential of IHFE-AgNPs can also be investigated.

DECLARATION

I declare that **"Green synthesis of silver nanoparticles from Indian hawthorn (*Rhaphiolepis indica*) and the investigation of their antimicrobial, antioxidant and cytotoxic effects"** is my own work, that it has not been submitted for any degree or examination in any other university, and that all the sources I have used or quoted have been indicated and acknowledged by complete references.

Full name: Aurelie Ngalula Nsumpi **Date:** 8th January 2024

Signed:

ACKNOWLEDGMENTS

I would like to start by thanking the Almighty God for the strength that I had found through His Word. Thank you for your magnificent love and mercy on my life, I would never have done this without your Grace.

To my supervisor Prof Abram Madiehe, thank you for offering me this opportunity. It has allowed me to grow into a resilient and strong scientist. Thank you for your guidance, your mentorship and trust throughout this journey. To Dr Nicole Sibuyi, thank you for your motherly guidance, your encouragement and support, I am forever grateful. To Prof Mervin Meyer, thank you for your support and for your willingness to assist in trying times, I am sincerely grateful.

To my lovely parents, Leonard and Isabelle Nsumpi Tshimanga, I am forever grateful for your love, your support and the values you have instilled in me. From my childhood until today, your love has carried me through all the challenges faced in life. This is for me the expression of the gratitude I have for you both.

To my sisters, Laetitia Nsumpi and Huguette Kenda Misenga, words can never express my gratitude towards everything you have done for me. From the financial support to the moral support, you have been there since the beginning of this journey. Thank you for always being there and for never giving up on me. To my siblings, Tanya, Divine, David, Deborah and Miriam Nsumpi, thank you for the love and support.

To my friend Henri Kisimba, thank you for your support, your encouragements, it meant a lot to me. To my NIC friends, Toni Oliver, Miche Meyer, Jodi Couert, Antoinette Ajmal, Letoya Williams, Tswellang Mgijima, Samson Oselusi, Nive Dudley, Alexandria Erasmus, Keletso Modise and Thendo Mabuda, thank you for all the love and support. From the trainings, the help and all the fun conversations we have had, my time in the lab would not have been the same without you. I will forever cherish these moments.

I would like to express my gratitude to the DSI NIC/Mintek Biolabels Node for the financial support to further my studies. To the Nanobiotechnology Research Group (NBRG) and the

University of the Western Cape, thank you for all the support and resources required to complete my postgraduate studies.

DEDICATION

To my dad whom I love so much, you have always been able to encourage me since my first steps. You who instilled in me the value of always wanting to excel in everything I do. Your love and sacrifices paid off today. May the Lord continue to make you smile every day.

Love, Bundini!

CONFERENCE CONTRIBUTIONS

Aurelie N. Nsumpi, Nicole R. S. Sibuyi, Mervin Meyer and Abram M. Madiehe. “Nanotechnology: a novel approach to eradicating antibiotic resistance using greener methods”, South African Society for Microbiology (SASM 2023 convention), 17-20 September 2023. **Stellenbosch, Western Cape. Poster presentation**

Aurelie N Nsumpi, Nicole R.S. Sibuyi, Mervin Meyer and Abram M. Madiehe. “Evaluation of the antimicrobial and antioxidant effects of silver nanoparticles synthesised from Indian Hawthorn (*Rhaphiolepis indica*) fruit extract”, Nanotechnology Innovation Centre annual workshop, Western Cape, 11-12 October 2023. **South African Medical Research Council, Tygerberg. Poster presentation (First place)**

Table of contents

LIST OF FIGURES

LIST OF TABLES

LIST OF ABBREVIATIONS

°C	Degrees Celsius or degree centigrade
%	Percentage
β	Beta
λmax	Maximum absorbance/ absorption maximum
µl	Microliter
ζ-potential	Zeta potential
ABTS	2,2'-azino-di-(3-ethylbenzthiazoline sulfonic acid)
Ag	Silver
Ag^+	Silver ion
Ag^0	Silver atom
AgNPs	Silver nanoparticle(s)
$AgNO_3$	Silver nitrate
AMR	Antimicrobial resistance
ATCC	American Type Culture Collection
CFU	Colony forming units
ddH_2O	Deionized distilled water
dH_2O	Distilled water
DLS	Dynamic Light Scattering
DPPH	2,2-diphenyl-1-picrylhydrazyl
EPS	Extracellular polymeric substances
EBSLs	Extended spectrum b-lactamases
ESKAPE	*Enterococcus faecium, Staphylococcus aureus, Klebsiella pneumoniae, Acinetobacter baumannii, Pseudomonas aeruginosa*, and *Enterobacter species*
FC	Folin-Ciocalteu
FDA	Food and Drug Administration
FRAP	Ferric reducing antioxidant power
FTIR	Fourier-transform Infrared spectroscopy
g	Gram(s)
GAE	Gallic Acid Equivalents
HCl	Hydrochloric acid
hr(s)	Hour(s)
HR-TEM	High Resolution-Transmission Electron Microscopy

IHFE	Indian Hawthorn fruit extract
IHFE-AgNPs	Indian Hawthorn fruit extract-silver nanoparticles
KBr	Potassium bromide
$K_2S_2O_8$	Potassium peroxidisulfate
MBC	Minimum bactericidal concentration
MDR	Multidrug resistant
mg	Milligram(s)
mg/ml	Milligram(s) per millilitre
MHA	Mueller Hinton agar
MHB	Mueller Hinton broth
MIC	Minimum inhibitory concentration
min(s)	Minute(s)
ml	Millilitre(s)
mm	Millimetre(s)
mM	Millimolar
NaOH	Sodium Hydroxide
Na_2CO_3	Sodium carbonate
nm	Nanometre
OD	Optical density
PBS	Phosphate buffered saline
PDI	Polydispersity index
RFU	Relative Fluorescence Units
ROS	Reactive oxygen species
rpm	Revolutions per minute
TPC	Total phenolic content
v/v	Volume per volume
w/v	Weight per volume
WST-1	Water soluble Tetrazolium salt

Chapter 1: Literature Review

1.1 Introduction

Infectious diseases can be caused by bacteria, viruses, fungi, or other pathogens. These diseases are treated using drugs such as antibacterial, antiviral, or antifungal all known as antimicrobials. Due to the misuse of these drugs, microbes, mainly bacteria, have acquired resistance to many antibiotics available in the market (WHO, 2015). The current antibacterial agents are not effective against a large range of bacteria due to their resistance. This situation has led to the emergence of antimicrobial resistance (antibiotic resistance, AMR) which poses a major threat to human health worldwide (Murray et al., 2022, WHO, 2015). According to Lancet's report published in 2022, it was estimated that 4.95 million deaths were associated with antibacterial resistance and 1.27 million deaths were caused by antimicrobial resistance bacteria with western sub-Saharan Africa being the region with the highest deaths attributable to AMR in 2019 (Murray et al., 2022). Therefore, there is an urge to find medical alternatives to treat diseases caused by resistant bacteria.

Scientists are currently researching for antimicrobial agents which will have a broad-spectrum potential activity against Gram-positive and Gram-negative bacteria with reduced or no side effects. Plants (including their leaves, stem and fruits) have gained interest globally and have been widely exploited due to the different bioactive compounds present as well as their healthy properties which have been known for centuries (Aung et al., 2020, Durazzo et al., 2018, Nazhand et al., 2020, Omer et al., 2021). They are used to produce plant-based drugs/medicines which has brought a glimpse of hope in the biomedical field for the treatment of diseases caused by AMR. The use of medicinal plants has been approved by the World Health Organization (WHO) based on scientific research confirming that it's safe and effective to use (WHO, 2013). About 80% of population worldwide make use of medicinal plants for the treatment of many diseases; however, more scientific research is required to improve our knowledge about their chemical compounds, their safety as well as their mechanisms of action

(Alirezalu et al., 2020, Benabderrahmane et al., 2021, Cuevas-Durán et al., 2017, Ngoc et al., 2019). One of these interesting common medicinal plants is Indian hawthorn (*Rhaphiolepis indica*), a perennial, deciduous and thorny shrub (Nazhand et al., 2020, Singh et al., 2018). The fruits/berries of the Indian Hawthorn have been reported to have cardiovascular properties, protect from high blood pressure, angina, heart failure, cardiac arrhythmias, myocarditis, arteriosclerosis, anxiety, and insomnia (Nazhand et al., 2020, Singh et al., 2018). Crataegus spp. are the commonly used species of the Rosaceae family due their medicinal properties (Nazhand et al., 2020, Singh et al., 2018).

Nanotechnology is the science of manipulating atoms and molecules to produce materials that are widely used in the biomedical field; these materials are known as nanoparticles (NPs) and have a size range between 1-100 nm (Kaushal et al., 2021). NPs can be classified as polymeric (natural and synthetic), lipid NPs (biodegradable) and metal-based (gold NPs (AuNPs), AgNPs, and iron oxide NPs) NPs (Nagaich et al., 2016). Amongst those, metal-based NPs (MNPs) have been reported to exhibit antimicrobial activity and can be synthesised using plants or plant extracts to overcome the drawbacks of the current antimicrobial agents. NPs can be made using physical and chemical approaches (Kruis et al., 2000, Pal et al., 2019). Each method has advantages and limitations in their applications (Samuggam et al., 2021). The chemical approach is the commonly used method, examples include co-precipitation, micro-emulsion, sol-gel synthesis, and hydrothermal techniques (Kaushal et al., 2021). Physical methods (grinding and milling) are time consuming and require specific conditions such as high temperatures or pressures which renders the process expensive (Ahmed et al., 2016, Borah et al., 2020, Gahlawat and Choudhury, 2019). Although the chemical methods are preferred to produce NPs of desirable sizes, makes use of toxic reducing agents such as sodium dodecyl sulphate, potassium bitartrate and sodium borohydride, which are carcinogenic, cytotoxic as well as genotoxic (Ahmed et al., 2016, Iravani et al., 2014). Due to all the concerns on the previous methods, there is an urge to use greener processes to resolve health and environmental problems. Green nanotechnology makes use of biological materials such as plants and microorganisms to overcome the drawbacks of the chemical reducing agents. This greener approach is eco-friendly, cost effective compared to the conventional methods used to

synthesise NPs (Kaushal et al., 2021). Among MNPs, AgNPs are commonly known for their various beneficial antiviral, anti-inflammatory, antibacterial, and antifungal properties (Nagaich et al., 2016). They have also been incorporated in products such as antiseptic sprays, antibacterial coating agents to sterilise air, textiles as well as surfaces in hospitals, and wound dressing (Chaloupka et al., 2010). Considering all the different health properties present in AgNPs synthesised with plants extracts, this study will be focusing on the green synthesis of AgNPs using Indian Hawthorn (*Rhaphiolepis indica spp.)* berries and the evaluation of their antimicrobial, antioxidant, and cytotoxic effects.

1.2 Bacterial infections and drug resistance

Infectious diseases are a major cause of morbidity and mortality in the world, caused by a variety of organisms such as fungi, bacteria and viruses. Hospital acquired infections (HAI) are the main cause of death worldwide (Santajit and Indrawattana, 2016) and can be acquired by contact between patients or contaminated hospital equipment**.** The WHO has reported that 49 % of hospitalized patients with sepsis contracted the infection in the hospital, and estimated that 27 % of these patients and 42 % of patients in intensive care units will die (WHO, 2020). HAIs are also associated with multi-drug resistant (MDR) pathogens which is a burden on medical care systems as well as economic sector due to the increase in the cost of intensive care and medication (WHO, 2020).

A wide range of antimicrobial drugs including β-lactams group A (i.e penicillin, ampicillin, amoxicillin etc.) and group B aminoglycosides are available in the market for the treatment of infectious diseases (Ullah and Ali, 2017). Antimicrobial drugs are classified as bactericidal (able to kill bacteria) and bacteriostatic (able to inhibit bacterial growth) agents (Ullah and Ali, 2017). Their misuse has facilitated bacterial resistance, which became a threat to public health (Mammari et al., 2022). The different drug-resistant bacteria comprise penicillin-resistant, methicillin-resistant, sulfonamide-resistant, vancomycin-resistant *Staphylococcus aureus* (*S. aureus*), penicillin-resistant *Streptococcus pneumoniae*, macrolide-resistant *Streptococcus pyogenes*, *Enterobacter cloacae* (*E. cloacae*), *Escherichia coli* (*E. coli*), *Klebsiella pneumoniae* (*K.*

pneumoniae), *Acinobacter baumannii* (*A. baumannii*), multidrug-resistant *Mycobacterium tuberculosis*, *Vibrio cholerae*, and *Pseudomonas aeruginosa* (*P. aeruginosa*) (Giurazza et al., 2021, Tacconelli et al., 2018) Methicillin resistant *S. aureus* (MRSA), which are resistant to multiple antibiotics and associated with a higher percentage of deaths are common HAIs (Murray et al., 2022), and responsible for 37.4 % of bloodstream infections (WHO, 2023).

The consequences of AMR are high treatment cost, uncertainties in diagnostics and a lack of trust in conventional medicine (Freitas and Werner, 2023). Nosocomial pathogens classified as "ESKAPE" (Rice, 2008, Bush and Jacoby, 2010), i.e. *Enterococcus faecium* (*E. faecium*), *S. aureus, K. pneumoniae, A. baumannii, P. aeruginosa, and Enterobacter species* were classified as health priority (Santajit and Indrawattana, 2016). These bacteria are the most prevalent cause of severe nosocomial infections amongst immunodeficient, and critically ill patients (Hetta et al., 2023). ESKAPE pathogens are associated with a high risk of mortality and raises the cost of treatments (Founou et al., 2017)

AMR is more prevalent in deadly bacterial infections such as lower respiratory diseases, tuberculosis, syphilis, meningitis and gonorrhoea (Chandra et al., 2017, Tacconelli et al., 2018, Santajit and Indrawattana, 2016). *E. coli* is commonly known to cause urinary tract and cholecystitis infections (Lim et al., 2010); *Salmonella typhimurium* is responsible for invasive nontyphoidal Salmonella (NTS) infections such as severe gastroenteritis (Scallan et al., 2011). *K. pneumoniae* is the second most prevalent disease-causing gram-negative bacterium after *E. coli* that is responsible for infectious illnesses such as meningitis and pneumonia (Podschun and Ullmann, 1998, Vading et al., 2018). Gram-positive bacteria such as streptococcus species are known to cause dental caries (Metwalli et al., 2013). In 2018, the WHO published 12 pathogens which are in demand of new antibiotics (Tacconelli et al., 2018), and classified the demand into three categories: critical, high, and medium priority based on the urgent state of need for new antibiotics (Mulani et al., 2019). *A. baumannii*, *P. aeruginosa* and Enterobacteriaceae are classified under "Critical Urgency". These are carbapenem and third generation-cephalosporin resistant Gram-negative (Mammari et al., 2022). The "High Urgency" include vancomycin-resistant *E. faecium*, *S. aureus* exhibiting resistance to methicillin and vancomycin, *Salmonella* spp. and *Campylobacter* spp. being resistant to fluoroquinolone and third generation

cephalosporin and fluoroquinolone-resistant *Neisseria gonorrhoea*. The "Medium urgency" includes ampicillin-resistant *Haemophilus influenzae*, penicillin non-susceptible *Streptococcus pneumoniae* and *Shigella* spp. resistant to fluoroquinolone (Duval et al., 2019, Tacconelli et al., 2018).

1.2.1 Classification of antimicrobial drugs

Antimicrobial drugs used to treat infectious diseases caused by bacteria have been categorised based on their mode of action, spectrum activity, source, function and their chemical structure (Adzitey, 2015). Antibacterial agents are generally grouped based on their action; it can either be bacteriostatic or bactericidal as summarised in Table 1.1. Bactericidal agents target and destroy the cell wall of the bacterium; while bacteriostatic agents slow or inhibit the growth of bacteria by inhibiting certain metabolic pathways involved in protein synthesis (Ullah and Ali, 2017).

Table 1. 1 Bactericidal and bacteriostatic drugs and their functions adapted from (Ullah and Ali, 2017)

A. Bacteriostatic antibacterial	**Function**
Sulphonamides	Inhibit synthesis of folate
Spectinomycin	Interrupts protein synthesis by binding to the 30S ribosomal subunit
Amphenicols, e.g., chloroamphenicol	Amphenicols inhibit protein synthesis
Trimethoprim	Interrupts synthesis of tetrahydrofolate pathway
Erythromycin, clarithromucin and azithromycin are macrolides	Protein synthesis inhibitors
Tigecycline (from the glycylcycline class)	Inhibits protein synthesis and binds to the 30S bacterial ribosomal subunit.
Linezolid (member of the oxazolidinone class)	Protein synthesis inhibitors
Doxycycline, tetracycline, and minocycline (belong to tetracyclines class)	
B. Bactericidal antibacterial	**Function**
Penicillin such as pen V, penicillin G, procaine penicillin G, benzathine penicillin G, methicillin, oxacillin, cloxacillin, dicloxacillin and flucloxacillin. All members of the β-lactams antibiotic class	Interfere with the synthesis of the bacterial cell wall
Carbapenems such as imipenem, meropenem,	

aztreonam, ticarcillin clavulanate and piperaciintazobactam are β-lactam/β lactamase inhibitors. Other β-lactam inhibitors known as cephalosporin, e.g., ceftazidime, cefotaxime, ceftriaxone, and cefepime	
Gentamicin, amikacin, and tobramycin are known as aminoglycosides	Protein synthesis inhibitors
Fluoroquinolones and Quinolones such as Ciprofloxacin, levofloxacin and oxifloxacin	Block the replication of bacterial DNA
Vancomycin which are glycopeptide	Inhibit synthesis of the cell wall
Polymyxin B and colistin are polymyxins	Destroy the cell membrane

1.2.2 Mechanisms of resistance against antimicrobial drugs

Bacteria have different ways to acquire resistance against antimicrobial agents these include, low uptake of antibiotic, antibiotic target modification, inactivation of antibiotics, efflux mechanisms of resistance and biofilm formation as shown in Figure 1.1 (Wilson, 2014, Wright, 2005). There are 3 main steps leading to the development of drug resistance, the first one is acquisition of resistant genes by microorganisms against single and multiple drugs, this occurs through horizontal gene transfer including transformation, conjugation, and transduction (Hajipour et al., 2012). The second step involves the expression of resistant genes by bacteria as a response to their exposure to antibacterial drugs (Kareem et al., 2021). Lastly, selection for microbes expressing resistance genes against the antimicrobial agent resulting in resistance widespread. This occurs when treatment was stopped before destroying bacteria (Hajipour et al., 2012). Bacteriostatic drugs are more likely to cause antimicrobial resistance than bactericidal drugs (Lara et al., 2010). Furthermore, AMR can also be the result of antimicrobial drug misuse (either by taking insufficient doses or missing the scheduled doses); which may increase the risk of drug resistance. The five mechanisms used by pathogens to develop resistance to antimicrobial drugs are summarized in Table 1.2.

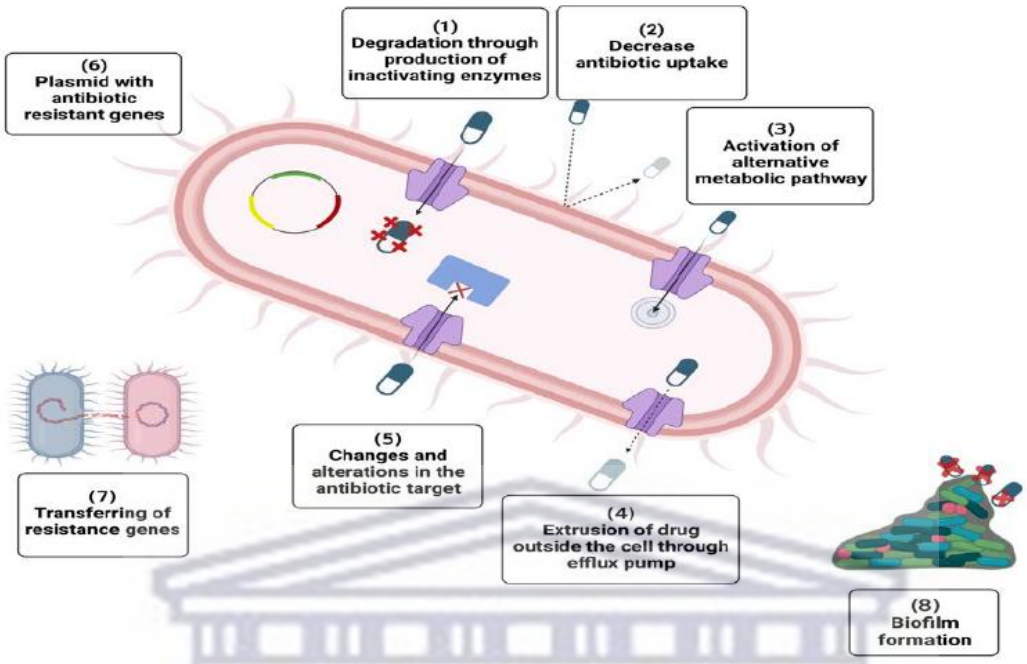

Figure 1. 1. The different mechanisms of antibiotic resistance. AMR develops through: (1) breakdown of drugs through production of inactivating enzyme, (2) decrease in antibiotic uptake, (3) alteration of metabolic pathway, (4) extrusion of drug outside the cell by efflux pump, (5) change and alteration in antibiotic target, (6) presence of plasmid carrying multiple resistance genes, (7) sharing resistance gene between different bacteria, (8) formation of protective extracellular polymeric matrix. (Hetta et al., 2023)

Table 1.2 Antimicrobial resistance mechanisms on different antibiotics (Wanda, 2018)

Drug	Drug uptake action	Drug target modification	Drug inactivation	Efflux pumps
β-Lactams	Porins number decreased and no outer cell wall	Alterations in penicillin-binding proteins in Gram-positive bacteria	Gram-positive and Gram-negative-β-lactamases	Resistance-nodulation-cell division family (RND)
Carbapenems	Selectivity of porin is altered	-	-	-
Cephalosporins	Changed in porin selectivity	-	-	-
Monobactams	-	-	-	-
Penicillins	-	-	-	-
Glycopeptides	Condensed cell wall, no outer cell wall	Altered peptidoglycan	-	-
Lipopeptides	-	Modification of net cell surface charge	-	-

Aminoglycosides	Polarity of the cell wall	Ribosomal mutation, methylation	Acetylation, phosphorylation, adenylation and aminoglycoside modifying enzymes	RND
Tetracyclines	Reduced numbers of porins	Ribosomal protection	oxidation and antibiotic modification	Major facilitator superfamily (MFS), RND
Chloramphenicol	-	Ribosomal methylation	Acetylation of drug	MFS, RND
Lincosamides	-	Gram-positive ribosomal methylation	-	ABC, RND
Macrolides	-	Ribosomal mutation, methylation	-	ABC, MFS, RND
Oxazolidinones	-	Ribosomal methylation	-	RND
Streptogramins	-			ABC
Fluoroquinolones	-	Gram-negative DNA gyrase alteration	Acetylation of drug	Multidrug and toxic compound extrusion family, MFS, RND
	-	Gram-positive topoisomerase IV	-	
Sulfonamides	-	Reduction in dihydropteroate synthase (DHPS) binding, overproduction of resistant dihydropteroate synthase	-	RND
Trimethoprim	-	Reduction in dihydrofolate reductase (DHFR) binding, overproduction of DHFR	-	RND

1.2.2.1 Inactivation of antibacterial agent

The inactivation of antibacterial agents can occur in two ways: by degradation of the drug or by transfer of functional groups such as acetyl, phosphoryl, and adenylyl groups to the drug

(Wanda, 2018). The pathogen produces enzymes that will inactivate the antibacterial drug causing it to lose its biological function (Wanda, 2018). Certain pathogens can become resistant to β-lactam antibiotics by producing enzymes such as β-lactamases that inactivate the activity of the antibiotic leading to a loss of its biological function (Hetta et al., 2023). β-lactam rings including antibiotics such as ampicillin, amoxicillin, penicillin, ceftazidime etc. are rendered ineffective when β-lactamases hydrolyse the amide bond in the ring (Wilke et al., 2005). Several transferases' have been identified to inactivate antibiotics, these include adenylyl transferase, phosphotransferase, and acetyltransferase (Abd El-Baky et al., 2020, El-Kazzaz et al., 2020, Farhan et al., 2019, Makharita et al., 2020). Acetylation is one of the most used mechanisms to inactivate a wide range of antibiotics including chloramphenicol, aminoglycosides, fluoroquinolones, and streptogramin (Wanda, 2018). Other mechanisms such as adenylation and phosphorylation are mainly used against aminoglycosides (Blair et al., 2015, Ramirez and Tolmasky, 2010, Robicsek et al., 2006, Schwarz et al., 2004).

1.2.2.2 Modification of antibiotic binding sites/targets

Antibacterial drugs act on specific target sites, where they attach and modify the normal function of the bacterium (Chandra et al., 2017). Bacterial cells can develop drug resistance through alteration or modification of these target sites; they express genes that code for a modified version of the target substrate to which the drug usually binds, resulting in lower binding affinity and reduced drug activity (Pelgrift and Friedman, 2013). One example is the structural modification of the penicillin-binding proteins (PBPs) of the β-lactam drugs by gram-positive bacteria in most cases MRSA (Algammal et al., 2020). The structural change of the PBP2a in *S. aureus* by addition of *mecA* gene may reduce the binding ability of the drug or completely inhibit its binding (Beceiro et al., 2013, Reygaert, 2009). Another example, is the alteration of peptidoglycan precursors by acquisition of *van* genes resulting in vancomycin-resistant enterococci and *S. aureus* particularly MRSA; this modification reduces the ability of vancomycin to bind (Beceiro et al., 2013, Cox and Wright, 2013). In the case of the antibiotic

erythromycin, methylation of an adenine residue in the peptidyl-transferase of rRNA 23S reduce its binding affinity to the enzyme without protein synthesis impairment (Hetta et al., 2023).

1.2.2.3 Reduced intracellular drug accumulation

The balance between the accumulation and elimination of antibiotics determines the sensitivity of bacteria to that specific drug (Pelgrift and Friedman, 2013). Two important resistance mechanisms are utilised by bacteria; reduced uptake and increased efflux of the drug (Jayaraman, 2009). These mechanisms impede the drug concentration to rise to toxic levels, thus reducing the amount of drug that passes through the bacterial cell wall (Jayaraman, 2009, Pelgrift and Friedman, 2013). This is achieved through reduction of protein channels on the outer membrane of bacteria to limit drug entry and uptake through efflux pumps within the bacterial cells (Santajit and Indrawattana, 2016). Bacteria can alter their cell wall to reduce drug accumulation; it has been observed that Gram-negative bacteria have a lipopolysaccharide layer which act as a barrier to certain molecules. Diffusion of drugs occurs through porin channels which allow entry of hydrophilic drugs in two ways: modification or reduction in the amount of porins and porin gene mutation leading to the development of resistance (Abd El-Baky et al., 2020, Al-Kadmy et al., 2020, Kareem et al., 2021). As an example, *Enterobacteriaceae* can develop resistance by reducing the number of porins or in certain cases hindering the production of certain porins. This group of bacteria use this mechanism to build resistance against carbapenems (Chow and Shlaes, 1991, Cornaglia et al., 1996, Cornaglia et al., 1992). Mutations leading to changes within the porin channel have been observed in *E. aerogenes* causing resistance to imipenem and some cephalosporins (Gill et al., 1998, Thiolas et al., 2004). *Neisseria gonorrhoea* became resistant to β-lactams and tetracycline (Gill et al., 1998, Thiolas et al., 2004). Gram-positive bacteria do not have an outer membrane; thus, restriction of drug uptake is not as common. *S. aureus,* is resistant to vancomycin and makes use of an unknown mechanism through which the cell wall is obstructing drug access (Santajit and Indrawattana, 2016). Another example is observed in Enterococci species, they have developed intrinsic

resistance to aminoglycosides due to the difficulty of polar molecules penetrating their cell wall (Reygaert, 2009).

1.2.2.4 Drug efflux

Bacteria can get rid of toxic substances using extruder membrane proteins known as efflux pumps; these pumps can transfer a variety of molecules within the bacterial cell (Wanda, 2018). These are energy-driven systems that remove antibiotics exposed to bacteria; this occurs at a high rate meaning that the drug concentrations are not sufficiently accumulated to cause toxic effects on the bacterium (Hetta et al., 2023). Most of these pumps are multidrug exporters/transporters that can expel a wide variety of antibiotics causing MDR. The 5 families of efflux pumps are: the resistance-nodulation division family, the ATP binding cassette family, the major and small multidrug resistance family, as well as the multidrug and harmful substance extrusion family (Sun et al., 2014). Many bacteria use this mechanism, as an example, *P. aeruginosa* possesses an inner membrane consisting of H^+/drug antiporter protein attached to a linker protein which is then bound to an outer membrane channel protein (Poole, 2002). The function of this protein is to repress genes coding for efflux proteins, however, when mutation occurs, these proteins are overexpressed rendering *P. aeruginosa* multi-drug resistant (Poole, 2002). An increase in efflux pump can cause resistance against fluoroquinolones, particularly in Gram-negative bacteria (Poole, 2002). Furthermore, resistance against macrolide in Gram-positive bacteria has been associated with this mechanism; the same was also observed in *E. faecalis* which shows resistance to streptogramins including dalfopristin and quinupristin (Jayaraman, 2009).

1.2.2.5 Biofilm formation

Biofilms are bacterial communities that live as a small layer on surfaces, embedded in a matrix which consist of extracellular polymeric substances (EPS) (Santajit and Indrawattana, 2016). The EPS mainly include proteins, lipids, polysaccharides, and extracellular DNA from bacteria (Sharma et al., 2014). Three steps are involved in the formation of biofilm: firstly, cells adhere

and are fixed onto a surface, this is known as adhesion. This is followed by growth and maturation of the pathogens as they produce EPS that create the matrix and grow from small colonies to multi-layered cell clusters. Lastly, detachment which can be passive or active; active detachment is established by the microorganisms themselves and in contrast, passive detachment is initiated by outside forces including human involvement, scraping and liquid stress caused by fluid shear (Laverty et al., 2014). Biofilms protect pathogens against the immune system of the host and antimicrobial drugs (Wanda, 2018). The thick consistency of the biofilm matrix restricts antimicrobial agents to adhere to the pathogen; therefore, higher concentrations of drugs are required (Wanda, 2018). Biofilm formation can therefore cause bacteria to be resistant to high doses of multiple antibiotics causing chronic infections despite the treatment (Ferreira et al., 2010, Hajipour et al., 2012, Huh and Kwon, 2011, Jayaraman, 2009).

1.3 Nanotechnology to combat AMR

Nanotechnology is a discipline of science that involves the manipulation of atoms and molecules to produce nanomaterials at a size range of 1 to 100 nm (Figure 1.2). Their unique size, shape, structure, and physio-chemical properties contribute to their innovative properties in various applications (Madiehe et al., 2022). Nanoparticles (NPs) have a large surface area to volume ratio which enables attachment of large amounts/quantities of drugs (Mauricio et al., 2018). They are composed of the core and the shell (Kaushal et al., 2021); the different layers display distinct attributes (Kaushal et al., 2021) that were explored in medical field as diagnostics (Sahana et al., 2014), and therapeutic agents (Zonooz and Salouti, 2011).

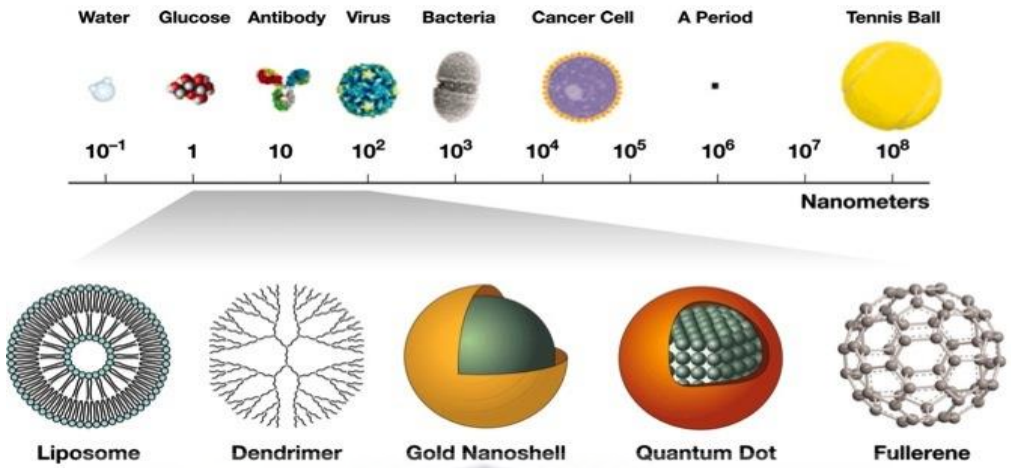

Figure 1. 2. Types of organic and inorganic nanomaterials and their size range (1-100nm) in relation to biomolecules (McNeil, 2005).

NPs are classified into 3 principal groups based on their chemical compounds: organic, inorganic, and carbon-based groups as shown in Figure 1.3. Organic NPs include liposomes, polymers, micelles and dendrimers (Martinelli et al., 2019, Zaidi et al., 2017). Inorganic NPs are comprised of semiconductor nanomaterials such as metal oxides, MNPs (silver, gold, and copper), quantum dots (QDs) and ceramic NPs (Hetta et al., 2023, Zaidi et al., 2017). Carbon-based NPs include fullerene, graphene and carbon nanotubes (Aqel et al., 2012, Khan et al., 2017, Zaidi et al., 2017). NPs can have different morphologies such as rods, spheres, wires, etc. which may influence their biological applications (Huang et al., 2007, Kesharwani et al., 2014, Liu et al., 2014).

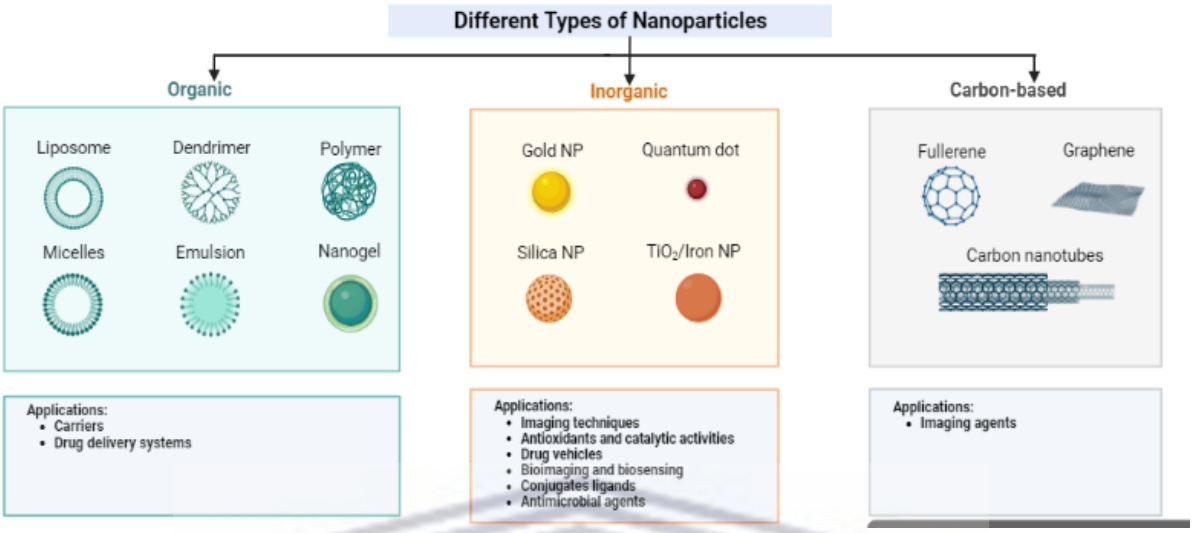

Figure 1. 3. Classification of NPs and their main applications in biomedicine. NPs are classified in three groups: Organic, inorganic and carbon-based. Created with BioRender.com

Organic NPs, especially liposomes, are the most advanced in medicine due to their biodegradability and biocompatibility (Zaidi et al., 2017). They were approved by FDA as delivering agents for chemotherapeutic drugs in cancer treatment (Mauricio et al., 2018, Martinelli et al., 2019). Due to their degradable characteristics, these NPs are considered less toxic and good candidates for drug delivery systems (Zaidi et al., 2017). Despite the advantages, some of their pitfalls such as low loading efficacy and instability have also been observed (Zaidi et al., 2017); leading to the interest in inorganic NPs or MNPs. MNPs offer several advantages over organic NPs, such as more loading capacity, high surface area to volume ratio, ease of surface modification, stability, exclusive optical and thermal properties (Zaidi et al., 2017). AuNPs and AgNPs are the widely used MNPs in biomedical application. AuNPs are used in both diagnostics (Martin et al., 2021), and therapy (Aboyewa et al., 2021); however, they have limited antimicrobial agents compared to AgNPs (Hetta et al., 2023, Zaidi et al., 2017).

1.3.1 AgNPs as candidate antibacterial agents

AgNPs are among the most studied MNPs that have gained great interest owing to their broad-spectrum antimicrobial activities (Fadaka et al., 2022). AgNPs can kill different bacteria through several mechanisms; hence, it is difficult to develop resistance against them (Qayyum and Khan,

2016, Rai et al., 2012). AgNPs can attach and damage the cell membrane of bacteria by increasing porosity; produce free radicals and increase reactive oxygen species (ROS) concentration which induces inflammatory responses resulting in apoptosis (cell death) (Kulshrestha et al., 2017, Misba et al., 2016). Furthermore, AgNPs have a range of different applications including water filtering devices (Deshmukh et al., 2019), catalysis (Nguyen et al., 2020), surface plasmon resonance research (Gangwar and Agarwal, 2023), colorimetric label free devices for enzyme detection (Nguyen et al., 2018), visual receptor in biolabeling (Ling et al., 2008), wound bandage (Iqbal et al., 2020), antiviral research (Jeremiah et al., 2020), antiseptics in the medical field (e.g. catheters, needles, and blades coated with AgNPs) (Croes et al., 2011), antiplatelet drugs (Shrivastava et al., 2009), medical face masks (Valdez-Salas et al., 2021), preservatives in bone cement (Kehribar et al., 2023), paints (Kumar et al., 2008), packaging of food (Mohammed Fayaz et al., 2009), as well as in water distillation (Dankovich and Gray, 2011).

1.3.1.1 AgNPs synthesis

MNPs including AgNPs can be synthesised using the bottom-up and top-down approaches, classified as physical, chemical, and biological approaches (Figure 1.4). In the top-down approach, bulk materials are mechanically reduced into fine particles (Mallick et al., 2004) while the bottom up uses the biological and chemical methods that involve the assembly of atoms to form a nuclei which grows into a particle of nanoscale (Ahmed et al., 2016). The physical method involves preparation of NPs by evaporation-condensation (Kruis et al., 2000), pyrolysis and spark discharging (Tien et al., 2008); this approach holds many advantages including speed, and exclusion of harmful chemical reducing agents (Mallick et al., 2004). However, low yield, contamination of solvent, high consumption of energy and the lack of uniform distribution render this method unfavourable (Elsupikhe et al., 2015, Shameli et al., 2010). Chemical method makes use of organic solvents as reducing and capping/stabilizing agents in the synthesis of AgNPs (Tao et al., 2006, Wiley et al., 2005). The reduction of silver salts occurs in two steps: nucleation and subsequent growth (Deepak et al., 2011). The chemical methods offer

advantages over the physical ones by generating higher yields and ease of synthesis. However, the chemical and physical methods are costly and time consuming (Pal et al., 2019). Moreover, the chemical method uses toxic chemicals such as borohydride, and citrate as reducing reagents (Mallick et al., 2004, Pal et al., 2019), they are labour intensive as further downstream processes are required to stabilize the AgNPs to avoid aggregation (Malik et al., 2002).

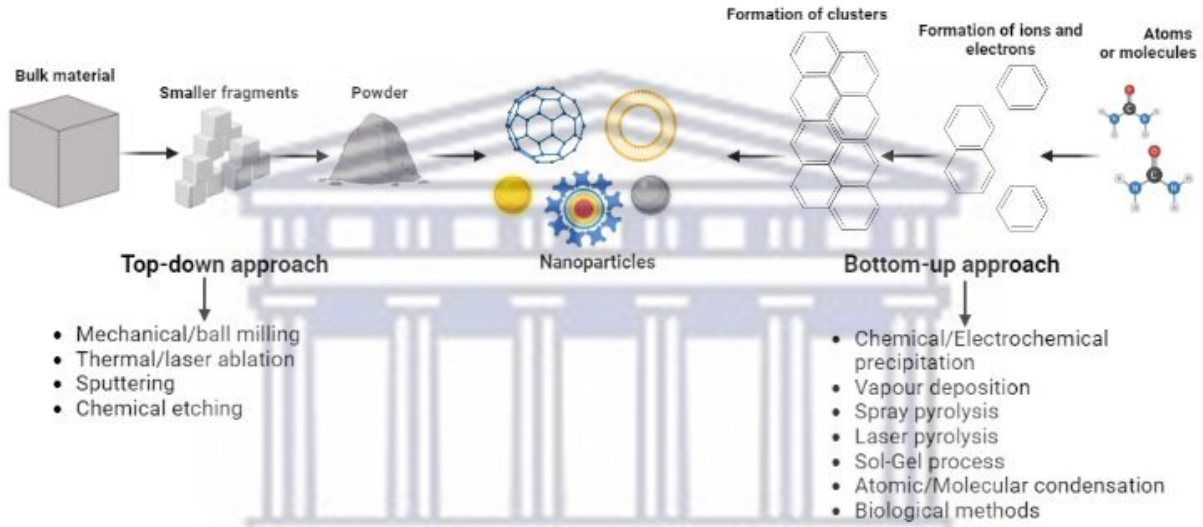

Figure 1. 4 Top-down and Bottom-up approach for the synthesis of NPs. Bulk materials are broken down into smaller fragments via physical methods in the top-down approach, while the bottom-up approach involves the assembly of atoms to form clusters known as NPs. (Simon et al., 2022)

1.3.1.2 Green synthesis of AgNPs

The major concern with chemical methods is the use of toxic substances such as sodium dodecyl sulphate, potassium bitartrate and sodium borohydride resulting in products that are carcinogenic, cytotoxic as well as genotoxic (Ahmed et al., 2016, Iravani et al., 2014). To overcome this, there is an urge to use greener or biological processes to resolve health and environmental problems (Massironi et al., 2019). Biological methods as shown in Figure 1.5, use plant or microbial (bacteria, fungi) extracts as reducing or capping agents to produce NPs that are eco-friendly and cost effective (Pal et al., 2019). Furthermore, the biological approach excludes secondary steps that require using capping or stabilizing agents; thus, reducing the reaction rate of synthesis (Gahlawat and Choudhury, 2019).

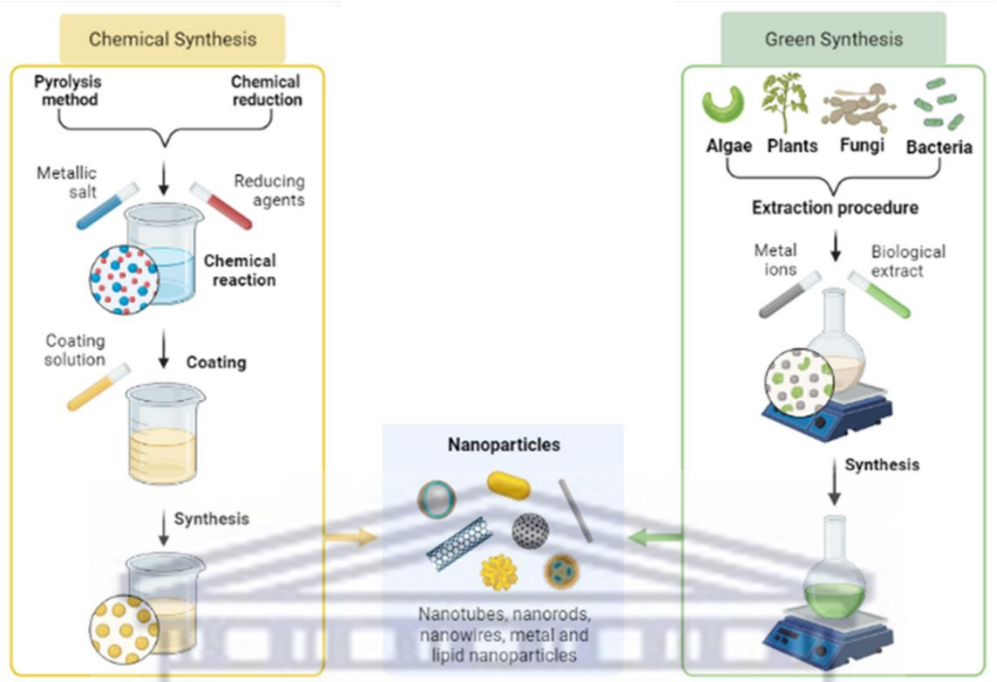

Figure 1. 5 Overview of chemical and biological/green methods used to synthesize AgNPs. The chemical method involves reducing metal precursors using chemical reducing agents to form NPs; while the green synthesis uses biological products to reduce metal salt into NPs. (Simon et al., 2022)

Several studies have reported on the synthesis of AgNPs using biological methods including microorganisms and plants (Ahmed et al., 2016). Even though AgNPs can be synthesised using microorganisms, this method cannot be industrialised due to certain constraints such as high maintenance and aseptic conditions (Ahmed et al., 2016). For this reason, using plant extracts to synthesise AgNPs is ideal, as it offers more advantages such as shorter reaction time, easy to scale up and it does not required many processes such isolation and bacterial culture maintenance (Samuel et al., 2022). Therefore, plant extracts are a safer option for AgNPs synthesis. Plants contain phytochemicals which can simultaneously act as capping and stabilisation in a one-step reaction (Samuel et al., 2022). The different phytoconstituents implicated in the synthesis include phenolics, saponins, tannins, vitamins, amino acids and proteins; which serve a role in the bioreduction of metal precursors into NPs and at the same time as stabilising agents (Kulkarni and Muddapur, 2014).

Biosynthesised AgNPs are widely used in biomedical systems due to the medicinal properties of plants. Several studies have reported on the biosynthesis of AgNPs using plant extracts such as

Pedalium murex (Anandalakshmi et al., 2015), *Artemisia princeps* (Gurunathan et al., 2015), *spondias mombin* (Samuggam et al., 2021), *Cotyledon orbiculata* (Tyavambiza et al., 2021), etc. The biological properties of biosynthesised AgNPs are dependent on their shape and structure. Many studies confirmed that biosynthesised AgNPs with a small size (6 - 70 nm) have enhanced antimicrobial properties as opposed to the raw plant extract (Dube et al., 2020, Simon et al., 2021, Tyavambiza et al., 2021). This was observed with AgNPs synthesised with *Cotyledon orbiculata* plant extract, whereby a size range from 20 to 40 nm exhibited great antimicrobial activity towards bacteria (Tyavambiza et al., 2021). Furthermore, the antimicrobial effect of Cotyledon-AgNPs was comparable to ampicillin (one of the antibiotics found in the market); the AgNPs had a minimum inhibitory concentration (MIC) against MRSA and *P. aeruginosa* of 40 and 5 µg/mL, respectively, which was lower than ampicillin (Tyavambiza et al., 2021).

1.4 Antibacterial effect of MNPs

Although antibiotics are efficient against many bacterial infections, challenges are still being observed specifically with the development of bacterial resistance against multiple antibacterial drugs (Zaidi et al., 2017). These infections are a serious threat to healthcare and can lead to disastrous consequences. Therefore, several studies are underway to solve this issue by improving the potency of antimicrobial drugs through precise targeting with drug delivery systems (Zaidi et al., 2017). As mentioned previously, MNPs has been used to tackle the AMR issue (Hetta et al., 2023).

The antimicrobial potential of MNPs involves direct contact with the bacterial cells causing destruction of the cell membrane, thereby allowing entry of NPs through the cell wall; once inside, NPs interfere with the cellular components and metabolism of the microorganisms and eventually causing death (Hajipour et al., 2012, Simon et al., 2021, Tyavambiza et al., 2021). Some examples include Titanium dioxide (TiO_2), Zinc oxide (ZnO), Copper (Cu) and Nickel (Ni) NPs, which have been used due to their antimicrobial properties (Akhavan et al., 2011, Pant et al., 2013, Qu et al., 2016, Yin et al., 2016). The antimicrobial potential of MNPs follow various

mechanisms; the common ones are oxidative stress, and non-oxidative stress mechanisms in response to metal ions release (Li et al., 2015, Zhao and Ashraf, 2015).

1.4.1 Antimicrobial mechanisms of NPs

Many antibiotics target bacteria by inhibiting the synthesis of proteins, nucleic acids, and the cell wall (peptidoglycan being the main target) or by modifying the membrane permeability of bacteria (Mammari et al., 2022). As a response to antimicrobial drugs, bacteria can develop resistant mechanisms by expressing enzymes that can alter or degrade antimicrobial drugs (Blair et al., 2015, Tenover, 2006), modify bacterial cell wall (Mammari et al., 2022), cause ribosomal mutations (Lin et al., 2018) or change porin expression (Christaki et al., 2020, Fernández and Hancock, 2012).

MNPs make use of various mechanisms to tackle microbial drug resistance (Pelgrift and Friedman, 2013), or can be used as drug delivery agents to overcome drug resistance (Blecher et al., 2011, Zhang et al., 2010). Bacterial mechanisms of actions such as the increase in efflux pumps, decrease in drug uptake and biofilm formation have been targeted by MNPs (Hajipour et al., 2012, Huh and Kwon, 2011). MNPs induce their antibacterial activity by releasing metal ions to damage the cell wall of bacteria, and have potential in the development of novel strategies that will combat bacterial resistance. This is achieved through the interaction between the charged MNPs and the negatively charged molecules on the bacterial cell walls (Mammari et al., 2022). MNPs mode of action against AMR follows a series of reactions: attachment to the bacterial surface, disruption of bacterial cell wall and membrane, followed by the modification of its permeability, initiation of toxicity and oxidative stress due to the production of reactive oxygen species (ROS) and free radicals, and lastly, the adjustment/ modulation of signal transduction pathways as shown in Figure 1.6 ((Zhang et al., 2019). The most prominent mode of actions of MNPs are: release of metal ions, non-oxidative stress and oxidative stress mechanisms.

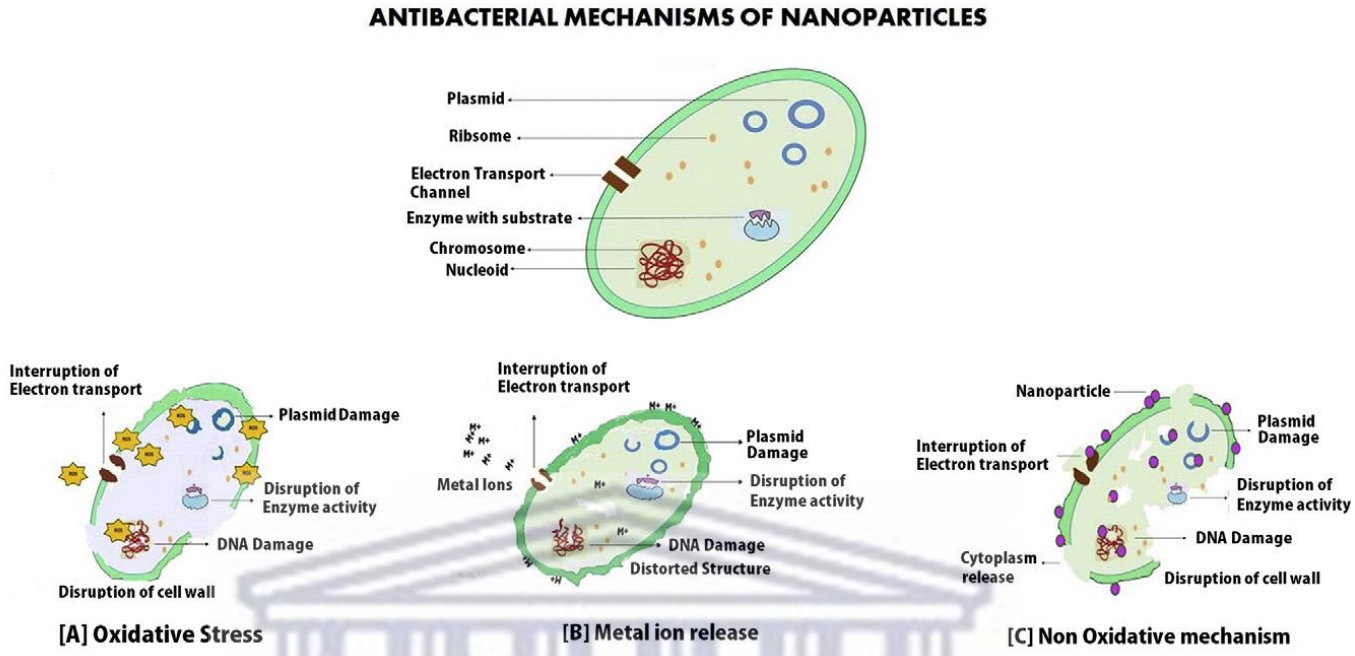

Figure 1. 6. Overview of the antibacterial mechanisms of MNPs. (A) Oxidative stress mechanism; (B) Metal ion release and (C) Non-oxidative mechanism. Reprinted with permission from (Zaidi et al., 2017).

1.4.1.1 Release of metallic ions

It has been reported that positively charged AgNPs can strongly attach to the bacterial surface resulting in higher antibacterial activity; this is done by releasing the metal ions which then are adsorbed on the cell membrane (Mammari et al., 2022, Zaidi et al., 2017). These metal ions react with mercapto (-SH), amino(-NH) and carboxyl (-COOH) groups present in DNA and proteins subsequently disrupting the cell structure of bacteria and preventing the bacterial metabolic pathways (Zaidi et al., 2017). On the contrary, neutral or negatively charged AgNPs have low antimicrobial activity due to less electrostatic attraction with the cell wall of bacteria which is negatively charged (Zaidi et al., 2017). DNA fragmentation was observed after treatment with AgNPs, this was due to the high affinity of Ag^{+} to the phosphate group present in nucleic acids (Muthukrishnan et al., 2019).

1.4.1.2 Non-oxidative processes

The non-oxidative mechanism involves NPs interacting with the bacterial cell wall covered with multi-layers whose role is to defend bacteria against unpredictable hostile environments (Zaidi et al., 2017). The difference between gram-negative and gram-positive bacteria is based on the composition and structure of the cell membrane; this results in varying effects of the drugs (Breijyeh et al., 2020, Jubeh et al., 2020, Lesniak et al., 2013). The cell wall of gram-negative bacteria is composed of lipopolysaccharide on the outer membrane and teichoic acids (Breijyeh et al., 2020). In the case of gram-positive bacteria; these two components include carboxyl or phosphate groups and give a negative charge to the surfaces of the bacteria (Hetta et al., 2023). The phosphate group in teichoic acids draws and delivers NPs onto the surface avoiding any aggregation. Furthermore, it has been confirmed that the antibacterial potential of NPs is more noticeable for gram-positive bacteria as opposed to gram-negative bacteria (Breijyeh et al., 2020, Jubeh et al., 2020, Zaidi et al., 2017). The cell wall of gram-negative bacteria prevents the entry of NPs due to its non-porous composition; however, in gram-positive bacteria, the cell wall is permeable allowing different molecules to penetrate, forming covalent bonds with adjacent proteins and components of the cell wall (Sarwar et al., 2015). Furthermore, proteins and enzymes involved in the metabolism of the cells will be inhibited leading to malfunctioning of the bacterial cell (Wang et al., 2017). Some examples include TiO_2 NPs treatment causing bacterial cell swelling, resulting in cytoplasmic leakage (Joost et al., 2014); this treatment can also cause bacterial cells to aggregate causing their inactivation (Zhukova, 2015). Moreover, MNPs can inhibit the synthesis of proteins and DNA of bacterial cells; an example include treatment with CuO NPs which can hinder different mechanisms involved in the proper functioning of bacterial cells such as nitrogen metabolism and electron transport chain (Su et al., 2015). Furthermore, AgNPs synthesised using fucoidan isolated from *Spatoglossum asperum* exhibited enhanced protein leaking of cellular components by increasing the membrane permeability of *K. pneumoniae* (Ravichandran et al., 2018).

1.4.1.3 Oxidative stress

Oxidative stress is the term used to describe the imbalance among the making and consumption of ROS, reactive nitrogen species (RNS) and unstable molecules (Samrot et al., 2022). ROS are chemically reactive molecules including free radicals and various species all derivative of molecular oxygen such as hydroxyl radicals (-OH), hydrogen peroxide (H_2O_2), singlet oxygen ($^1O_2$), superoxide anion radical (O_2^-) as well as hydroxyl radicals (Boonstra and Post, 2004, Keren et al., 2013). ROS are produced as a natural response to the normal metabolism of oxygen and play an important role in several signalling pathways (Liu and Imlay, 2013, Sena and Chandel, 2012, Shadel and Horvath, 2015); one of which is known as phagocytosis, an important defence mechanism against pathogens in the human body (Akter et al., 2018). However, excessive amounts of ROS can result in damaging effects on biomolecules including proteins, DNA and RNA as well as lipids (Sarangarajan et al., 2017). These negative effects including chemical, physical, and biological factors induce oxidative stress leading to pathological illnesses in humans. In accordance with the previously mentioned evidence, there is a correlation between oxidative stress and diseases caused by oxidative stress (e.g Alzheimer's disease (Cooke et al., 2003), atherosclerosis (Su and Groves, 2010), cardiovascular diseases (Förstermann, 2010), cancer (Ghaffari, 2008, Nazem and Mansoori, 2008, Phaniendra et al., 2015), but also, psychic impairments, such as attention-deficit/hyperactivity disorder (ADHD) or schizophrenia (Katta and Brown, 2015, Klaunig and Kamendulis, 2004). Under normal conditions, cells are able to circumvent the adverse effects of oxidative stress by producing intracellular or extracellular molecules known as antioxidants.

1.4.1.3.1 Antioxidants

Antioxidants are natural or synthetic substances that can hinder or slow down the harmful effects caused by oxidants including ROS and free radicals (Bedlovičová et al., 2020). Antioxidants react with oxygen or nitrogen radicals to deactivate the target molecule resulting in less harmful products (Bedlovičová et al., 2020). Antioxidant defence systems can be generated through *in vivo* processes which include the synthesis of enzymes (superoxide reductases, superoxide dismutase, catalases, and glutathione peroxidases (Bedlovičová et al., 2020). Antioxidants are found in nutrients such as vitamins (A, C, D, E), polyphenols, flavonoids,

amino acids, riboflavin, carotenoids, folic acid, and elements (Se, Fe, Zn, Mg) (Cillard et al., 1980, Halliwell and Gutteridge, 2015, Piao et al., 2011).

MNPs have been reported to display antioxidant properties which allows them to scavenge free radicals and reduce excessive amounts of ROS (Samrot et al., 2022), and offer great potential for the treatment and prevention of diseases caused by excessive ROS (Akhtar et al., 2017, Mohammad et al., 2008, Lushchak et al., 2018). The main antioxidant properties displayed by MNPs include catalase, oxidase, superoxide dismutase and glutathione peroxidase mimicking activity (Samrot et al., 2022). These NPs can move between various oxidation states, allowing them to have great antioxidant potential (Lushchak et al., 2018). Plant-based MNPs have been reported to have enhanced antioxidant scavenging activity (Samrot et al., 2022). The ability of MNPs to scavenge free radicals depends on their physico-chemical properties such as size, surface charge (Khalil et al., 2019, Valgimigli et al., 2018).

Many studies have reported on the use of AgNPs as radical scavengers due to their redox potential and this is true for biosynthesised AgNPs particularly those made using plant extracts. The ability of these NPs to reduce free radicals depends on the method used for their synthesis, as mentioned previously, plants possess compounds such as terpenes, flavonoids, polyphenols, carbohydrates, aldehydes to cite a few (Ahmed et al., 2016, Gurunathan et al., 2009, Pallavicini et al., 2017). An example of biosynthesised AgNPs exhibiting great antioxidant potential was AgNPs synthesised from *Brassica oleracea* leaves extract which exhibited 60 to 80% scavenging activity (Ansar et al., 2020). Additionally, Cotyledon AgNPs could scavenge 2'-Azino-Bis-3-Ethylbenzotiazolin-6- Sulfonic Acid radical (Tyavambiza et al., 2022). These studies demonstrated that biosynthesised AgNPs have enhanced antioxidants properties.

1.4.1.3.2 Oxidative stress mediated antibacterial activity of MNPs

The toxicity of MNPs is also described by the production of ROS, which subsequently results in the induction of oxidative stress and microbial death (Mammari et al., 2022). Studies have reported that higher levels of ROS production during treatment with MNPs is dependent on

their chemical structure, smaller size and surface composition (Mammari et al., 2022, Zaidi et al., 2017). Different MNPs, while displaying similar inhibitory effects on bacterial growth can have diverse ROS damage (Bellanger et al., 2020). AgNPs promote the generation of ROS, resulting in cellular, proteins, and DNA damage (Krce et al., 2020, Quinteros et al., 2016). Different MNPs can generate different types of ROS including hydrogen peroxide (H_2O_2), hydroxyl radical (·OH), singlet oxygen ($^1O2$) and superoxide radical (O^{-2}). For instance, Calcium (Ca) and Magnesium (Mg) NPs can produce O_2^- ; Copper oxide (CuO) NPs have been reported to generate all 4 types of ROS (Zaidi et al., 2017). When bacterial cells are treated with MNPs, the permeability of their cell membrane is altered due to oxidative stress. Subsequently, intracellular ROS causes membrane integrity loss, as well as protein and enzyme damage which leads to high expressions of oxidative proteins causing cell death and apoptosis (Wang et al., 2017, Zaidi et al., 2017).

1.5 Medicinal use of plants

The use of medicinal plants has emerged as an advantage in medical field due their availability and almost no side effects (Chandra et al., 2017). A crude extract is traditionally made using different parts of the plants such as the stem, root, fruits, peels, twigs and flowers which contain a variety of phytochemicals such as flavonoids, tannins, saponins, alkaloids, terpenoids, carbohydrates and proteins (Kaushal et al., 2021, Ravichandran et al., 2018). These phytochemicals found in plants are known to possess antimicrobial and antioxidants properties (Chandra et al., 2017). Some medicinal plants have been used in the treatment of chronic diseases such as Hepatitis B and C, human immunodeficiency virus (HIV), Dengue fever, Tuberculosis, Swine flu etc. (Bhaskar et al., 2020, Chandra et al., 2017). A few examples of medicinal plants for the treatment of diseases include leaf extract of Bhumiamla (*Phyllanthus niruri*) which was reported to have anti-Hepatitis B activity (Li et al., 2017, Venkateswaran et al., 1987). Some plants are known to have antimicrobial activity such as roselle (*Hibiscus sabdariffa*), rosemary (*Rosmarinus officinalis*), clove (*Syzygium aromaticum*), and thyme (*Thymus vulgaris*) (Gonelimali et al., 2018). The leaves of *Plectranthus amboinicus* and root of *Glycyrrhiza glabra*

have been reported to have anticancer properties (Caroline et al., 2023). Additionally, some berries such as strawberry (*Fragaria virginiana*) , Blackberry (*Rubus fruticosus L.*) and Indian gooseberry (*Phyllanthus emblica L.*) have been reported to have anticancer and antioxidant properties (Baby et al., 2018).

1.5.1 Indian Hawthorn (*Rhaphiolepis indica*)

Indian Hawthorn (*Rhaphiolepis indica*) is a perennial, deciduous and thorny shrub from the family of Rosaceae originally discovered in China (Heflish et al., 2023). The plant is being cultivated in over 30 countries worldwide such as South Africa, Kenya, Madagascar, New Zealand, Japan, India, Europe and Australia (Heflish et al., 2023). The shrubs can grow up to 1.8 m in height and can be cultivated in most parts of Asia (Myers, 2023). The fruits/berries are small, dark blue and often used to make jam (Myers, 2023). This plant has been commercialised in only a few countries and holds nutritional and medicinal properties which are of great profit in the medical field. The medicinal properties of this plant are due to the different phytochemicals such as flavonoids and phenols which are present in most hawthorn fruits (Heflish et al., 2023, Singh et al., 2018). The fruit of a related species *Crataegus crenulata* showed ability to treat hypertension in animal models (Negi et al., 2018), confirming that the fruits of this species have anti-hypertensive characteristics. The berries hold antioxidant activities, which minimize the damage caused by free radicals as well as anti-inflammatory, diuretic, and antispasmodic properties (Singh et al., 2018).

Another commonly known hawthorn is the *Pyracantha crenulata* or "Ghingaroo" in Uttarakhan in Northern India (Singh et al., 2018). These shrubs are 1.5 to 6 m in height, with dark greenish leaves; the fruits known as "pomlet" are small and with an approximate mass of 250 mg for each berry (Singh et al., 2018). The fruits of this plant are comestible, profuse in sugar and its leaves used for herbal tea (Singh et al., 2018). This plant possess medicinal and nutritional properties (Heflish et al., 2023, Singh et al., 2018). Additionally, the fruits (berries) hold various therapeutic properties including coronary vasodilator, cardiotonic and hypotensive attributes (Singh et al., 2018). Vasodilating agents can dilate blood vessels by controlling/managing severe

heart failure (Levy et al., 2014). The berries are composed of a variety of bioactive compounds including flavonoids, vitamin A, B_{12}, C and E, protein, potassium, magnesium, and calcium. The most prominent bioactive compounds in the berries are flavonoids and oligomeric proantho-cyanidins (Singh et al., 2018). *Pyracantha* and other hawthorn species have been catalogued as herbal treatments in countries such as China, France, England, and Germany (Singh et al., 2018). A recent study reported the antifungal activity of *Rhaphiolepis indica* fruit extract against *Rhizoctonia solani* and *Fusarium solani*, which was attributed to the presence of flavonoids and phenolic content in the extracts (Heflish et al., 2023). The images of *Rhaphiolepis indica* flowering plant and fruits (berries) are shown in Figure 1.7, there are currently no reports on the biological activities of this specific plant.

Figure 1. 7. Flowers and berries of Indian Hawthorn (*Rhaphiolepis indica*). (McJaje-commonswiki, 2006, Grazio, 2021)

1.6 Aim and Objectives

1.6.1 Aim

The aim of this study was to synthesise AgNPs using Indian Hawthorn (*Rhaphiolepis indica spp.*) fruit extracts and to evaluate their in vitro antibacterial, antioxidant, and cytotoxic effects.

1.6.2 Objectives

The objectives of the study were as follows:

- To synthesise AgNPs using aqueous Indian Hawthorn berries fruit extract (IHFE)
- To characterise IHFE-AgNPs using UV-Vis, DLS, HR-TEM and FTIR
- To investigate the antibacterial effects of IHFE-AgNPs on seven human pathogens using agar well diffusion and microdilution assays

- To evaluate the antioxidant effects of IHFE-AgNPs
- To investigate the cellular toxicity of IHFE-AgNPs on KMST-6 cells

1.6.3 Hypothesis

The aqueous IHFE can synthesise AgNPs with antibacterial and antioxidant properties

1.6.4 Null hypothesis

The aqueous IHFE cannot synthesise AgNPs with antibacterial and antioxidant properties

Chapter 2: Material and methods

2.1 Materials: Reagents, equipment, and suppliers

Table 2. 1 Materials used and their suppliers

Materials	Supplier	Company location
AlamarBlue™ cell viability reagent	Thermo Fisher Scientific	Massachusetts, United States of America (USA)
ABTS (2,2'-Azino-Bis-3-Ethylbenzotiazolin-6-sulfonic Acid)	Thermo Fisher Scientific	Kandel, Germany
Ascorbic acid	Merck	Gauteng, South Africa
Cell culture flasks (25 cm^2 and 75 cm^2)	SPL Life Sciences	Kyonggi-do, South Korea
Ciprofloxacin	Sigma-Aldrich	Missouri, USA
Conical tubes (15 ml and 50 ml)	SPL Life Sciences	Kyonggi-do, South Korea
Disposable cuvette (DTS0012)	Malvern Instruments	Worcestershire, United Kingdom (UK)
Disposable folded capillary cell (DTS1070)	Malvern Instruments	Worcestershire, UK
Dimethyl sulphoxide (DMSO)	Sigma-Aldrich	St Louis, Missouri, USA
DPPH (2,2-diphenyl-1-picrylhydrazyl)	Sigma-Aldrich	Steinheim, Germany
Dulbecco's Modified Eagle's Medium (DMEM)	Gibco	Scotland, UK
Folin-Ciocalteu (FC) reagent	Sigma-Aldrich	St Louis, Missouri, USA
Gallic acid	Sigma-Aldrich	St Louis, Missouri, USA
Hydrochloric acid (HCl)	Merck	New Jersey, USA
Millipore Ultra-purified distilled water (18.2 MΩ cm at 25 °C)	Thermo Fisher Scientific	Massachusetts, USA
Müeller Hinton agar	Sigma-Aldrich	St Louis, Missouri, USA
Müeller Hinton broth	Sigma-Aldrich	St Louis, Missouri, USA
Sodium carbonate (Na_2CO_3)	Sigma-Aldrich	St Louis, Missouri, USA
Phosphate buffered saline (PBS)	Thermo Fisher Scientific	Massachusetts, USA
Polystyrene 96-well microtiter™ plates	Greiner Bio-One (Lasec)	Cape Town, RSA
Potassium peroxydisulfate ($K_2S_2O_8$)	Thermo Fisher Scientific	Kandel, Germany
TPTZ (2, 4, 6-tripyridyl-S-triazine)	Sigma-Aldrich	Switzerland
Trypan blue	Thermo Fisher Scientific	Massachusetts, USA
Trypsin	Sigma-Aldrich	Missouri, USA
Silver nitrate ($AgNO_3$)	Sigma-Aldrich	Missouri, USA
Sodium hydroxide (NaOH)	Sigma-Aldrich	Missouri, USA

Sterile cotton swabs	Lasec	Cape Town, RSA
Sterile loops	Lasec	Cape Town, RSA
Whatman No. 1 filter paper	Sigma-Aldrich	Missouri, USA
WST-1: Water-soluble Tetrazolium, 2-(4-Iodophenyl)-3-(4-nitrophenyl)-5-(2,4 disulfophenyl)-2H-tetrazolium	Roche	Mannheim, Germany

Table 2. 2 Equipment used and their suppliers

Equipment	**Supplier**	**Company location**
Analytical weighing balance	Ohaus Adventurer	New Jersey, USA
Blender	Panasonic	Osaka, Japan
Centrifuge 5415D	Eppendorf	Hamburg, Germany
Countess cell counting chamber slide	Thermo Fisher Scientific	Massachusetts, USA
Countess automated cell counter	Thermo Fisher Scientific	Massachusetts, USA
Desiccator	Thomas Scientific	New Jersey, USA
Evos XL Core inverted microscope		
High-Resolution Transmission Electron Microscope (FEI Tecnai G2 20 FEG)	Thermo Fisher Scientific	Massachusetts, USA
IncoTherm Oven	Labotec	Cape Town, RSA
Incubator	Thermo Fisher Scientific	Massachusetts, USA
Fourier-Transform Infrared Spectrophotometer Perkin Elmer Spectrum 400	Perkin Elmer	Waltham, USA
Laminar flow hood	Thermo Fisher Scientific	Massachusetts, USA
pH meter – Crison Basic 20	Lasec	Cape Town, RSA
POLARstar Omega Plate Reader	BMG Labtech	Ortenberg, Germany
Sorvall Lynx 6000 Centrifuge	Thermo Fisher Scientific	Massachusetts, USA
Stuart Heat-Stir CB162 Hot Plate	Lasec	Cape Town, RSA
Thermomixer Comfort	Eppendorf	Hamburg, Germany
Vacuum Filtration System	KNF Labotech	Cape Town, RSA
Varian 710-ES Inductively Coupled Plasma Optical Emission Spectrometer	Varian	California, USA
VirTis freeze dryer - BenchTop Pro with Omnitronics	SP Scientific	Pennsylvania, USA
Zetasizer – Nano-ZS90 System	Malvern Instruments	Worcestershire, UK

Table 2. 3 Bacterial strains and their suppliers

Bacterial strain	ATCC number	Gram reaction	Supplier
Staphylococcus aureus	25923	Gram-positive	American Type Culture Collection (ATCC) Virginia, USA
Methicillin-resistant *staphylococcus aureus*	33591	Gram-positive	ATCC
Klebsiella pneumoniae	13883	Gram-negative	ATCC
Escherichia coli	35218	Gram-negative	ATCC
Acinetobacter baumannii	19606	Gram-negative	ATCC
Enterobacter cloacae	13047	Gram-negative	ATCC
Pseudomonas aeruginosa	27853	Gram-negative	ATCC

2.2 Research methodology

2.2.1 Collection and preparation of IHFE fruit extract

Indian Hawthorn berries were provided by Prof. Abram Madiehe. Using a coffee grinder, the dried berries were ground until a fine powder was obtained. The preparation of the fruit extract was performed following the method from (Dube et al., 2020). A 10 % aqueous extract was then prepared by mixing the 40 g of the berry powder into 400 ml of deionised distilled water (ddH_2O). Subsequently, the mixture was boiled in a microwave for approximately 5 min. The mixture was stirred for 24 hrs at room temperature and centrifuged on a Sorvall Lynx 6000 Centrifuge at 9000 rpm for 30 min. The clarified supernatant was collected and vacuum filtered using Whatman No.1 filter paper, followed by centrifugation for 5 min at 13 200 rpm. The clarified supernatant was frozen at - 80 °C. The frozen aqueous extract was freeze dried for three days using the VirTis Freeze Dryer – BenchTop Pro with Omnitronics. Furthermore, the freeze-dried extract was stored in a desiccator for future use. Figure 2.1 depicts the process for the preparation of IHFE.

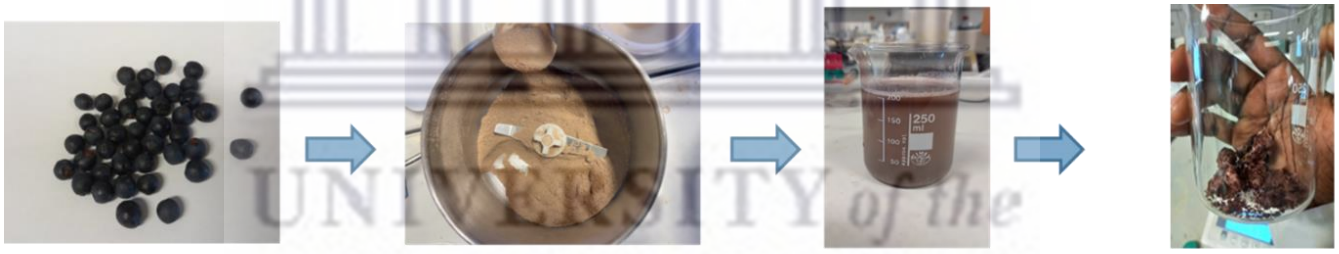

Figure 2. 1 schematic representation for the preparation of the Indian Hawthorn fruit extract (IHFE)

2.2.2 Optimisation of AgNPs synthesis using IHFE

The synthesis optimisation was performed following the method from (Simon et al., 2021). The AgNPs were synthesised by mixing the IHFE and $AgNO_3$ solution in a 1:10 (v/v) ratio to a final volume of 400 µl (i.e., 40 µl extract: 360 µl $AgNO_3$) in Eppendorf tubes. Different parameters were used for optimising the synthesis such as the concentration of IHFE, pH, temperature, and the concentration of $AgNO_3$. The reactions were incubated in the dark for 1 hr at their set

conditions while shaking at 750 rpm using the Eppendorf thermomixer comfort. The optimum conditions for the synthesis of IHFE-AgNPs for each parameter were determined.

2.2.2.1 Effect of pH vs temperature on the synthesis of IHFE-AgNPs

From a stock solution of 125 mg/ml IHFE, the pH of the extract was adjusted to different values (3, 4, 5.7, 7, 8, 9, 10, and 11) using 0.1 M HCl and 0.1 M NaOH for acidic and basic pH, respectively. The natural pH of the IHFE was established to be 5.7. Subsequently, each sample was made up to a final concentration of 12.5 mg/ml. The extract at each pH value was centrifuged for 10 min at 13 200 rpm, the pellet was discarded and supernatants were used for the synthesis of IHFE-AgNPs. Thereafter, 12.5 mg/ml of the IHFE at the different pH values were mixed with 1 mM $AgNO_3$ in 1:10 (v/v) ratio (40 µl IHFE: 360 µl $AgNO_3$). The samples were placed on an Eppendorf thermomixer comfort and mixed at 750 rpm for 1 hr at different temperatures (25 °C shaking and non- shaking, 45, 50, 55, 60, 70, 80, 90, and 99°C). After the synthesis was complete, the samples were cooled at room temperature and centrifuged (Centrifuge 5415D, Eppendorf) at 13 200 rpm for 15 min. The pellets were resuspended in 400 µl sterile ddH_2O. Lastly, the optimum pH and temperature for the synthesis were determined.

2.2.2.2 Effect of IHFE concentration on the synthesis of IHFE-AgNPs

Different concentrations of IHFE (1.56, 3.125, 6.25, 12.5, 25, 50 and 100 mg/ml) were used to determine the optimum extract concentration for synthesis. At the determined pH, the different concentrations of IHFE were mixed with 1 mM $AgNO_3$ in a 1:10 (v/v) ratio (40 µl IHFE: 360 µl AgNO3). The samples were placed on an Eppendorf thermomixer comfort and mixed at 750 rpm for 1 hr using the previously determined temperature. Upon synthesis completion, the samples were allowed to cool off and centrifuged at 13 200 rpm for 15 min. The supernatants were removed and the pellets resuspended in 400 µl sterile ddH_2O. Lastly, the optimum concentration of IHFE was obtained. This experiment was performed in triplicate.

2.2.2.3 Effect of $AgNO_3$ concentration on the synthesis of IHFE-AgNPs

To assess the effect of varying the concentration of $AgNO_3$, different concentrations were used including 0.5, 1, 2, 3, 4 and 5 mM. The optimum concentration of $AgNO_3$ was determined by combining each concentration of $AgNO_3$ with the preceding determined IHFE concentration in a 1:10 (v/v). The reactions were incubated in the dark for 1 hr at their set conditions while shaking at 750 rpm. The experiment was done in triplicate.

2.2.2.4 Effect of reaction time on the synthesis of IHFE-AgNPs

To establish the optimum time at which the reactants have reached saturation, the reaction time for synthesis was determined. From the previously determined synthesis conditions, the IHFE and 1 mM $AgNO_3$ were mixed in a 1:10 (v/v). The samples were placed onto the Eppendorf thermomixer comfort and mixed while shaking at 750 rpm. The spectrum was measured after 0, 5, 10, 15, 30, 45, 60, 180, 240, 300, 360, 480, 600, 720 min.

2.2.3 Synthesis upscale of IHFE-AgNPs

The synthesis of the IHFE-AgNPs was upscaled to a final volume of 50 ml using the optimum conditions obtained previously. Once the synthesis was complete, the samples were centrifuged at 14 000 rpm for 45 min (at 15 min intervals) and the pellet was resuspended to a final volume of 50 ml using sterile ddH_2O. The experiment was done in triplicate. The upscaled samples were used for further analysis including stability testing, biological analysis as well as other characterisation techniques.

2.2.4 Characterisation of IHFE-AgNPs

The IHFE-AgNPs were characterised using Ultraviolet-Visible (UV-vis) spectroscopy, Dynamic light Scattering (DLS), Fourier-Transform infrared (FTIR) spectroscopy and High-resolution transmission electron microscopy (HR-TEM).

2.2.4.1 UV-Vis analysis

Preliminary characterisation of the synthesised IHFE-AgNPs was done using the UV-Visible spectroscopy (POLARstar Omega microplate reader). The formation of IHFE-AgNPs was confirmed by observing a colour change as well as the Surface Plasmon Resonance (SPR) peaks at a wavelength (λ) ranging from 300 to 800 nm. In a 96 well Greiner plate, the IHFE-AgNPs samples were diluted with sterile ddH_2O in a ratio of 1:10 (v/v) in a final volume of 300 µl. The obtained spectra were analysed using Omega Mars and Microsoft Excel software.

2.2.4.2 Dynamic light scattering (DLS) analysis

DLS analysis was performed using a Malvern Zetasizer Nano ZS90 to determine the hydrodynamic size, Polydispersity Index (PDi) and Zeta Potential (ζ-potential) of the IHFE-AgNPs. The IHFE-AgNPs samples were diluted in a 1:10 (v/v) ratio with sterile ddH_2O and then transferred into a 10 mm optical density square polystyrene cuvette. The IHFE-AgNPs samples were analysed at 25 °C and 90° angle using DLS. For ζ-potential measurements, 1 ml of the diluted IHFE-AgNPs sample was transferred into a disposable folded capillary cell and analysed at a voltage of 4 mV at 25 °C and 90° angle. The PDi gave an estimation of the average uniformity of the nanoparticles formed and the ζ-potential was used to determine the stability of the IHFE-AgNPs in colloidal substances.

2.2.4.3 Fourier transform infrared spectroscopy (FTIR) analysis

FTIR was conducted at the Chemistry department, UWC Bellville. The analysis was performed to identify the biomolecules responsible for reducing, capping, and stabilizing the IHFE-AgNPs. 20 µl of IHFE-AgNPs was mixed with potassium bromide (KBr) on a filter paper; the mixture was then pressed into a pellet preceding FTIR analysis. The background correction was done using a reference blank KBr pellet. All the samples were analysed between 4000cm^{-1} and 400cm^{-1} wavenumber using the PerkinElmer spectrum two spectrometers FTIR instrument. The data was analysed using OriginPro 8 software.

2.2.4.4 High resolution transmission electron microscopy (HR-TEM) analysis

HR-TEM was used to analyse the morphological and structural features of the biosynthesised AgNPs. The core size of the IHFE AgNPs was determined using OriginPro 8 and ImageJ analysis software (National Institute of Health, USA). To prepare the samples, one drop of the IHFE-AgNPs was placed onto a carbon-coated copper grid and allowed to dry for 10 min under a xenon lamp prior to analysis. The samples were viewed using an FEI Tecnai G2 20 field-emission gun HR-TEM microscope at the University of Cape Town (UCT). The microscope was operated in a bright field mode at an accelerating voltage of 200 kV.

2.2.5 Stability test of the IHFE-AgNPs in biological media

The *in vitro* stability of the IHFE-AgNPs was evaluated in various biological media (water, 1× phosphate buffered saline (PBS), Mueller-Hinton Broth (MHB), complete Dulbecco's modified eagle medium (DMEM) and non-complete DMEM over 24 hrs. In a 1.5 ml Eppendorf tube, IHFE-AgNPs was mixed in a 1:2 (v/v) ratio in a final volume of 1 ml with the different media. The samples were incubated at 37 °C for 24hrs. The stability of the biosynthesised AgNPs was determined by observing the changes in the UV–vis spectra using the POLARstar Omega microplate reader, after incubation in the different media at 0, 1, 3, 6, 12 and 24 hrs. This was done in triplicate.

2.2.6 Antibacterial activity determination

2.2.6.1 Bacterial strain and MacFarland standardization

Antibacterial potential of the IHFE and IHFE- AgNPs was tested against the following bacteria: *S. aureus,* MRSA, *K. pneumoniae*, *A. baumannii*, *P. aeruginosa*, *E. Cloacae*, and *E. coli*. The bacterial cultures were purchased from ATCC and used for the testing of the antibacterial activity of the IHFE and IHFE-AgNPs.

MacFarland turbidity standard was used for the standardization of the antimicrobial tests that were performed according the method described by (Balouiri et al., 2016) with modifications. Bacterial strains were each streaked onto Mueller Hinton agar (MHA) plates and incubated at 37 °C for 24 hrs. Single colonies from the different bacterial cultures were inoculated in 2 ml of Mueller Hinton broth (MHB) and incubated for 1 hr at 37 °C in a shaking incubator at 200 rpm. The bacterial cultures were adjusted to 0.5 McFarland standard at OD_{600nm} of 0.08 to 0.12.

2.2.6.2 Agar well diffusion assay

The agar well diffusion assay was used to investigate the antibacterial activity of the IHFE-AgNPs. This assay was performed according to the method previously described by Dube et al. (2020) with modifications. Using sterile cotton swabs, the different bacterial cultures at 0.5 McFarland turbidity standard were evenly spread on Mueller Hinton agar (MHA). Additionally, five wells of 6 mm diameter were made into the MHA plates using a sterile P200 pipette tip. IHFE-AgNPs and IHFE (50 µl) was added into separate wells. For the positive control, 50 µl of 15 µg/ml ciprofloxacin was added into the wells for all the strains except for *E. coli* where 10 µg/ml ciprofloxacin was used. 50 µl of MHB was added into the well and served as a negative control, The plates were allowed to dry prior to incubation at 37 °C for 24 hrs. The experiment was done in triplicate. After incubation, the antibacterial activities of the IHFE-AgNPs were assessed by formation of a clear zone (or zone of inhibition) around the wells. The clear zones were measure using a vernier calliper.

2.2.6.3 Micro-dilution assay

The micro-dilution assay was performed following the method described by (Bariş et al., 2006)with modifications. MHB was used to dilute the bacterial suspensions and as a negative control. Furthermore, ciprofloxacin was used as a positive control.

2.2.6.3.1 Minimum inhibitory concentration (MIC)

Micro-dilution assay was used to determine the minimal inhibitory concentrations (MIC) of IHFE-AgNPs which is the lowest concentration that inhibits visible growth of bacteria. A colony

of each bacterial strain was mixed with MHB, and the suspensions were adjusted to 0.5 McFarland turbidity standard as described in section 2.2.6.1. Following this step, 1: 150 (v/v) dilutions were done using fresh MHB before the experiment. Serial dilutions of the biosynthesised-AgNPs (100, 50, 25, 12.5, 6.25, 3.125, 1.56 and 0.78 µg/ml) were prepared. In 96 well Greiner plate, 50 µl of IHFE was mixed with 50 µl of the bacterial suspensions, and the same was done with IHFE-AgNPs at each concentration. 50 µl MHB served as the negative control, and 50 µl of 15 µg/ml ciprofloxacin served as the positive control, with the exclusion of *E. coli* where 10 µg/ml was added. The plates were then covered with foil and incubated at 37 °C for 24 hrs. After incubation, AlamarBlue™ dye (10 µl) was added to each well followed by incubation for 4 hrs in the dark. AlamarBlue™ (resazurin) is non-fluorescent which is reduced to resofurin, a pink compound that is highly fluorescent in the presence of viable bacteria. Therefore, the intensity of the pink colour and the fluorescence is proportional to the number of viable cells present. The MIC was determined using a spectrophotometer (POLARstar Omega microplate reader) at an absorbance of 600 nm and a fluorescence excitation/emission wavelength of 530-560/590 nm. The experiment was performed in triplicate.

2.2.6.3.2 Minimum bactericidal concentration (MBC)

The MBC was determined by sub-culturing on MHA a loopful of the mixture of bacterial cultures treated with IHFE-AgNPs and IHFE from the wells which did not show bacterial growth (wells that did not turn pink) during the MIC experiment. The plates were incubated at 37°C for 24 hrs. The MBC was recorded as the lowest concentration of IHFE-AgNPs that showed no growth on the plates. The experiment was performed in triplicate.

2.2.7 Phytochemical profiling and Antioxidant activity analysis

2.2.7.1 Total phenolic content (TPC)

The TPC of IHFE and IHFE-AgNPs was determined by the Folin-Ciocalteu assay using Gallic acid as the standard following the method described by (Alirezalu et al., 2020). Different concentrations of gallic acid (15.6, 31.25, 62.5, 125, 250, 500 µg/ml) were prepared. Furthermore, into a 96 well Greiner plate, 20 µL of IHFE, IHFE-AgNPs and gallic acid standards

were added in their respective wells. Afterward, 100 µl of 10% Folin–Ciocalteu reagent (FC) was added into each well, then incubated for 5 min. Following this, 80 µl of 7.5% aqueous Na_2CO_3 was placed into the wells and incubated for 30 min at room temperature. The TPC was measured using a spectrophotometer (POLARstar Omega microplate reader) at a wavelength of 765 nm and was expressed in terms of gallic acid equivalent (µg GAE/ml). The concentration of phenols in the samples was derived from the standard curve of gallic acid standards. The experiment was done in triplicate.

2.2.7.2 Antioxidant studies

2.2.7.2.1 2,2'-azino-di-(3-ethylbenzthiazoline sulfonic acid (ABTS) scavenging assay

The antioxidant ability of IHFE and IHFE-AgNPs was determined using the ABTS (2,2'-azino-di-(3-ethylbenzthiazoline sulfonic acid) assay. This assay was performed following the method used by (Re et al., 1999) with modifications. 7 mM of ABTS was made in deionised water and mixed with 2.45 mM of $K_2S_2O_8$ in a 1:1 ratio; the mixture was covered in foil and kept in the dark at room temperature for 12- 16 hrs until a blue green colour was produced. The blue green coloured ABTS solution was adjusted to an absorbance of 0.70 at 734 nm by diluting with ethanol. Different concentrations of aqueous IHFE, IHFE-AgNPs and the standard ascorbic acid were made. In a 96 well Greiner plate, 20 µl of IHFE, IHFE-AgNPs and ascorbic acid standard was mixed with 200 µl of ABTS. The plate was then incubated in the dark for 6 min at room temperature and the samples were read at of 734 nm. The ABTS radical scavenging calculation was calculated using **equation 2.**

Equation 2: Radical scavenging (%) = $\frac{OD\ blank - OD\ sample}{OD\ blank} \times 100$

2.2.7.2.2 2,2-diphenyl-1-picrylhydrazyl (DPPH) scavenging assay

DPPH scavenging assay was used to calculate the total antioxidant content of the IHFE and IHFE-AgNPs. This assay was performed using the method described by (Khorrami et al., 2018). In a typical procedure, 100 µl of DPPH solution (0.25 mM in methanol) was transferred to each well of a 96-well plate. Subsequently, different concentrations of IHFE, IHFE-AgNPs and ascorbic acid

(5–400 µg/ml) were added to each well. The plate was incubated in the dark for 1–2 hrs at room temperature. The UV-Vis spectra of the samples were measured at 517 nm. The percentage radical scavenging activity calculated using the same equation as ABTS (**Equation 2)**

2.2.7.2.3 Ferric reducing antioxidant power (FRAP) scavenging assay

This method was used to assess the reducing ability of antioxidants from ferric ion (Fe^{3+}) to ferrous ion Fe^{2+}. The ferric reducing capacity of IHFE and IHFE-AgNPs was determined according to the method described by Benzie and Strain (1996) (Benzie and Strain, 1996). To prepare the FRAP reagent, 10 ml of acetate buffer (300 mM) was mixed with 1 ml of 2, 4, 6-tripyridyl-Striazine (TPTZ) (10 mM) and 1 ml of ferric chloride hexahydrate (20 mM $FeCl_3.6H_2O$). Subsequently, 10 µl of the samples IHFE, IHFE-AgNPs and the standard (ascorbic acid) were mixed with 300 µl of the FRAP solution in a 96 well Greiner plate; the mixture was incubated in the dark for 30 min. The absorbance readings were measure at 593 nm using a spectrophotometer. A calibration curve was plotted using ferrous sulphate ($FeSO_4.7H_2O$) and the absorbance of the samples were compared to the calibration curve. The values were expressed as µg/ml $FeSO_4.7H_2O$ equivalent.

2.2.8 Cytotoxicity study

2.2.8.1 Cell culture and maintenance

KMST-6 cells were purchased from ATCC. The frozen stocks in cryovials were allowed to thaw, then transferred to a 15 ml conical tube filled with cold 5 ml DMEM supplemented with 10 % Fetal bovine serum (FBS) and 1 % Penicillin/ Streptomycin. Subsequently, the mixture was centrifuged at 3000 rpm for 5 min using a E-C4.5-6.50 CP centrifuge. Afterward, the supernatant was discarded and the pellet was resuspended in 5 ml of pre-warmed DMEM media; which was then transferred into a T25 cell culture flask. The flasks were incubated at 37 °C in a Forma series II Water Jacketed CO_2 incubator. The cells were frequently monitored on an Evos XL Core inverted microscope to assess their growth; and the media was replaced every 2 to 3 days as required.

2.2.8.2 Trypsinization of cells

Once the cells have reached 70-80 % confluence, trypsin was used to detach adherent cells from the T25 flask. The media was removed from the flask and the cells were washed with 2-5 ml of 1 X PBS. 2 ml of 2 X trypsin was added and the flask was incubated at 37 °C. The cells were observed using Evos XL Core inverted microscope at 2-5 min intervals to check if the cells were detached. To stop the trypsinization process, 5 ml of growth medium was added. This mixture was transferred into a 15 ml tube and subjected to centrifuged for 5 min at 3000 rpm. The pellet was resuspended in 1-2 ml of complete media.

2.2.8.3 Cryo-preservation of cells

The cells were trypsinised as described in section 2.2.8.2. and resuspended in in DMEM containing 10 % DMSO. Afterward, 1.5 ml of the mixture was aliquoted into 2 ml labelled cryovials and stored at - 80 °C.

2.2.8.4 Cell count

Following the trypsinization process described in section 2.2.8.2, 10 µl of the resuspended cells was mixed with 10 µl trypan blue (a dye that aid in the identification and counting of live or dead cells). Afterward, 10 µl of the mixture was added into a Countess cell counting chamber slide and the cells were counted. After the total number of cells was counted, the cells were diluted with complete DMEM to obtain the ideal cell density to be used for further analysis.

2.2.8.5 Water soluble Tetrazolium salt (WST-1) protocol: cell viability assay

The cytotoxicity of the IHFE and IHFE-AgNPs was assessed on non-cancerous human fibroblast (KMST-6) cells using the water-soluble Tetrazolium salt or WST-1 assay following the manufacturer's instructions (Roche). The cells were seeded in 96 well Greiner plates at a cell density of 1×10^5 cells/ml and 100 µl of the cell suspension per well. The plates were incubated

for 24 hrs at 37 °C. After 24 hours, the cells were treated with various concentrations of IHFE and IHFE-AgNPs (0.78 µg/ml - 100 µg/ml-). The positive control was a mixture of DMSO and DMEM media in a 1:9 (v/v) ratio. Untreated cells (DMEM plus WST-1) were used as a negative control. The treatments were removed and the cells were washed thrice with 1 X PBS. Subsequently, 100 µl of DMEM containing 10 % WST-1 reagent was added into all wells except the interference wells in which only 100 µl complete media was added. The plate was covered with foil and incubated at 37 °C for 3 hrs and the absorbance was read at 440 nm with a reference wavelength of 630 nm. The percentage (%) cell viability was calculated using **Equation 3**:

Equation 3: Cell viability (%) = $\frac{\text{Test absorbance at 440 nm} - \text{Absorbance at 630 nm}}{\text{Negative control absorbance at 440 nm} - \text{Absorbance at 630 nm}} \times 100$

2.2.9 Statistical analysis

Statistical analysis of the data was performed using the GraphPad Prism6 software and One-way ANOVA test. Multiple-comparison analyses were performed within each group of the assays in this study. All the assays were performed in triplicates and the data were expressed as the mean ± standard error of the mean (SEM) of the three replicates. Statistical significance was indicated as * for $p < 0.05$, ** p for < 0.01, *** $p < 0.001$ and **** for $p < 0.0001$.

Chapter 3: Results and Discussion

Green synthesis of MNPs has gained significant interest in recent years and offers various advantages which are desirable for biomedical applications. Due to the use of biological entities such as plant materials (i.e fruit extracts and leaf extracts), this approach has been recognised as rapid, cost-effective, eco-friendly and sustainable to synthesise NPs (Samuel et al., 2022, Simon et al., 2022). Additionally, plant extracts contain phytochemicals which provide reducing agents which contributes to a rapid synthesis time as well as natural capping agents for the stabilisation of NPs (Gahlawat and Choudhury, 2019, Samuel et al., 2022). Phytochemicals such as flavonoids and oligomeric proantho-cyanidins, which are abundant in the berries from Indian Hawthorn have been used as herbal medicine to treat several diseases (Singh et al., 2018), and their activities were enhanced when used in green synthesis. MNPs synthesised using this approach have been reported to display enhanced biological activities prompting their application in drug delivery, targeted therapy and diagnostics (Khan et al., 2017). AgNPs have played several roles in therapeutics as antibacterial, antifungal, antioxidant and anti-inflammatory agents. And as antioxidants, green synthesised AgNPs offer great potential in the treatment and prevention of ailments caused by excessive ROS (Mohammad et al., 2008, Lushchak et al., 2018).

This study focused on the synthesis of biogenic IHFE-AgNPs using a green nanotechnology approach and evaluation of their antimicrobial and antioxidant activities. Green synthesis of AgNPs was performed using an aqueous berry extract (IHFE) and the synthesised IHFE-AgNPs were characterised using UV-Vis spectroscopy, DLS, ζ-potential, HR-TEM and FTIR. The stability of the IHFE-AgNPs was investigated in biological media. The *in vitro* antibacterial properties of the biosynthesised IHFE-AgNPs were assessed against *S. aureus,* MRSA*, K. pneumoniae, A. baumannii, P. aeruginosa, E. coli and E. cloacae* using agar well diffusion and microdilution assay to determine the MIC and MBC of the IHFE-AgNPs. The antioxidant scavenging abilities effects of IHFE-AgNPs were also tested using DPPH, ABTS and FRAP antioxidant assays, and their biocompatibility was studied using the WST-1 cell viability assay.

3.1 Synthesis and optimisation of AgNPs using IHFE (Indian Hawthorn fruit extract)

3.1.1 Optical properties of the synthesised IHFE-AgNPs

Using a green synthesis approach, AgNPs were synthesised from IHFE as described in Section 2.2.2. During the synthesis, a peach coloured IHFE was used as the reducing and stabilising agent which when mixed with a clear solution of $AgNO_3$ resulted in a yellowish-brown colour solution indicative of IHFE-AgNPs formation (Figure 3.1). This colour change was due to the excitation of the surface plasmon resonance (SPR) of AgNPs (Thakur and Reddy, 2017, Tyavambiza et al., 2021). This is explained by a collective oscillation of electrons of AgNPs which interacts with light waves generating a unique SPR absorption peak around 400 nm (Amendola et al., 2010). The visual colour change confirmed the formation of AgNPs and that the phytochemical found in the IHFE could reduce Ag^+ ions to Ag^0. This observation was in accordance with a previously reported studies, in which a colour change has been observed which confirmed the formation of AgNPs (Dube et al., 2020).

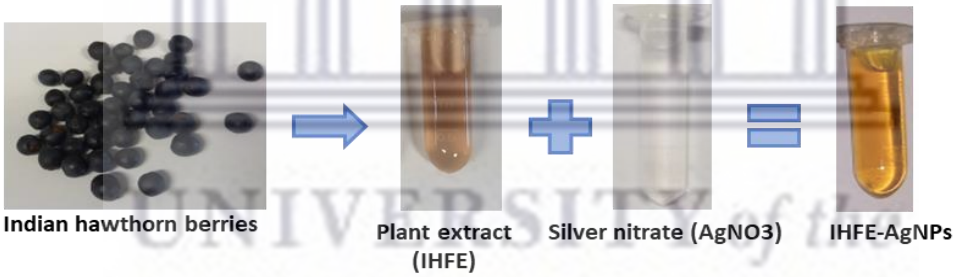

Figure 3. 1 Schematic of the green synthesis of Indian Hawthorn fruit extract biosynthesised silver nanoparticles (IHFE-AgNPS)

3.1.2 Optimisation of the IHFE-AgNPs synthesis

The synthesis of IHFE-AgNPs from IHFE were optimised by adjusting various reaction parameters such as pH, temperature, extract concentration and $AgNO_3$ concentration. These conditions are fundamental for a successful synthesis as they influence the physicochemical characteristics of the NPs which consequently have an impact on their downstream applications (Zaidi et al., 2017). The formation of IHFE-AgNPs was further confirmed by monitoring the colour change and SPR peak characteristics of AgNPs using UV-Vis spectroscopy. UV-Vis is a fast, simple and delicate

technique which can be used to evaluate the stability as well as the optical characteristics of AgNPs (Silva et al., 2019). Generally, AgNPs exhibit a SPR band in the range of 400-500 nm (Dube et al., 2020). However, it is important to note that the SPR is dependent on the size, shape and the state of aggregation of AgNPs (Silva et al., 2019). Different parameters were optimised to determine optimal conditions for synthesis of IHFE-AgNPs using UV-Vis spectroscopy (Bhattacharjee, 2016).

3.1.2.1.1 Effect of temperature vs pH on IHFE-AgNPs synthesis

The bio-reduction of AgNPs was observed with a colour change from clear to yellowish-brown followed by the SPR analysis shown in Figure 3.2. The colour of the synthesised IHFE-AgNPs was dependent on the pH which is responsible for the various size, shape and reduction rate (Liaqat et al., 2022). The colour changed observed during synthesis of IHFE-AgNPs, correlated with the UV-Vis spectra indicating successful formation of IHFE-AgNPs. A sharp or narrow peak indicated that AgNPs are likely to be monodispersed as opposed to a broader peak which indicates polydispersity of the NPs (Ndikau et al., 2017).

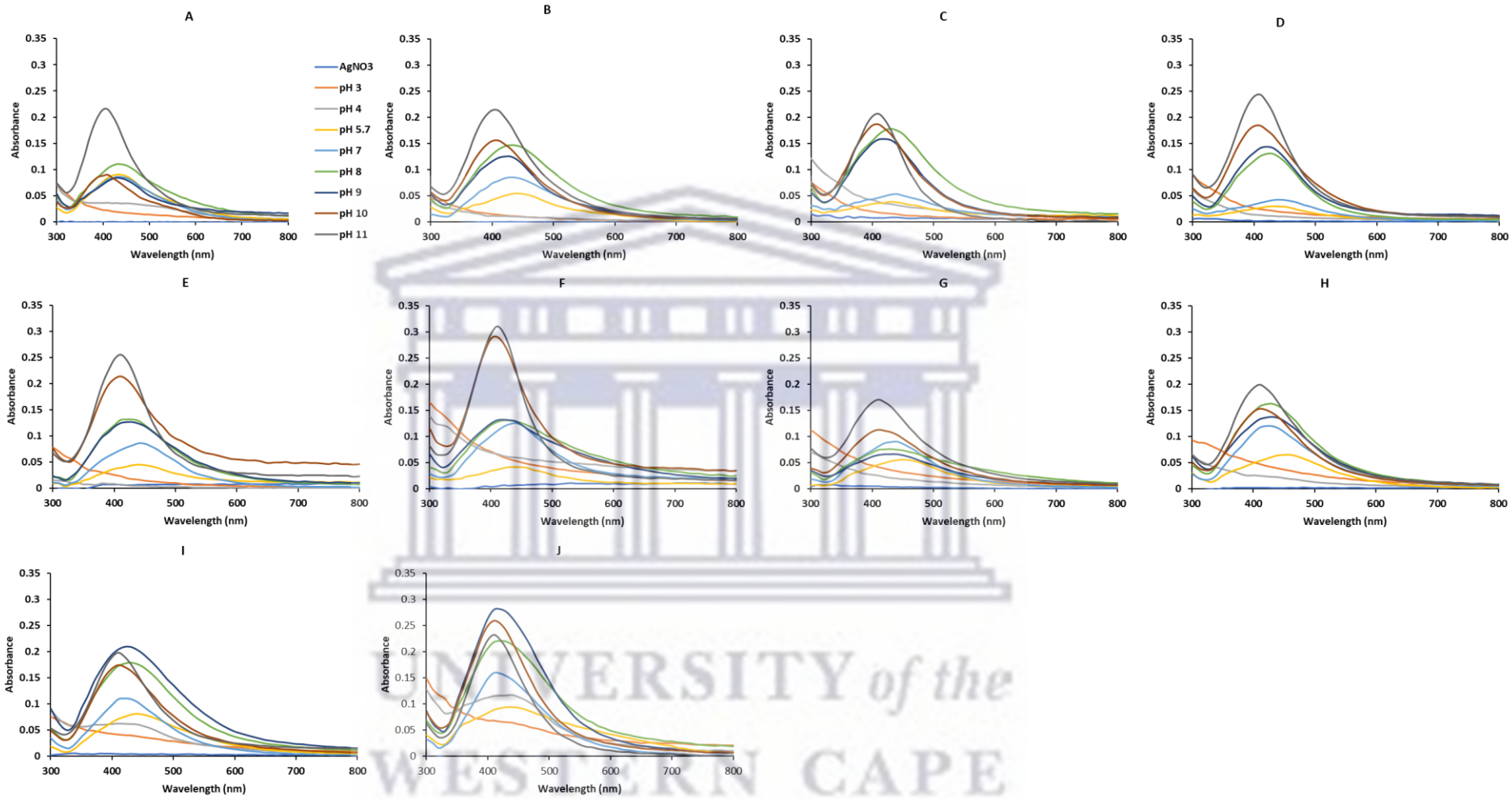

Figure 3. 2 UV-Vis spectra of Indian Hawthorn fruit extract biosynthesised silver nanoparticles (IHFE-AgNPs) showing the effect of different pH and temperatures. A: 25°C, B: 25 °C not mixed; C: 45 °C, D: 50 °C, E: 55 °C, F: 60 °C: G: 70 °C, H: 80 °C, I: 90 °C and J: 99°C. The [$AgNO_3$] and [IHFE] used were 1 mM and 12.5 mg/ml respectively.

The UV-vis spectra in Figure 3.2 (A-I) shows that IHFE-AgNPs synthesised at basic pH (8,9, 10 and 11) exhibited more distinct peaks; and no synthesis was observed at lower acidic pH (3 and 4). This is in agreement with Tarannum et al., 2019, who stated that synthesis at basic pH is more favourable than at acidic pH which produces unstable NPs (Tarannum et al., 2019). This is because at acidic pH, the biomolecules from the plant extract may have been protonated by H^+ from HCl, causing aggregation of NPs (Ndikau et al., 2017, Pal et al., 2019). Furthermore, at higher temperatures and pH, the peaks became well defined.

There was no significant bio-reduction of Ag^+ to Ag^0 observed for pH 3 and pH 4 at 25 °C as no SPR peaks were observed on the UV-Vis spectra (Figure 3.2 A), this was also associated with no colour change in the reaction. This observation has been previously reported in the study performed by Simon et al., 2021, pear fruit extract did not synthesize AgNPs at lower acidic pH 4 and 5 (Simon et al., 2021). At pH 5.7 which is the natural pH of the IHFE, a broad peak was formed which corresponds to agglomeration of the IHFE-AgNPs (Ndikau et al., 2017). At pH 7 to 10, IHFE-AgNPs were formed, the absorbance peaks were broad and red shifted (except for pH 10 which was blue shifted) indicating polydispersed IHFE-AgNPs. Furthermore, pH 11 displayed a narrow absorbance peak and was blue shifted. According to literature, a blue shift with a sharp or narrow absorbance peak corresponds to smaller AgNPs (Ndikau et al., 2017). IHFE-AgNPs formation occurred at 25 °C without shaking; here, the samples were incubated in the dark overnight. A similar trend observed in Figure 3.2 A can be seen for acidic pH as no spectra was formed. IHFE-AgNPs were formed at pH 5.7 to pH 9, however the absorbance peaks were broad and red shifted. There was a blue shift as the pH increased at pH 10 and 11, this indicated that the size of the IHFE-AgNPs became smaller as pH increased. It was evident that a longer incubation time allowed the formation of IHFE-AgNPs at low temperature.

IHFE-AgNPs formation at 45 °C, 50 °C and 55 °C followed a similar trend. There were no absorbance peaks at pH 3 and 4 indicating that no biosynthesis took place. Broader peaks were observed at pH 5.7 and pH 7 with lower yield. Higher yields of IHFE-AgNPs were observed from pH 8 to 11 with pH 8 and 9 being red shifted. A blue shift coupled with narrow peaks were observed for pH 10 and pH 11; with the latest displaying higher yield of IHFE-AgNPs. According

to literature, the absorbance correlates to the concentration of NPs in solution (Tyavambiza et al., 2021). Therefore, at pH 11 more IHFE-AgNPs were synthesised.

IHFE-AgNPs synthesis at 60 °C did not form at pH 3 and 4 (Figures 3.2 F), this could be due to the protonation of phytochemicals under acidic conditions, which prevented conversion of Ag^+ ions into AgNPs (Omran *et al.*, 2018). Broadening of peaks coupled with red shift were observed from pH 5.7 to pH 9, in higher or basic pH (pH 10 and 11), more intense and narrow peaks were observed with a blue shift. This phenomenon is associated with formation of smaller IHFE-AgNPs. With increase in the pH, a large number of functional groups are available facilitating higher number of Ag^+ to bind and later form a large number of NPs (Ndikau et al., 2017, Kumar et al., 2019). Furthermore, at this temperature, IHFE-AgNPs at pH 10 and 11 showed the highest yield with OD value of 0.29 and 0.31, respectively.

At 70 °C and 80 °C, IHFE-AgNPs were successfully synthesised at all pH except for pH 3 and 4 (Figures 3.2 G and H). Broadening of peaks were observed from pH 5.7 to pH 11; with the highest OD value of 0.17 at pH 11. A decrease in OD value was observed at 70 °C as opposed to the increase in absorbance seen at lower temperatures (25 - 60 °C). Although higher temperatures are known to facilitate the synthesis of NPs, it has been shown that NPs synthesised using certain plant extracts require heat activation but only to some extent, this is because certain phytochemicals in plant extracts become inactive at higher temperatures (Liaqat et al., 2022, Madiehe et al., 2022).

Synthesis of IHFE-AgNPs at 90 °C and 99 °C displayed no synthesis at pH 3 as shown in Figures 3.2 I and J. Broad SPR peaks were observed from pH 4 which indicated polydispersity. High yield of IHFE-AgNPs was observed at pH 9, ideal synthesis of IHFE-AgNPs was observed at pH 10 and 11.

Overall, the synthesis of IHFE-AgNPs was observed at all temperatures starting at the natural pH of the IHFE (pH 5.7). Previous studies reported that lower pH hardly synthesised AgNPs. AgNPs synthesised from *Crataegus douglasii* fruit extract confirmed that acidic pH does not favour formation of AgNPs (Ghaffari-Moghaddam and Hadi-Dabanlou, 2014). Synthesis of IHFE-AgNPs was observed from pH 5.7 to pH 11, as hydroxide ions altered the charge on the NPs. More

functional groups are available to bind with Ag^{+}, resulting in a large number of NPs with smaller diameters (Ndikau et al., 2017). Therefore, based on the prior results, the optimum pH and temperature used for the synthesis were pH 11 and 60 °C.

3.1.2.1.2 Effect of IHFE concentration on IHFE-AgNPs synthesis

As shown in Figure 3.3, the reduction of Ag^{+} into Ag^{0} by IHFE and the formation of IHFE-AgNPs was observed at all plant concentrations by the UV-vis spectra. IHFE-AgNPs synthesised with 1.56 and 3.25 mg/ml IHFE had the lowest absorbance which could be due to the limited amounts of phytochemicals available to reduce Ag^{+} into Ag^{0}, thus leading to less NPs produced (Ngungeni et al., 2023). According to literature, at lower plant extract concentrations, a small number of nucleation sites are available which results in more reduction taking place at one nuclei leading to larger NPs which is indicated by broadening of the peak (Ndikau et al., 2017).

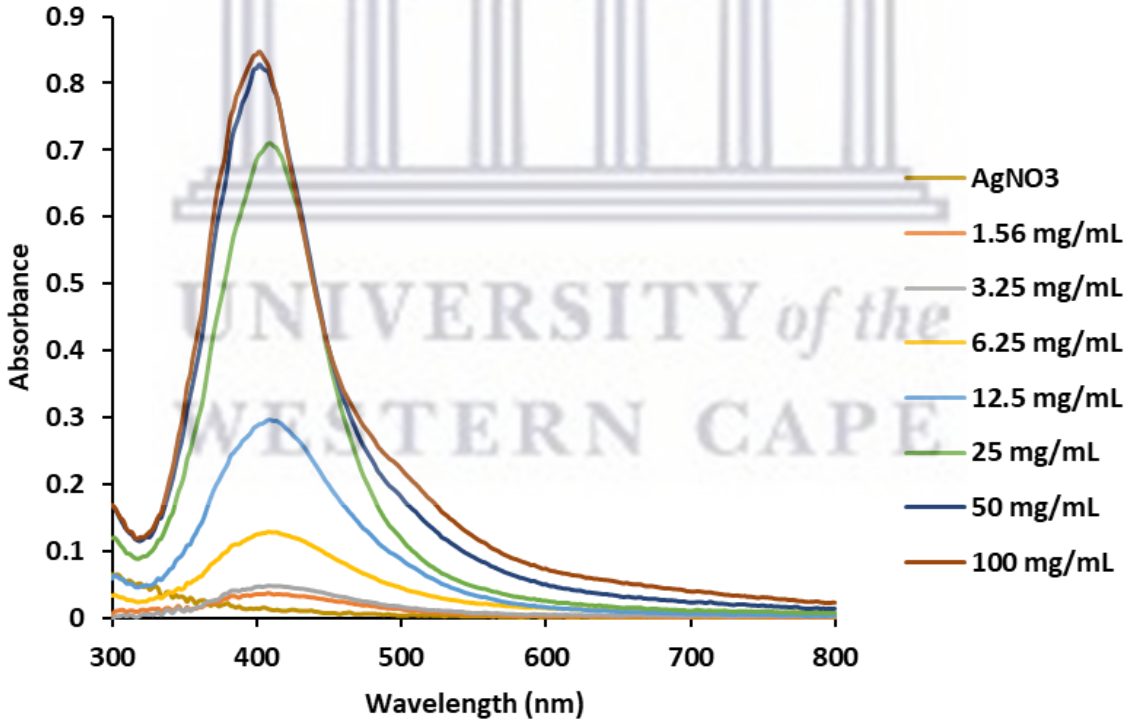

Figure 3. 3 UV-Vis spectra of the synthesis of Indian Hawthorn fruit extract biosynthesised silver nanoparticles (IHFE-AgNPs) showing the effect of varying IHFE concentrations.

The intensity of the absorption spectra increased with increase in concentrations of IHFE. At 100 mg/ml, IHFE-AgNPs were produced with a λ_{max} of 402 nm and an OD value of 0.847. This behaviour was reported in literature confirming that at extremely high plant extract concentrations, more phytochemicals are available to react with $AgNO_3$ which forms large NPs that absorbs light at higher wavelengths (Tyavambiza et al., 2021). Increasing yields of IHFE-AgNPs was observed at concentration from 6.125 mg/ml. When comparing λ_{max} values of 6.125, 12.5, 25 and 50 mg/ml, it can be observed that 50 mg/ml was blue shifted with λ_{max} of 402 nm suggesting that the NPs were smaller in size. This was followed by 25 mg/ml with λ_{max} of 410 nm indicating a red shift; 12.5 and 6.125 mg/ml were also red shifted with λ_{max} of 408 nm. At higher concentration of plant extract, more phytochemicals are available to reduce Ag^{+} ions to Ag^{0} providing enough capping agents for the stabilisation of IHFE-AgNPs and prevent aggregation (Ndikau et al., 2017).

Subsequently, to decide which concentration of the aqueous fruit extract should be used, DLS was performed on 50, 25 and 12.5 mg/ml. After performing DLS, the optimum concentration of the fruit extract used for the synthesis of IHFE-AgNPs was 12.50 mg/ml with a hydrodynamic size of 142.80 nm and a PDi value of 0.31 which indicated that the IHFE-AgNPs synthesised at this concentration were smaller in size and monodispersed compared to IHFE-AgNPs synthesised at 25 mg/ml and 50 mg/mL with a hydrodynamic size of 144.40 and 152.00 nm and PDi of 0.43 and 0.55, respectively (Table 3.1). The DLS results confirms that at extremely high plant extract concentrations (50 and 25 mg/ml), IHFE-AgNPs size were bigger and that they are polydisperse in the solution indicating that their sizes are not uniform compared to IHFE-AgNPs synthesised at low concentrations (12.5 mg/ml). Therefore, the optimum concentration of IHFE was determined to be 12.5 mg/ml.

Table 3. 1 Dynamic light scattering representing the hydrodynamic size and PDi of the IHFE-AgNPs synthesised using different IHFE concentrations (12.5 mg/ml, 25 mg/ml and 50 mg/ml).

IHFE concentrations (mg/ml)	Hydrodynamic size (nm)	PDi
12.5	142.80	0.31
25	144.40	0.43
50	152.00	0.55

The optimum IHFE is highlighted in blue.

3.1.2.1.3 Effect of IHFE concentration vs $AgNO_3$ (salt) concentration on IHFE-AgNPs synthesis

The concentration of the $AgNO_3$ was optimised using pH 11 IHFE at 12.5 mg/ml and 60 °C described in Sections 3.1.2.1.1 and 3.1.2.1.2. The effect of $AgNO_3$ concentration on the synthesis of IHFE-AgNP**s** is shown in Figure 3.4, synthesis of IHFE-AgNPs was observed at all the $AgNO_3$ concentrations. The results showed that the absorption peaks increase with an increase in $AgNO_3$ concentration. The SPR (λ_{max}) at 0.50 and 1 mM was 410 nm with absorbance values of 0.31 and 0.40, respectively. IHFE-AgNPs synthesised at 2, 3 and 5 mM were red shifted and had λ_{max} at 414 nm and 412 nm for 4 mM $AgNO_3$ as summarized in Table 3.2. At 0.50 and 1 mM the SPR peaks were narrower compared to higher $AgNO_3$ concentrations. The broad SPR peaks at higher concentrations suggested that the IHFE-AgNPs are polydisperse. These findings aligns with literature which confirmed that increasing the concentration of $AgNO_3$ influenced the rate of AgNPs formation (Simon et al., 2021), and produce larger AgNPs (Liaqat et al., 2022). The optimum $AgNO_3$ concentration was thus selected to be 1 mM as there was smaller size IHFE-AgNPs were produced.

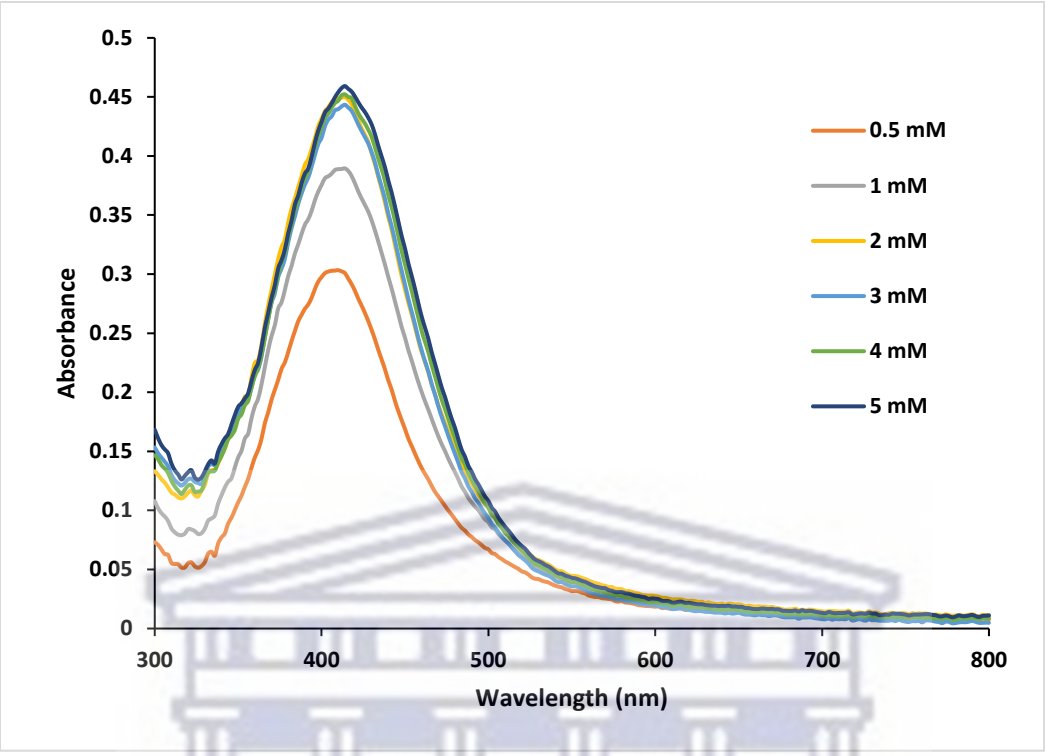

Figure 3. 4. UV-Vis spectra of Indian Hawthorn fruit extract biosynthesised silver nanoparticles (IHFE-AgNPs) showing the effect of varying $AgNO_3$ concentrations with [IHFE]: 12.5 mg/ml.

Table 3. 2 Effect of $AgNO_3$ concentration on the synthesis of IHFE-AgNPs.

[$AgNO_3$] (mM)	SPR (nm)	Abs(au)
0.5	410	0.31
1	410	0.40
2	414	0.46
3	414	0.46
4	412	0.47
5	414	0.49

The optimum $AgNO_3$ concentration was highlighted in blue.

3.1.2.1.4 Effect of reaction time on IHFE-AgNPs synthesis

The synthesis reaction time was assessed for a period of 720 min (12 hrs) using optimum conditions. Although a colour change was observed within a few seconds after addition of 12.5 mg/ml IHFE to 1 mM $AgNO_3$, formation of IHFE-AgNPs required more reaction time to be complete. Over a period of 720 min (12 hrs), the absorbance value of IHFE-AgNPs increased as

indicated in Figure 3.5. As the synthesis progressed over time, there was a rapid increase in the absorbance from 0.32 to 0.75 of IHFE-AgNPs between 0 to 300 min (5 hrs). As the reaction time increased, the absorbance increased and the synthesis of IHFE-AgNPs reached saturation at 300 min as there were no significant increase in the absorbance after this time point (Doan et al., 2020, Princy and Gopinath, 2018). This indicated that the synthesis was complete at 480 min as no further rise in the intensity of SPR was observed (Princy and Gopinath, 2018). As mentioned previously, the absorbance is directly proportional to the yield of AgNPs (Elbagory et al., 2016, Tyavambiza et al., 2021). Therefore, the results demonstrated that more IHFE-AgNPs were synthesised at 8 hrs (480 min) and chosen for the synthesis of IHFE-AgNPs.

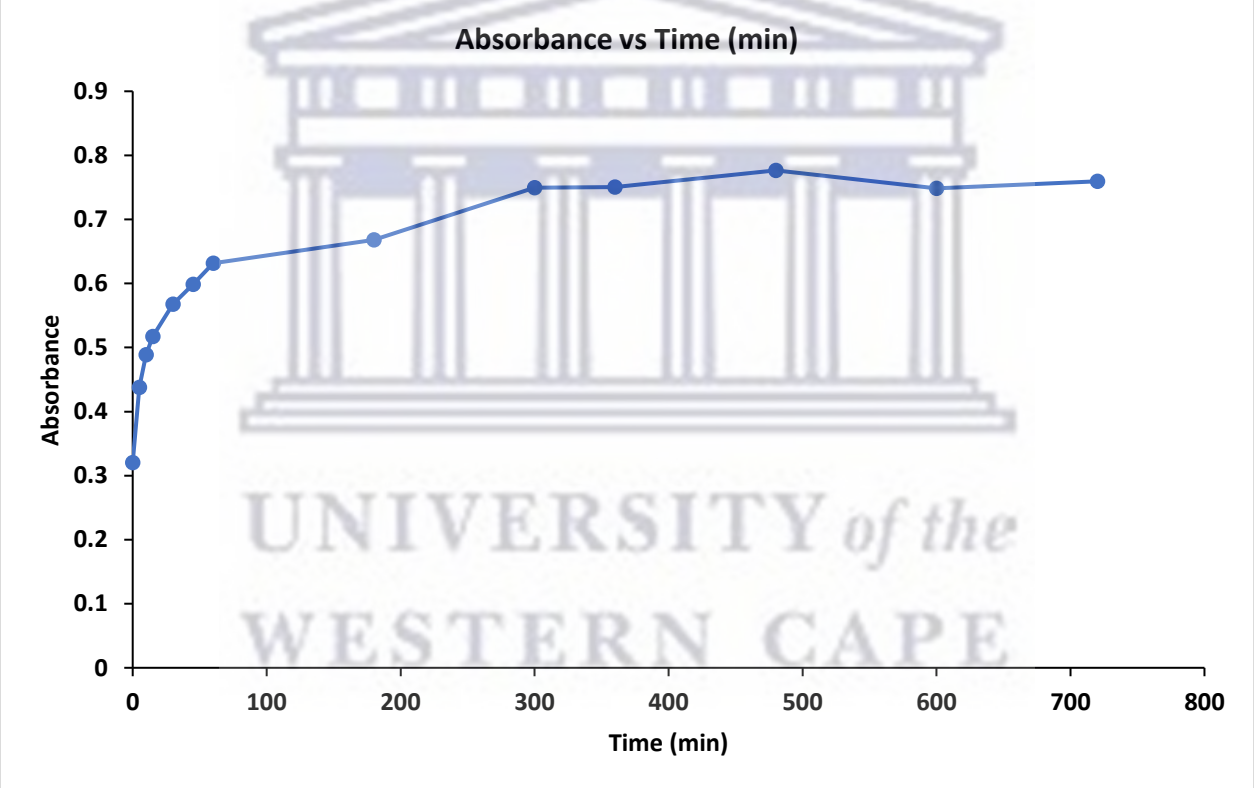

Figure 3. 5. UV-Vis spectra showing the effect of synthesis time on Indian Hawthorn fruit extract biosynthesised silver nanoparticles (IHFE-AgNPs) over a period of 720 min.

3.2 Large scale synthesis and characterisation of of IHFE-AgNPs using optimum conditions

Using the previously optimised conditions; i.e 1 mM $AgNO_3$, 12.5 mg/ml IHFE, 60 °C, pH 11 and 8 hrs, the reaction volume was upscaled from 2 ml to a final volume of 50 ml. The UV-vis

absorption spectrum of the IHFE-AgNPs is shown in Figure 3.6, with a SPR of 406 nm and OD of 0.824.

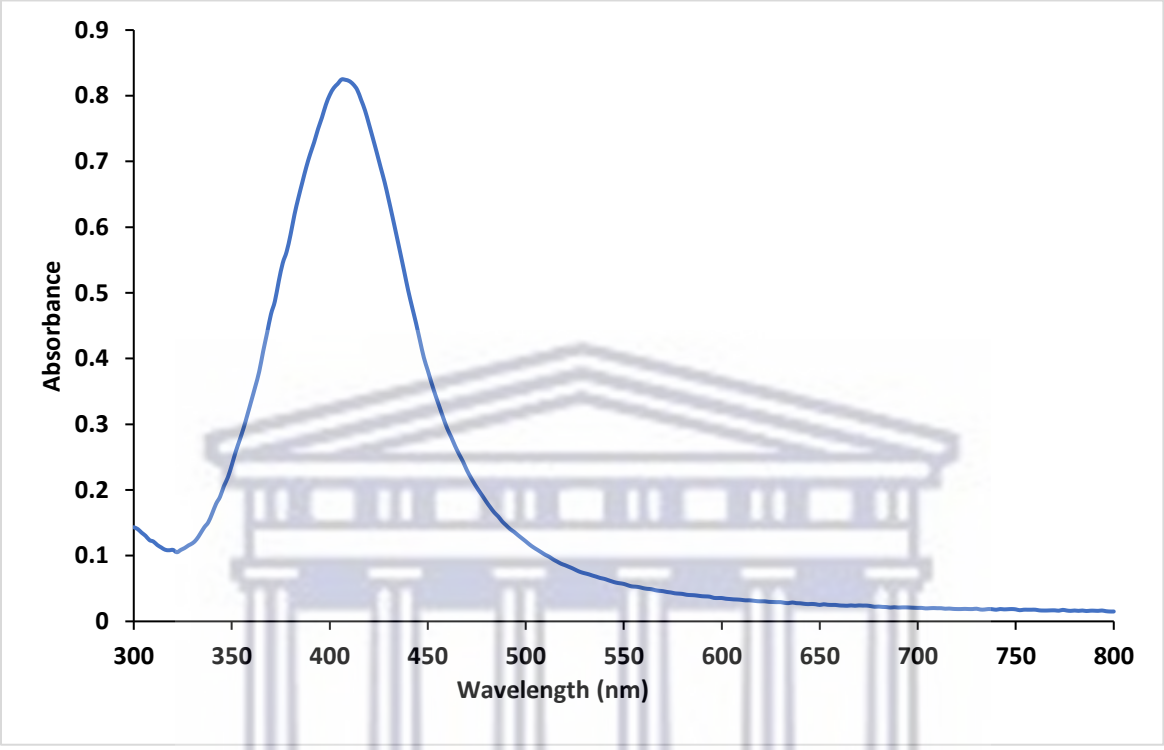

Figure 3. 6 UV-vis absorption spectra of the upscaled IHFE-AgNPs using optimum conditions. (IHFE concentration: 12.5 mg/ml, $AgNO_3$ concentration: 1 mM, temperature: 60 °C, pH 11, time of reaction: 8 hrs, shaking at 750 rpm).

Subsequently, DLS analyses were performed to determine the shape, hydrodynamic size, PDi and the ζ-potential of IHFE-AgNPs. The hydrodynamic size distribution indicated that 89.40 % of the IHFE-AgNPs had size of 123.60 ± 25.00 nm and 10.60 % had a hydrodynamic size of 16.69 ± 2.30 nm (Figure 3.7 A). The hydrodynamic size corresponds to the whole size of the NPs in colloidal suspension which takes into account the metal core size and the phytochemicals surrounding the surface of NPs (Mourdikoudis et al., 2018, Miranda et al., 2022).

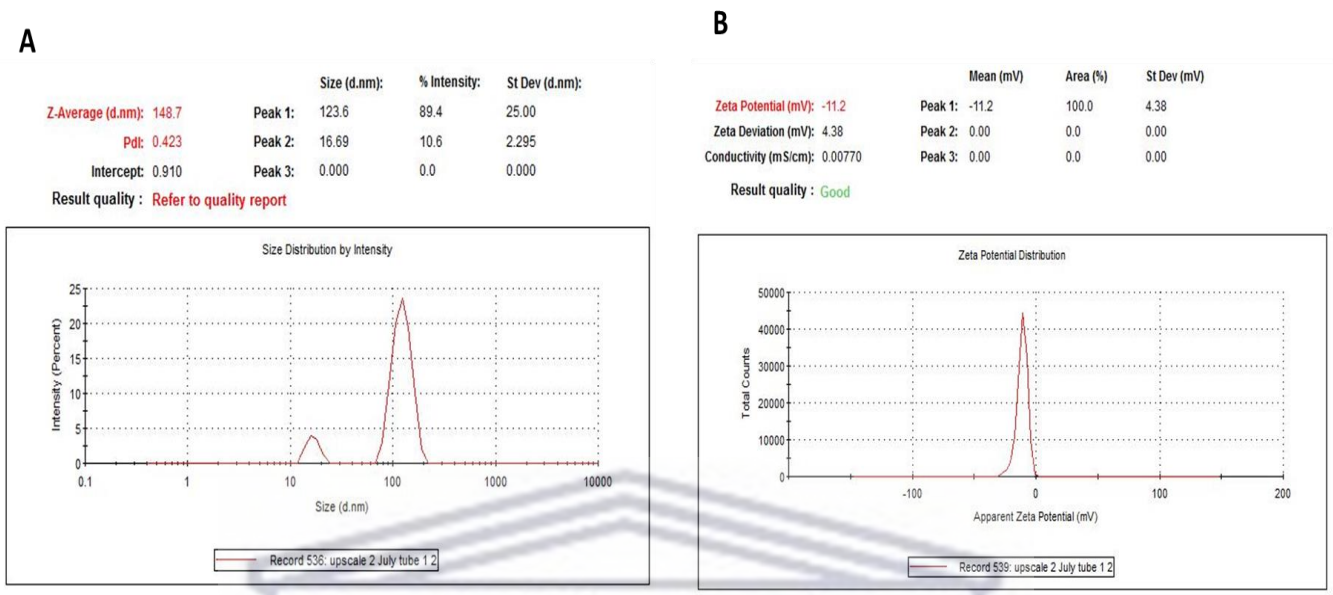

Figure 3. 7 DLS analyses of IHFE-AgNPs. (A) The Hydrodynamic size distribution, Pdi and (B) ζ-potential of the IHFE-AgNPs.

The Pdi measures the uniformity or homogeneity of the particles in colloidal suspension; with values ranging between 0 and 1 acceptable for downstream applications (Tyavambiza et al., 2021). NPs are considered monodispersed with similar size and shape when the Pdi value is between 0.01 and 0.50 (Tarannum et al., 2019), Pdi values higher than 0.70 are indicative of a broader size distribution (Mazzonello et al., 2017). Pdi of the IHFE-AgNPs was 0.423 (Figure 3.7 A) indicating that the NPs are slightly monodispersed. This corresponds to AgNPs synthesised using *E. camaldulensis* and *T. arjuna* with Pdi values of 0.399 indicating monodispersity (Liaqat et al., 2022). Another study reported polydisperse AgNPs from *Salvia Africana-lutea* and *Sutherlandia frutescens* aqueous extracts confirming that the phytochemicals composition of plants can affect the synthesis of AgNPs differently (Tyavambiza et al., 2021).

The surface charge of NPs was measured using the ζ-potential, defined as the electrical charge on the surface of NPs and determines the stability of the colloidal particles (Titus et al., 2019). The IHFE-AgNPs had an average ζ-potential of -11,20 ± 4.38 mV (Figure 3.7 B), which indicated that the IHFE-AgNPs were moderately stable while the negative charge indicated strong repulsive forces between the NPs preventing aggregation (Simon et al., 2021, Tyavambiza et al., 2021). NPs are considered neutral when ζ-potential is between -10 and + 10 mV; moreover, NPs

with values greater than +30 mV are strongly cationic and those with ζ-potential values less than -30 mV are known to strongly anionic (Clogston and Patri, 2011).

3.2.1 HRTEM analysis

HRTEM analysis was performed to determine the size and the morphology of the upscaled IHFE-AgNPs. The results obtained in this study confirmed that the IHFE-AgNPs were spherical in shape (Figure 3.8 A). These results were contrary to literature for biogenic AgNPs which are expected to have various size distribution and morphology due to the different phytochemicals present in plant extracts (Dube et al., 2020). Although some studies have reported on synthesis of well dispersed spherical AgNPs using *Atropa acuminata* (Rajput et al., 2020) and *Atropa belladonna* extracts (Das et al., 2019). Furthermore, from the HRTEM image, 108 individual NPs were selected to determine the average core size of the IHFE-AgNPs using ImageJ analysis. The core size distribution of the IHFE-AgNPs ranged from 5 to 14 nm (Figure 3.8 B) with an average core size diameter of 8.61 nm. As previously discussed, the hydrodynamic size from DLS analysis was larger than the core size because the hydrodynamic size considers molecules surrounding the organic layer of NPs. While the HRTEM analysis only accounts for the metal core size (Mourdikoudis et al., 2018, Saeb et al., 2014, Tyavambiza et al., 2021).

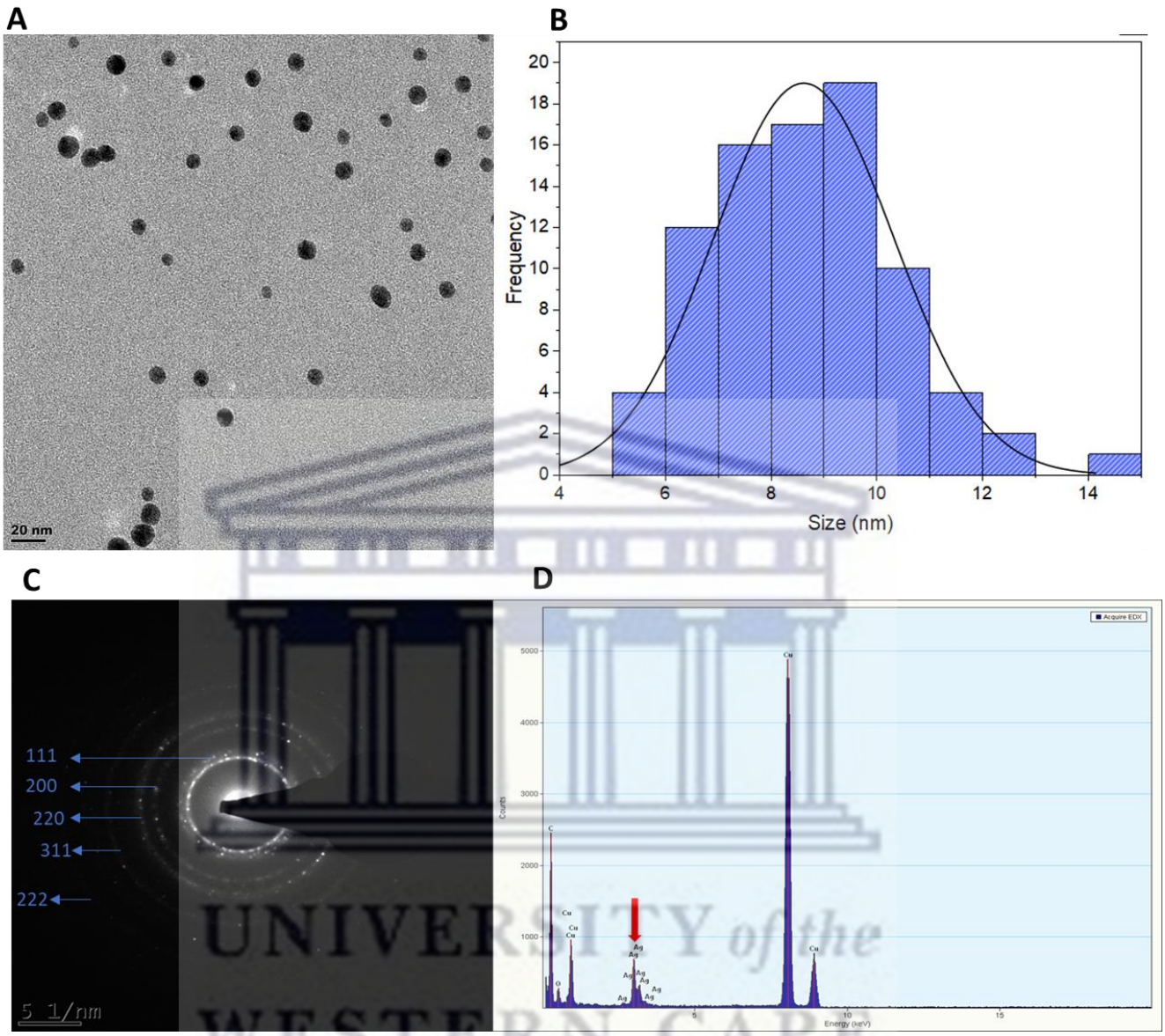

Figure 3. 8 HRTEM analysis of IHFE-AgNPs representing their shape and core size. (A) HRTEM images of IHFE-AgNPs at 20 nm resolution, (B) size distribution, (C) SAED pattern and (D) EDX spectrum of IHFE-AgNPs

The crystallinity of IHFE-AgNPs was determined by selected area electron diffraction (SAED) pattern shown in Figure 3.8 C, confirming the presence of the Miller indices at (111), (200), (220) and (311) in the IHFE-AgNPs corresponding to the face-centred cubic silver. The results concur with the patterns on *Atropa belladonna* AgNPs (Das et al., 2019, Elbahnasawy et al., 2021). The EDX spectrum shown in Figure 3.8 D, displays the elemental composition profile of

IHFE-AgNPs. The optical signal observed at 3 KeV corresponds to the presence of silver which display optical adsorption peak in this range (2.5 - 4 KeV) (Khan et al., 2013, Dube et al., 2020). Furthermore, adsorption peaks corresponding to copper, carbon and oxygen were observed which are from the copper grid used for HRTEM analysis; carbon and oxygen could be from plant extract present on the surfaces of NPs as capping agents (Khan et al., 2013).

3.2.2 Fourier-transform infrared (FTIR) of the IHFE and IHFE-AgNPs

To identify the different functional groups which are involved in the synthesis of the IHFE-AgNPs, FTIR analysis was performed on both the aqueous extract (IHFE) and the IHFE-AgNPs (Ngungeni et al., 2023). The absorption peaks/bands observed in the Infrared (IR) spectrum are equivalent to the frequencies of vibrations between the different atomic bonds in the NPs (Torres Rivero et al., 2021). The generated information can assist in identifying the phytochemicals that are involved in the bio reduction of $AgNO_3$, thus validating their relevance in the synthesis and capping of NPs (Dube et al., 2020). It is important to note that the IR spectrum consist of two main regions: a fingerprint region with functional groups between 1500- 600 cm^{-1} and a functional group region between 4000 - 1500 cm^{-1} (Dutta, 2017). The functional groups remain fairly constant in various samples which is not the case for the fingerprint region which contains functional groups that are exclusive to each sample, hence, it is unlikely that two compounds generate the same IR spectrum (Dutta, 2017).

The FTIR spectra of the IHFE and IHFE-AgNPs in Figure 3.9 displayed similar peaks between IHFE when compared to IHFE-AgNPs, whilst some peaks were slightly shifted indicating the presence of residual plant extract as a capping agent in the synthesis of IHFE-AgNPs (Table 3.3). A strong and broad peak was observed at 3367.26 cm^{-1} in the IHFE and was slightly shifted to 3368.67 cm^{-1} in the IHFE-AgNPs; this could be assigned to O-H or N-H stretching vibrations which indicate the presence of phenols, alcohols, carboxylic acids as well as primary and secondary amines (Dube et al., 2020). A similar band of 3261.15 cm^{-1} was observed in the IR spectrum of *Crataegus Oxyacanthus* which is a related species of Hawthorn; this band could be attributed to the presence of phenolic compounds (Omer et al., 2021). Additionally, a weak band was observed at 2082.11 cm^{-1} for IHFE and 2079.01 cm^{-1} for IHFE-AgNPs, this was assigned to C≡C stretching

vibrations corresponding to the presence of alkynes (Ngungeni et al., 2023). A strong sharp absorption peak was observed at 1638.15 and 1638.85 cm^{-1} in the IHFE and IHFE-AgNPs, respectively; this was assigned to bending vibrations of amide-I bond (NH-C=O) which could correspond to the presence of primary amine groups (Madiehe et al., 2022, Ngungeni et al., 2023). The respective peaks observed at 1400.86 and 1400.66 cm^{-1} for IHFE and IHFE-AgNPs were assigned to O-H bending vibrations which are associated to polyphenols (Madiehe et al., 2022). The absorption peaks at 1034.40 cm^{-1} in the IHFE which was shifted to 1031.79 cm^{-1} in the IHFE-AgNPs could be assigned to C-N vibrations corresponding to aromatic amines and C-O stretch corresponding to ether (Das et al., 2019). Lastly, the IHFE showed an absorption peak at 684.95 cm^{-1} which was shifted to 679.48 cm^{-1} in the IHFE-AgNPs, this band could be assigned to a C-Br stretch corresponding to alkyl halides and aliphatic bromo compounds. A previous study reported the presence of phenolic compounds, flavonoids, terpenoids and carbohydrates which were associated with the C-O and O-H stretching vibrations; thus confirming the involvement of phytochemicals in the capping and stabilization of IHFE-AgNPs (Dube et al., 2020).

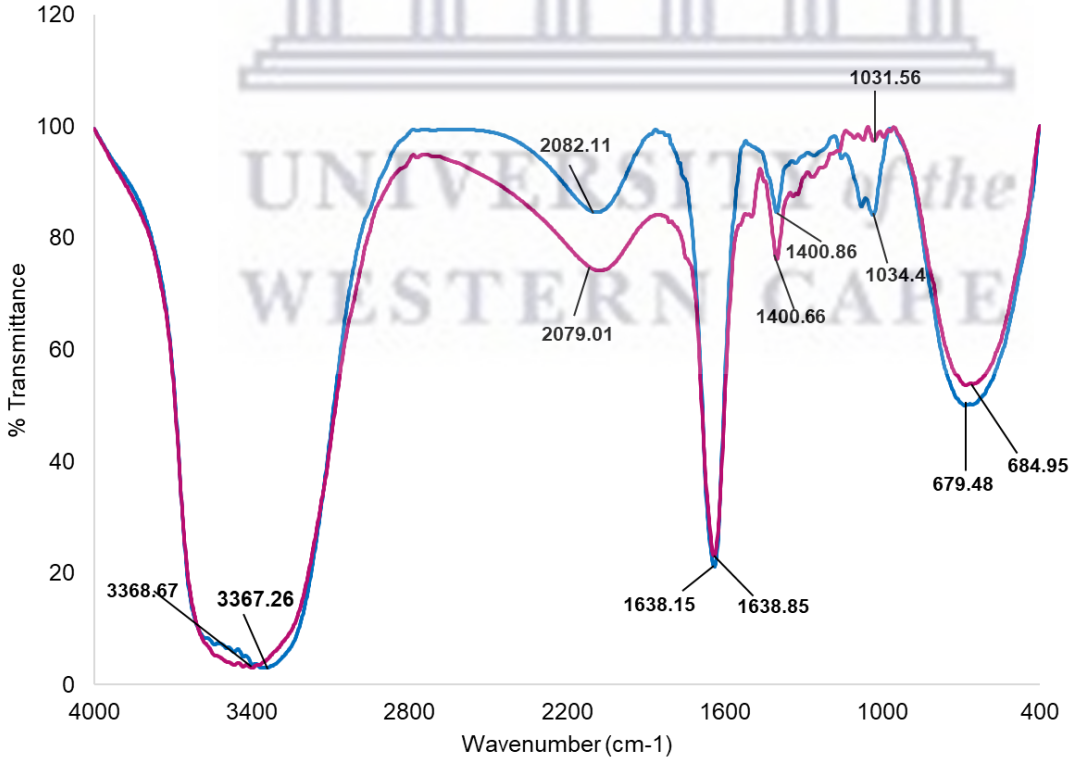

Figure 3. 9 FTIR spectra of IHFE and IHFE-AgNPs

Table 3. 3 Shifts of the FTIR spectra bands cm^{-1} of major peaks of IHFE and IHFE-AgNPs

Peak position in IHFE (cm^{-1})	Peak position in IHFE-AgNPs (cm^{-1})	Shift values (cm^{-1})	Functional groups
3367.26	3368.67	-1.38	O-H (Alcohols and phenols) N-H bend (Amine)
2082.11	2079.01	3.10	C≡C (Alkynes)
1638.15	1638.85	-0.70	C=O stretch (Carboxylic acid, Ethers, Esters) N-H bend (Primary amines)
1400.86	1400.66	0.20	O-H (Phenols) S=O (sulfoxide) C-F stretch (Alkyl and Aryl halides)
1034.40	1031.56	2.84	C-O (Aromtic esters, Ethers) C-N stretch (Aromatic amines)
684.95	679.48	5.47	C-Br stretch (alkyl halides and, aliphatic bromo compounds)

3.2.3 Stability analysis of IHFE-AgNPs

The stability of the IHFE-AgNPs was assessed in different biological media (dH_2O, ddH_2O, MHB, PBS, DMEM complete and DMEM non-complete media) for downstream biomedical applications. These media were selected because of their use in the different biological assays performed in this study. The stability of IHFE-AgNPs was evaluated at 37 °C as most biological assays are conducted under this temperature to mimic biological environments. Additionally, UV-Vis spectroscopy was used to monitor any change in the stability of the IHFE-AgNPs which is manifested through minimal changes in their UV-Vis spectra over time (Elbagory et al., 2016). It is important to note that unstable NPs can easily aggregate which can influence their intended properties for potential biomedical applications (Tyavambiza et al., 2021).

In this study, no significant change in the absorption spectra was observed after the IHFE-AgNPs was incubated in dH_2O, ddH_2O, MHB and PBS implying that they are stable in these media (Figure 3.10). On the other hand, IHFE-AgNPs were found to be relatively stable in complete and incomplete DMEM as indicated by moderate changes in their UV-Vis spectra which shows broadening as well as a downward peak observed at approximately 550 nm in both media. This could be explained by the high ion content and proteins which alters the surface morphology of the NPs leading to aggregation (Dube et al., 2020, Moore et al., 2015). Additionally, the downward peaks observed in complete and incomplete DMEM could be due to the phenol red present in the media resulting in absorbance of light around 550 nm. Aboyewa et al., 2021, reported the stability of MNPs (AuNPs) in DMEM and observed that Honeybush-AuNPs SPR and absorbance were altered, however, these changes were moderate (Aboyewa et al., 2021).

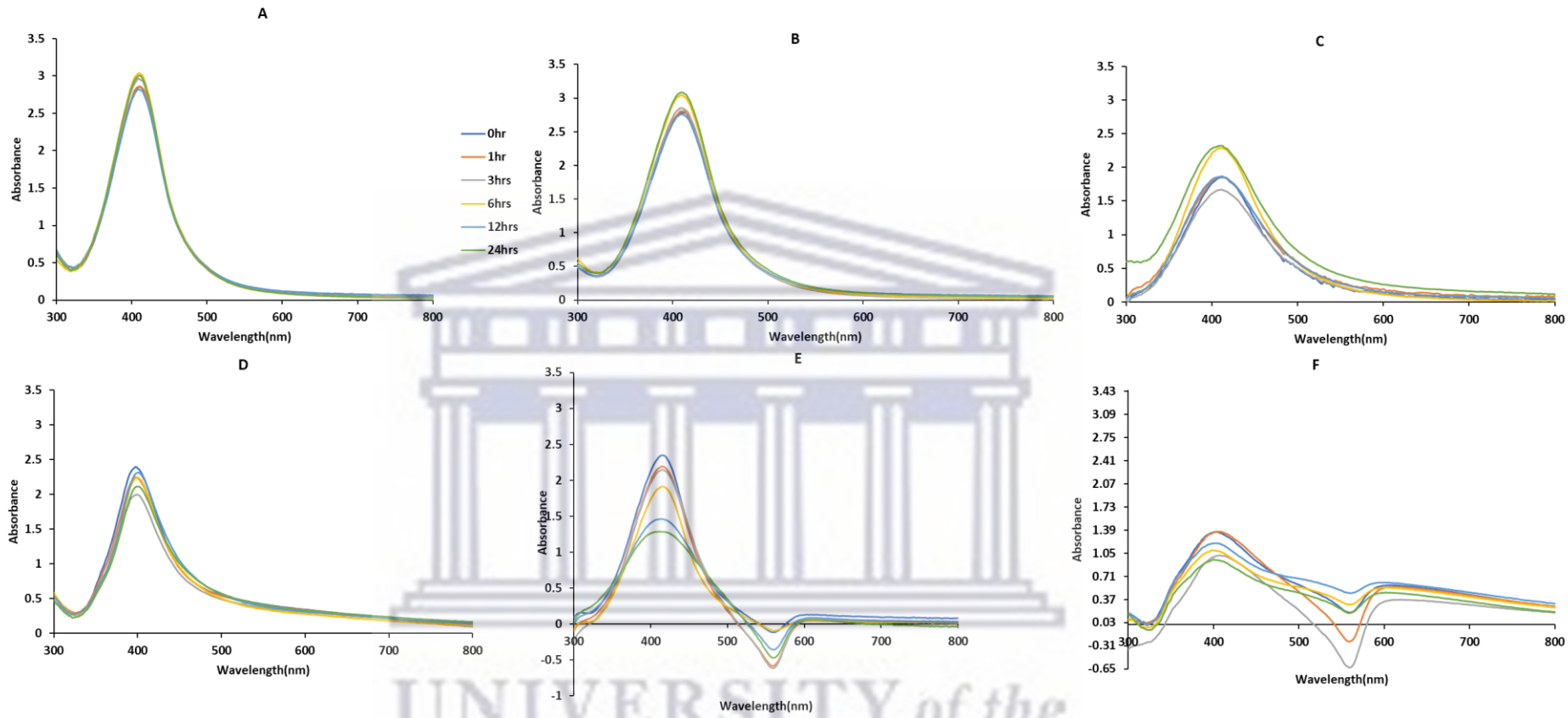

Figure 3. 10 Stability of Indian Hawthorn fruit extract biosynthesised silver nanoparticles (IHFE-AgNPs*)* during incubation in biological media at 37 °C over 24 hrs period. (A) dH_2O; (B) ddH_2O; (C) MHB; (D) PBS; (E) complete DMEM and (F) incomplete DMEM.

3.3 Antibacterial activity of IHFE-AgNPs

3.3.1 Agar well diffusion

The antibacterial activity of IHFE-AgNPs and IHFE was screened against *S. aureus*, MRSA, *K. pneumoniae*, *A. baumannii, P. aeruginosa*, *E. cloacae,* and *E. coli* using the agar well diffusion method. This assay evaluates the susceptibility of bacteria towards the antibacterial agents. An active agent will inhibit bacteria growth around the area where is added by creating a circular zone. The ZOI or a clear zone around the well of treatment was measured to assess the antibacterial effect of the IHFE-AgNPs as well as IHFE on the different bacteria. The positive control and negative control used in this study were Ciprofloxacin and MHB, respectively.

The results of this study showed that IHFE-AgNPs have antibacterial activity against Gram-positive and Gram-negative bacteria as observed in Figure 3.11. The ZOI of the different treatments: IHFE (unpH), IHFE (pH 11) and IHFE-AgNPs are shown in Table 3.4. For Gram-negative bacteria, IHFE-AgNPs demonstrated antibacterial activity against *P. aeruginosa* and *K. pneumoniae*. However, *P. aeruginosa* was more susceptible to IHFE-AgNPS than K. pneumoniae with ZOI of 10.00 ± 0 mm and 8.00 ± 0.00 mm, respectively. No ZOI was observed for *A. baumannii, E. coli and E. cloacae*. Bacteria use different mechanisms to develop resistant against antibacterial agents. For instance, *A. baumannii* is aerobic Gram-negative bacteria which is associated with many nosocomial infectious illnesses worldwide, and uses enzymes such as β-lactamases to inactivate β-lactams antibiotics; this is one of the main Multidrug (MDR) resistant mechanism (Breijyeh et al., 2020). For Gram-positive bacteria, only *S. aureus* was susceptible to IHFE-AgNPs with a ZOI of 10.00 ± 0.00 mm.

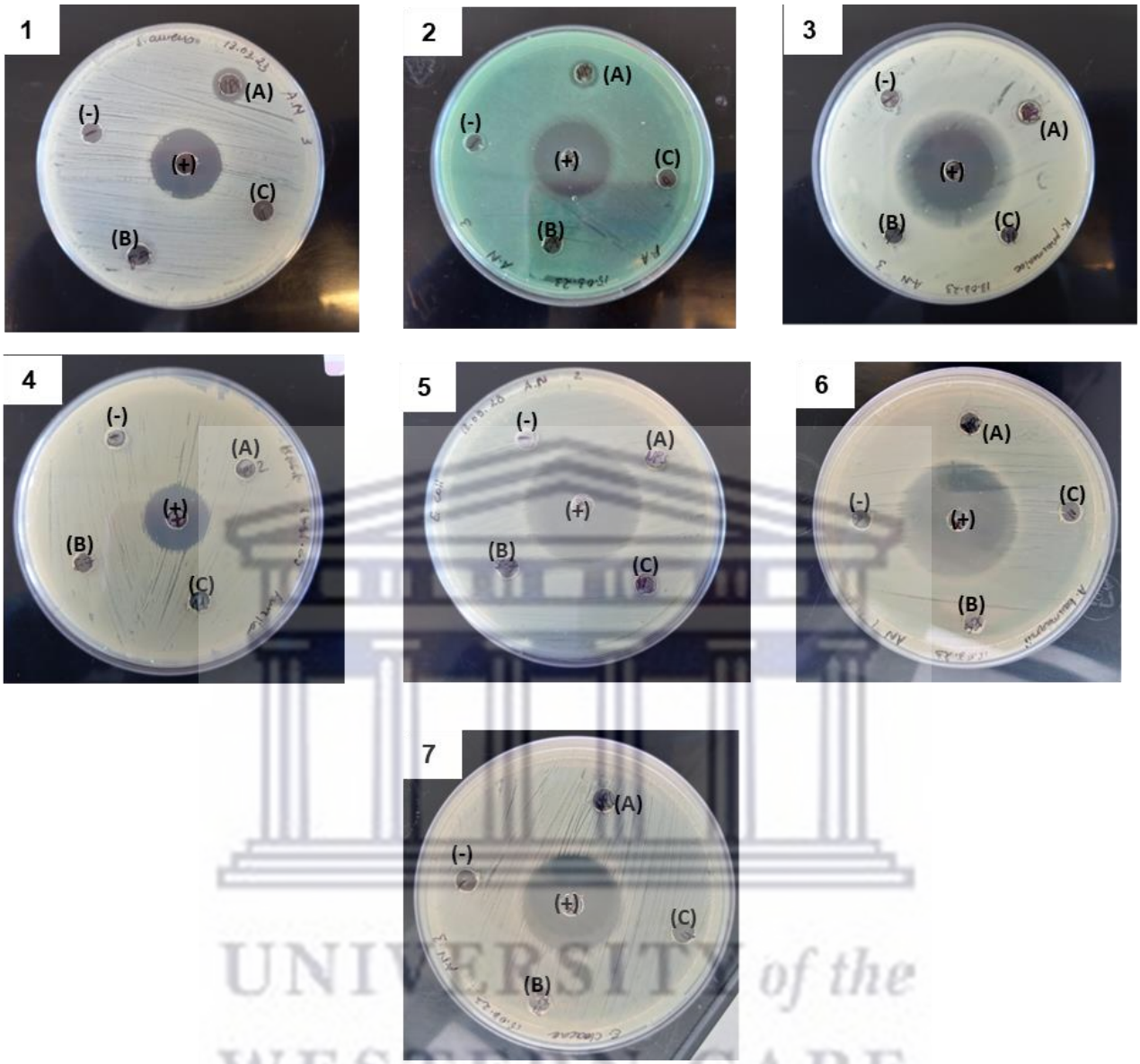

Figure 3. 11 Agar well diffusion results showing the antibacterial effect of Indian Hawthorn fruit extract biosynthesised silver nanoparticles (IHFE-AgNPs) against 7 pathogenic bacteria. The zone of inhibition of the biogenic IHFE-AgNPs against (1) *S. aureus*, (2) *P. aeruginosa,* (3) *K. pneumoniae,* (4) MRSA, (5) *E. coli*, (6) *A. baumannii* and (7) E. cloacae. Treatments: (A): IHFE-AgNPs, (B) IHFE at pH 5.7, (C) IHFE at pH 11. Ciprofloxacin is represented as (+) and MHB (-).

Table 3. 4 Zone of inhibition of 7 human pathogens treated with Indian Hawthorn fruit extract biosynthesised silver nanoparticles (IHFE-AgNPs), Indian Hawthorn fruit extract (IHFE) at pH 5. 7 and pH 11. Results are presented as mean ± standard deviation (n=3).

Treatment	*S. aureus*	MRSA	*E. coli*	*E. cloacae*	*P. aeruginosa*	*K. pneumoniae*	*A. baumannii*
				Zone of inhibition ± SD (mm)			
IHFE-AgNPs	10.00 ± 1.00	*	*	*	10.00 ± 0.00	8.00 ± 0.00	*
IHFE (pH 5.7)	*	*	*	*	*	*	*
IHFE (pH 11)	*	*	*	*	*	*	*
Ciprofloxacin (+)	20.70 ± 0.60	23.30 ± 0.60	26.30 ± 1.20	26.80 ± 0.60	23.33 ± 0.60	26.00 ± 1.00	30.70 ± 0.60
MHB (-)	*	*	*	*	*	*	*

*: no ZOI observed

IHFE did not exhibit any antibacterial activity against all microorganisms tested in this study. The antibacterial effects of hawthorn berries from *Crataegus oxyacanthus* has been reported by Omer et al. (2021), in their study, an ethanolic extract was used to test for the antibacterial effects in a range of 25 - 200 mg/ml. The results showed high antibacterial activity against *S. aureus* and *E.coli* (Omer et al., 2021). In another study by Bakour et al, pollen of *Quercux ilex* was extracted using ethanol and exhibited antibacterial effects against Gram-negative and Gram-positive bacteria (Bakour et al., 2021). The inactivity of the IHFE could impacted by the solvent (ddH_2O) used during the extraction process. The selection of the solvent is an important factor for the extraction of various phytoconstituents found in plants. It has been reported that phytoconstituents are more soluble in plant extracts made with solvents such as ethanol, acetone and methanol providing better antimicrobial effects compared to aqueous extracts (Heflish et al., 2023). In a study performed by Heflish et al (2023), *Rhaphiolepis indica* fruit extract was made using hexane and acetone which exhibited great antifungal effects against *Fusarium* infections. In the study previously mentioned, *Rhaphiolepis indica* was obtained in Egypt, therefore, geographical location could also play explain the inactivity observed in the IHFE used in the current study.

Ciprofloxacin, being the positive control inhibited the growth of all the bacterial strains used in the study. As expected, the negative control MHB did not display any antibacterial activity as there was no clear zone surrounding the well. This is a confirmation that the growth medium did not have any effect on the antibacterial activity observed. There was no antibacterial effect observed for the IHFE at its natural pH (unpH) and at pH 11. This could be because the extract concentration used was very low. A previous study by Omer et al., 2021, reported the antibacterial activity of a *Crataegus oxyacanthus* (species from the same family as Indian hawthorn) at concentration ranging from 25 mg/ml to 200 mg/ml which are higher than the concentration used in this study (12.5 mg/ml).

Due to their different structure, Gram-negative bacteria are known to be more resistant to antibiotics as compared to Gram-positive bacteria. The outer membrane of Gram-negative bacteria is the main cause of resistant to various antibiotics such β-lactams and quinolinones (Breijyeh et al., 2020). Although Gram-positive bacteria have a thick peptidoglycan layer, the outer membrane found on Gram-negative bacteria hinders hydrophilic antibiotics such as β-lactam to cross through, thus creating antibiotic resistance (Breijyeh et al., 2020). Resistant Gram-negative bacteria are the main cause for nosocomial diseases and the most important strains are *P. aeruginosa*, *A. baumannii* and *S. maltophilia* (Breijyeh et al., 2020).

3.3.2 Micro-dilution assay

The antimicrobial activity of IHFE-AgNPs was further investigated using microdilution assay to determine the minimum inhibitory concentration (MIC) and the minimum bactericidal concentration (MBC) of the IHFE-AgNPs against all aforementioned bacterial strains. The MIC of IHFE-AgNPs was determined using AlamarBlue™ dye also known as resazurin. It is a non-fluorescent dye that is reduced to resorufin, which turns pink in the presence of viable bacterial cells. The pink compound is highly fluorescent (Tyavambiza et al., 2021), the intensity of the pink colour is proportional to the number of live bacterial cells. In terms of the MBC, it is defined as the lowest concentration of the treatments that can kill 99.9% of bacteria.

These results demonstrated that IHFE-AgNPs displayed a broad-spectrum antibacterial effect against all the pathogens tested in this study as indicated in Figure**s** 3.12 and 3.13. The MIC was recorded as the lowest concentration that inhibits visible growth of bacteria. The MIC and MBC value for *S. aureus* and MRSA were found to be 100 µg/ml (Table 3.5). These two strains are known to be resistant to several antibiotics and are a major cause of high mortality rates (Jubeh et al., 2020). *S. aureus* causes severe illnesses such as skin and respiratory tract infections, hospital equipment related infections and infectious endocarditis (Jubeh et al., 2020). MRSA is a multi-resistant strain of *S. aureus* that is resistant to all β-lactam antibiotics. Furthermore, the lowest concentration of IHFE-AgNPs that inhibited *K. pneumoniae* was reported to be 50 µg/ml, this was similar for *A. baumannii* and *E. coli*. Moreover, the lowest concentration of IHFE-AgNPs able to kill 99.9 % of *A. baumannii*, *K. pneumoniae* and *E. coli* was similar to their MIC. Lastly, the highest antibacterial activity was observed against both *P. aeruginosa* and *E. cloacae* with a MIC and MBC of 25 µg/ml.

The micro-dilution technique has been reported to be more accurate than the agar well diffusion approach when determining the antimicrobial activity of a compound (Duval et al., 2019a). This is because AgNPs may not diffuse through the agar, however, the microdilution approach allows direct contact of the NPs and the medium used (Duval et al., 2019a, Eloff, 2019). Furthermore, reproducibility is a concern when using the agar diffusion approach (Eloff, 2019). Other authors have used agar well diffusion as a preliminary step to attest for the antimicrobial effects of the compound before determining the MIC of this compound (Duval et al., 2019a).

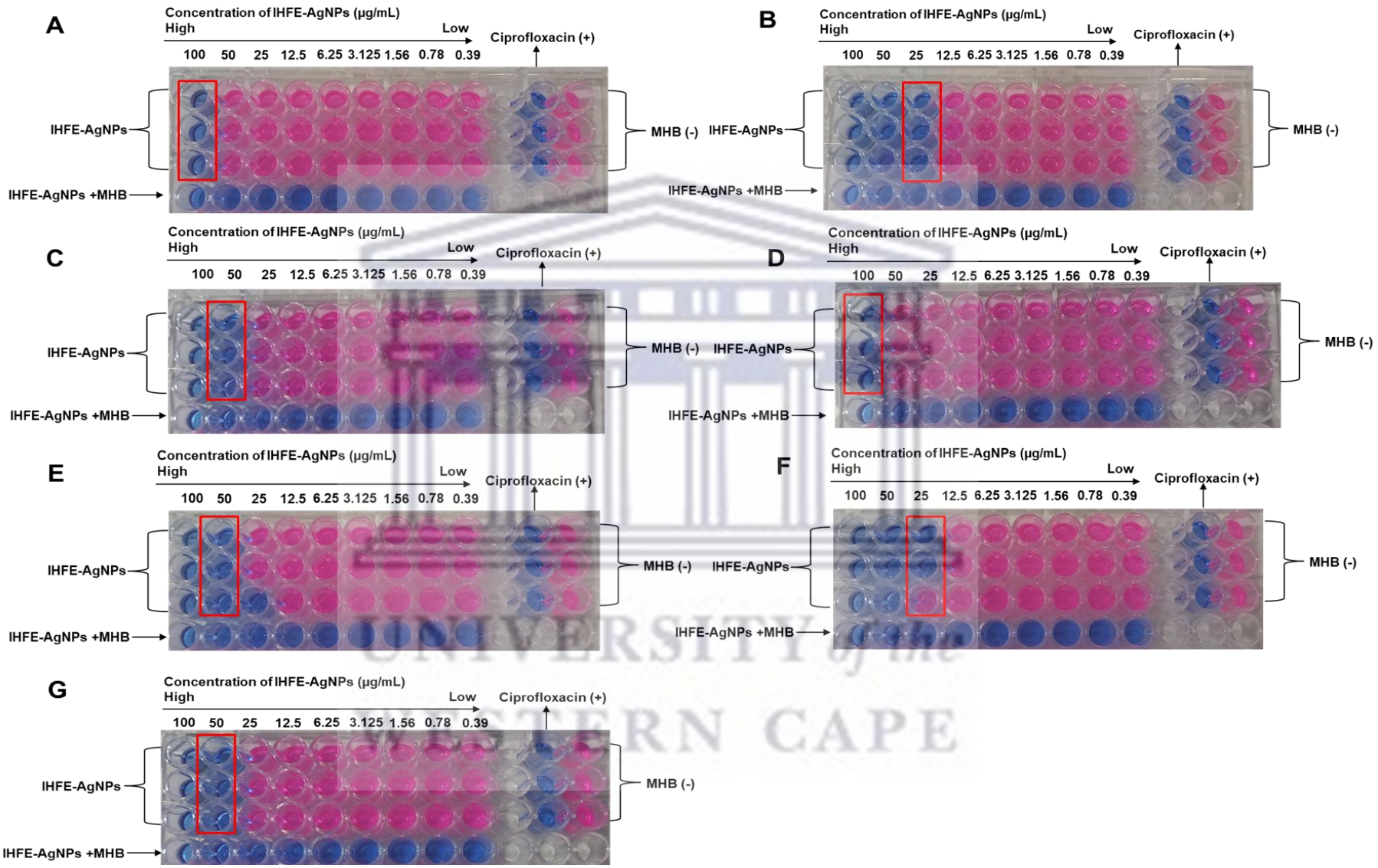

Figure 3. 12 Antibacterial effects of Indian hawthorn fruit extract biosynthesised silver nanoparticles (IHFE-AgNPs) using AlamarBlue™ dye assay to determine their minimum inhibitory concentration. A change in colour from blue to pink indicated the viable bacteria after treatments (A) *S. aureus*, (B) *P. aeruginosa*, (C) *K. pneumoniae*, (D) MRSA, (E) *E. coli*, (F) *E. cloacae* and (G) *A. baumannii*

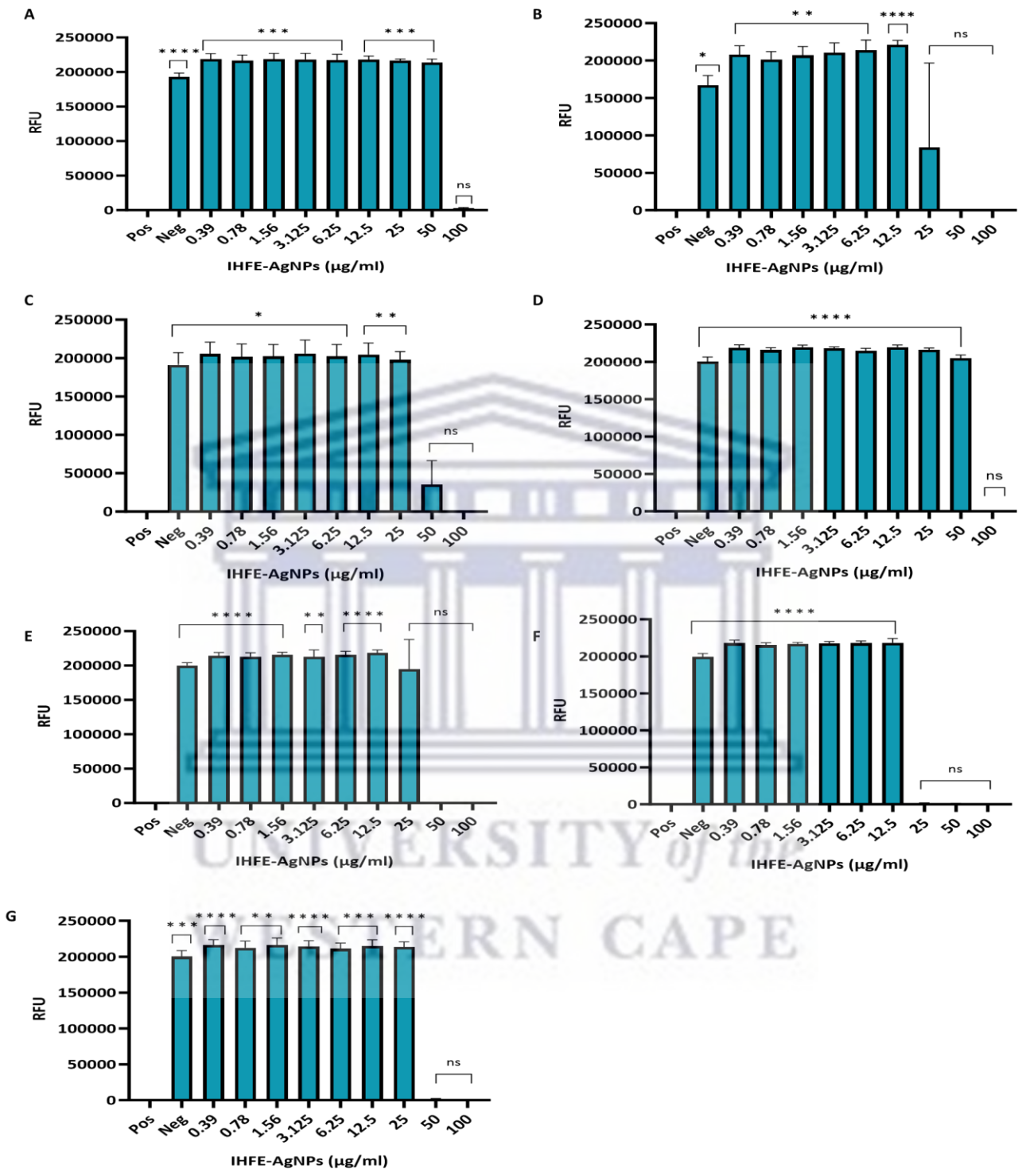

Figure 3. 13 Minimum inhibitory concentration analysis of Indian hawthorn fruit extract biosynthesised silver nanoparticles (IHFE-AgNPs) : (A) *S. aureus*, (B) *P. aeruginosa*, (C) *K. pneumoniae*, (D) MRSA, (E*) E. coli*, (F) *E. cloacae* and (G) *A. baumannii* . Graphs displaying the relative fluorescence units (RFU) after 24 hr treatment. Results represent the average of three independent experiments performed in triplicate. A One-Way ANOVA test was used to analyse statistical significance**.** The data is expressed in mean ± SEM (n=3). Statistical significance compared to the positive control is indicated by ^{ns} ($p > 0.05$), * ($p < 0.05$), ** ($p < 0.01$), *** ($p < 0.001$) and **** ($p < 0.0001$).

Table 3. 5 MIC and MBC values of IHFE-AgNPs against seven bacterial strains

Bacterial strains	**IHFE-AgNPS**		**Ciprofloxacin**	
	MIC (µg/ml)	MBC (µg/ml)	MIC (µg/ml)	MBC (µg/ml)
S. aureus	100	100	0.93	0.93
MRSA	100	100	0.46	0.46
P. aeruginosa	25	25	0.46	0.46
K. pneumoniae	50	50	<0.10	<0.10
A. baumannii	50	50	<0.10	<0.10
E. coli	50	50	<0.10	<0.10
E. cloacae	25	25	<0.10	0.23

It is obvious that Gram-negative bacteria were more susceptible to IHFE-AgNPs as opposed to Gram-positive bacteria. This is very significant because amongst the list of the twelve bacteria published by the WHO, nine are Gram-negative bacteria and pose a greatest risk of antibiotics resistance particularly Enterobacteriaceae such as *K. pneumoniae* and *E. coli* (Duval et al., 2019b). Furthermore, *K. pneumoniae* is the cause of infections in hospitals with resistance to β-lactam antibiotics including cephalosporin, penicillin and carbapenems (mostly used to treat infections caused Gram-negative strains) (Santajit and Indrawattana, 2016). Bacterial strains such *P. aeruginosa* and *E. cloacae* can cause infections in immunocompromised patients and have been reported to produce Extended spectrum b-lactamases (ESBLs) which allows them to develop MDR to almost all antibiotics except colistin which is known as the last-resort antibiotic and the most effective in all bacteria (Balestri et al., 2023). Furthermore, the different composition in the cell wall of Gram-positive and Gram-negative bacteria is an important factor in the development of AMR; although gram-negative bacteria are composed of a thin peptidoglycan cell wall, their outer membrane layer composed of lipopolysaccharides (LPS), proteins and phospholipids render NPs difficult to penetrate (Balestri et al., 2023). In contrast, Gram-positive strains have a thicker peptidoglycan cell wall with teichoic acid but lack an outer layer rendering the cell wall porous to foreign molecules, resulting in cell membrane injury and cell death (Balestri et al., 2023, Zaidi et al., 2017).

In comparison to the positive control (Ciprofloxacin), IHFE-AgNPs had similar inhibitory effect against *S. aureus* and MRSA at 100 µg/ml ($p > 0.05$). This was also observed for *A. baumannii*, *K.*

pneumoniae and *E. coli* from 100 to 50 µg/ml ($p > 0.05$). Lastly, IHFE-AgNPs showed comparable inhibitory effect with Ciprofloxacin against *P. aeruginosa* and *E. cloacae* from 100 to 25 µg/ml ($p > 0.05$). These results confirm that the IHFE-AgNPs were able to inhibit and kill bacteria and could potentially be used as an alternative antibacterial agent.

3.4 Phytochemical Analysis and Antioxidant Studies

3.4.1 Total phenolic content of IHFE-AgNPs

The TPC was extrapolated with the aid of a Gallic acid calibration standard curve (Figure 3.14: Appendix). The total phenolic content was higher in IHFE-AgNPs compared to the IHFE with 70.04 ± 2.66 µg GAE /ml and 27.4 ± 1.89 µg GAE /ml, respectively (Table 3.6). This implies that the phenolic compound present in IHFE took part in the reduction and capping of IHFE-AgNPs. These results are in accordance with literature where Salari et al, found that the AgNPs synthesised using *Prosopis farcta* fruit extract had higher phenolic content compared to the fruit extract alone (Salari et al., 2019).

Table 3. 6 Total phenolic content (TPC) analysis of Indian Hawthorn fruit extract (IHFE) and Indian Hawthorn fruit extract biosynthesised silver nanoparticles (IHFE-AgNPs). The values are expressed in gallic acid equivalents. The data is expressed in mean ± SD (n=3)

Treatment	TPC (µg GAE/ml)
IHFE	27.40 ± 1.89
IHFE- AgNPs	70.04 ± 2.66

3.4.2 Antioxidant studies

Oxidative stress can cause many diseases such cardiovascular diseases (Förstermann, 2010), cancer (Ghaffari, 2008, Phaniendra et al., 2015), inflammatory conditions and psychic impairments, such as ADHD or schizophrenia (Katta and Brown, 2015). MNPs such as AgNPs have been reported to possess antioxidant properties which offers advantages against oxidative stress by preventing diseases through free radical scavenging (Lushchak et al., 2018, Samrot et

al., 2022). MNPs functionalised with antioxidants can be used in drug delivery systems (Samrot et al., 2022). Green synthesis using plant extracts are reported to improve the antioxidant properties of NPs due to the phytochemicals present in plants (Khalil et al., 2019). The role of phytoconstituents is not limited to capping and reduction of NPs, they can also act as free radical scavengers (Tyavambiza et al., 2022). The antioxidants properties of IHFE and IHFE-AgNPs were determined using DPPH, FRAP and ABTS assays.

3.4.2.1 DPPH

The antioxidant activity of IHFE and IHFE-AgNPs was evaluated using DPPH assay. This is a rapid, simple and cost-effective method that helps to determine the antioxidant ability of NPs (Bedlovičová et al., 2020). In the presence of an antioxidant agent, the purple colour of DPPH turns yellow indicating reduction of free radicals (Bedlovičová et al., 2020). The disappearance of the purple colour is dependent on the concentration of the scavenging capacity of the tested sample. In this study, the antioxidant potentials of IHFE-AgNPs were investigated and compared to that of the IHFE and ascorbic acid as a standard. The results reflected a dose dependent scavenging ability of the IHFE as the concentration increased (1.56 to 400 µg/ml) as seen in Figure 3.15. However, both the IHFE-AgNPs and ascorbic acid exhibited higher scavenging activity against the free radical. Furthermore, there was a significant difference observed between the scavenging activity of IHFE and Ascorbic acid. No significant difference was observed between the IHFE-AgNPs and IHFE as well as ascorbic acid. The antioxidant activity of IHFE and IHFE-AgNPs can be attributed to the phytochemicals present in the IHFE which act as capping agents during the synthesis process (Elemike et al., 2017). The antioxidant potential of biogenic AgNPs against DPPH has been reported in literature. In the study conducted by Elemike et al., 2017, AgNPs synthesised with *Costus afer* (CA) leaf extract exhibited enhanced scavenging potential against DPPH in a dose dependent manner. It was found that the CA-AgNPs had higher antioxidant activity compared to the leaf extract (Elemike et al., 2017).

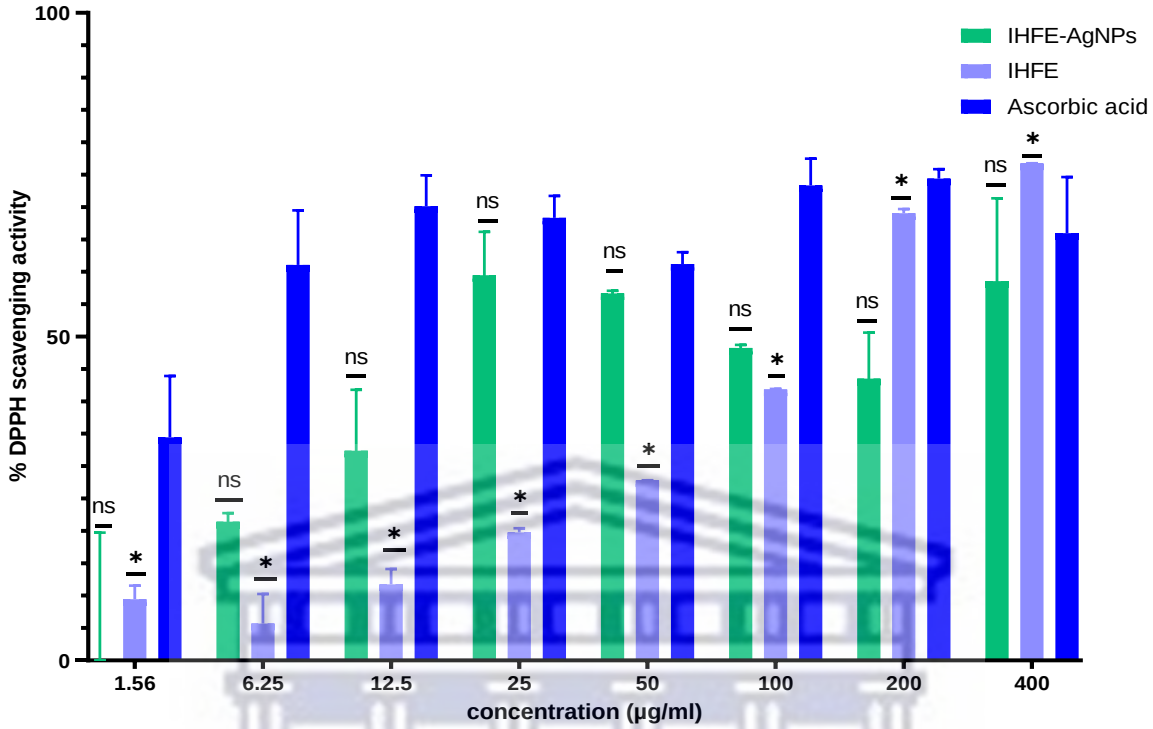

Figure 3. 14 DPPH radical scavenging activity of Indian Hawthorn fruit extract biosynthesized silver nanoparticles (IHFE-AgNPs), Indian Hawthorn fruit extract (IHFE) and ascorbic acid. A One-Way ANOVA test was used to analyse statistical significance. The data is expressed in mean ± SEM (n=3). Statistical significance in comparison to ascorbic acid (standard) is non-significant indicated by ^{ns} ($p > 0.05$) and significant indicated by * ($p < 0.05$).

3.4.2.2 ABTS

The antioxidant ability of IHFE and IHFE-AgNPs was determined using the ABTS method. This assay, also known as 2'-Azino-Bis-3-Ethylbenzotiazolin-6-sulfonic Acid is a method in which the cation radical $ABTS^{+}$ is generated through the emission of an electron from a nitrogen atom (Bedlovičová et al., 2020). The ABTS solution is a blue-green substance, in the presence of antioxidant, the solution turns clear (discoloration occurs) within a few minutes. As seen in Figure 3.16, the IHFE and IHFE-AgNPs exhibited some antioxidant activity. IHFE-AgNPs was able to reduce ABTS radical in a dose dependent manner, this was also observed for the IHFE and ascorbic acid. However, the percentage scavenging ability of the IHFE was lower compared to IHFE-AgNPs and Ascorbic acid. It was evident that the antioxidant properties were increased

with increasing concentrations of the different treatments (IHFE, IHFE-AgNPs and Ascorbic acid) in the range 1.56- 400 µg/ml. When comparing IHFE-AgNPs to ascorbic acid, it can be seen that ascorbic acid was able to scavenge a high percentage of ABTS radical from 1.56 µg/ml in a dose dependent manner. At the highest concentration of 400 µg/ml IHFE-AgNPs and ascorbic acid exhibited highest antioxidant activity which were 98.7 and 99.1 %, respectively. However, at this concentration, IHFE only exhibited 41% scavenging activity. As highlighted in section 3.5.1.1, IHFE-AgNPs contain high amounts of phenolic compounds from the IHFE which are responsible for their antioxidant's activity (Alirezalu et al., 2020).

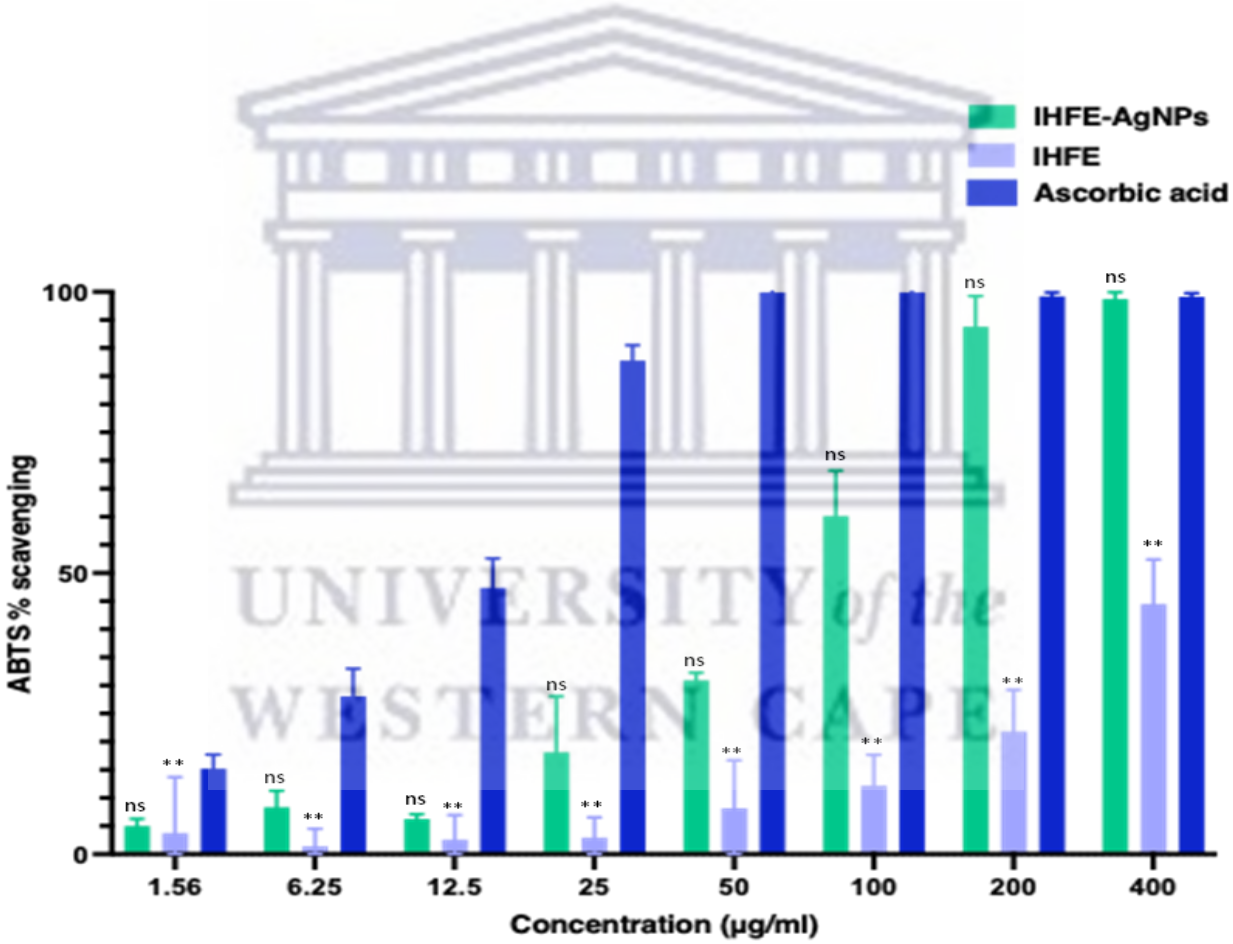

Figure 3. 15 ABTS % scavenging activity of IHFE-AgNPs, IHFE and ascorbic acid. A One-Way ANOVA test was used to analyse statistical significance. The data is expressed in mean ± SEM (n=3). . Statistical significance in comparison to the ascorbic acid (standard) is non-significant indicated by ^{ns} ($p > 0.05$) and significant indicated by * ($p < 0.05$) and ** ($p < 0.01$).

Several studies have confirmed the antioxidant activity of green synthesised AgNPs. Tyavambiza et al, assessed the antioxidant properties of green synthesised AgNPs from an aqueous extract

of *C. Orbiculata* using ABTS assay; the results showed that the *Cotyledon*-AgNPs exhibited better antioxidant activity than the extract (Tyavambiza et al., 2022). Additionally, it was reported that the various phytochemicals found in the *C. Orbiculata* were responsible for the scavenging activity of *Cotyledon*-AgNPs (Tyavambiza et al., 2022). AgNPs synthesised from *Salvia aethiopis* extract were found to be more active at scavenging ABTS radical than the aqueous extract and the standard (Gecer, 2021). These results could further imply that IHFE-AgNPs could potentially scavenge free radicals which may results in antioxidant properties.

3.4.2.3 FRAP

To determine the ferric-reducing activity IHFE and IHFE-AgNPs, the FRAP assay was used. This assay is based on the reduction of a colourless Fe^{3+}-2', 4, 6-tripyridyl-S-triazine (TPTZ) complex to an intense blue Fe^{2+}-TPTZ (Bedlovičová et al., 2020). The ferric reducing activity of different concentrations of IHFE-AgNPs is shown in Figure 3.17. In this study, the ability of IHFE-AgNPs to reduce Fe^{3+}-TPTZ to Fe^{2+}-TPTZ was significantly higher than that of the IHFE in a dose-dependent manner. On the other hand, ascorbic acid showed a dose-dependent reducing ability which was considerable higher than that of IHFE and IHFE-AgNPs. This finding corresponds to the study performed by Salari et al, who reported that the green synthesised AgNPs could significantly reduce Fe^{3+}-TPTZ to Fe^{2+}-TPTZ dose dependently compared to the extract (Salari et al., 2019). Furthermore, ascorbic acid exhibited higher reducing potential compared to both AgNPs and the extract (Salari et al., 2019). The aqueous *Cotyledon* plant extract exhibited higher reducing activity than the *Cotyledon*-AgNPs. Furthermore, they reported that the reducing activity of the *Cotyledon*-AgNPs could be attributed to high polyphenol content in the extract (Tyavambiza et al., 2022).

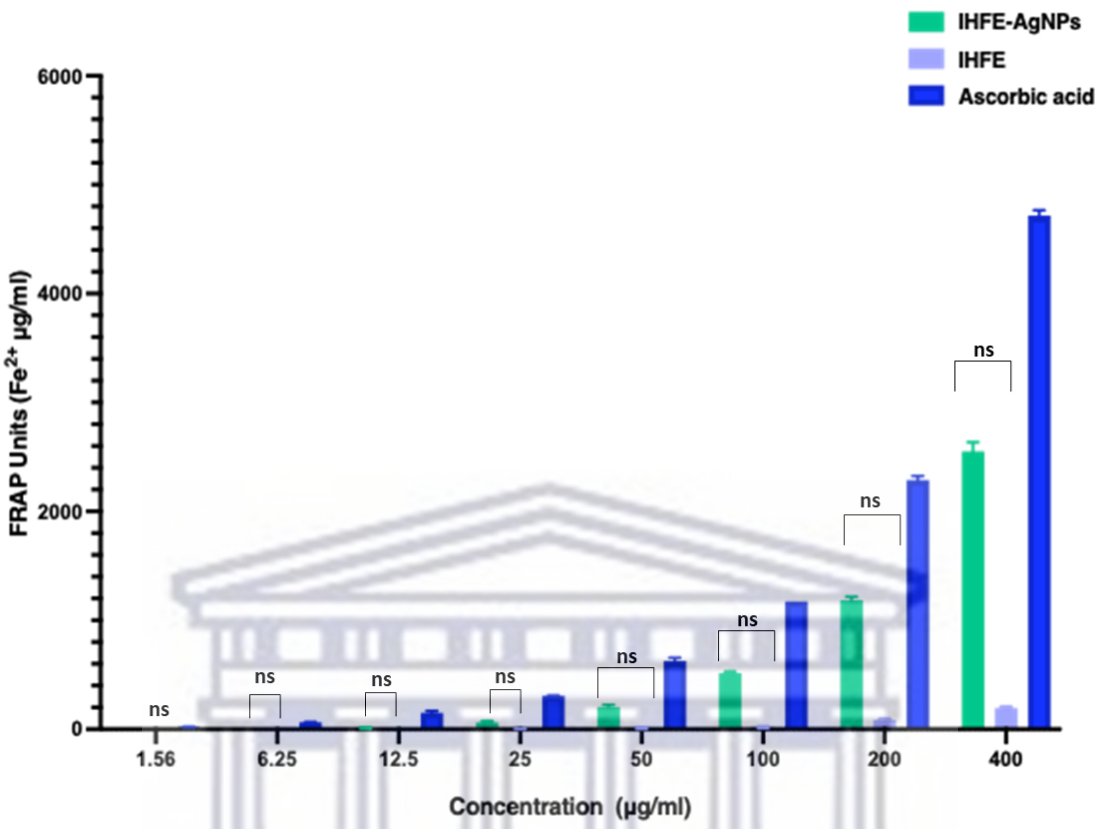

Figure 3. 16 FRAP of IHFE-AgNPs, IHFE and ascorbic acid. A One-Way ANOVA test was used to analyse statistical significance. The data is expressed in mean ± SEM (n=3). Statistical significance in comparison to the ascorbic acid (standard) is non-significant as indicated by ^{ns} ($p > 0.05$).

In summary, IHFE-AgNPs exhibited enhanced antioxidant potentials against all three free radicals tested in this study. This was due to the high phenolic content determined to be 70.04 ± 2.66 µg GAE /ml compared to 27.40 ± 1.89 µg GAE /ml in IHFE alone. The increased scavenging activity of IHFE-AgNPs can be significant in therapeutics to prevent or reduce oxidative stress related illnesses.

3.5 Cytotoxicity study

Cell viability was assessed using the WST-1 assay to determine the toxicity of IHFE and IHFE-AgNPs on KMST-6 cells which are normal human skin fibroblast cells. The number of viable cells were quantified following a 24 hrs exposure to increasing concentrations of IHFE and IHFE-AgNPs (0.78- 100 µg/ml). The principle is based on tetrazolium salt which in the presence of

metabolically viable cells breaks down to form formazan, a yellow-coloured product (Hiemer et al., 2016, Tyavambiza et al., 2021). This reaction is catalysed by succinate-tetrazolium reductase, an enzyme found in viable cells. The intensity of the yellow formazan product is proportional to the number of active cells in the culture which can be measured at 440 nm (Tyavambiza et al., 2021). To assess if the IHFE-AgNPs could interfere with WST-1 assay, the IHFE-AgNPs (at each concentration used in the study) without cells were incubated with the WST-1 dye and the absorbance was measured.

The results depicted in Figure 3.18 revealed that IHFE-AgNPs treatments had no effect on the viability of KMST-6 cells at concentrations lower than 100 µg/ml. However, IHFE-AgNPs were toxic to the cells at 100 µg/ml. These findings indicated that the IHFE-AgNPs were not toxic to the cells at ≤50 µg/ml. The positive control, 10 % DMSO was toxic to the cells with a cell viability of <30 %. DMSO has been previously been reported to be toxic to cells at concentration above 1% at room temperature (De Abreu Costa et al., 2017).

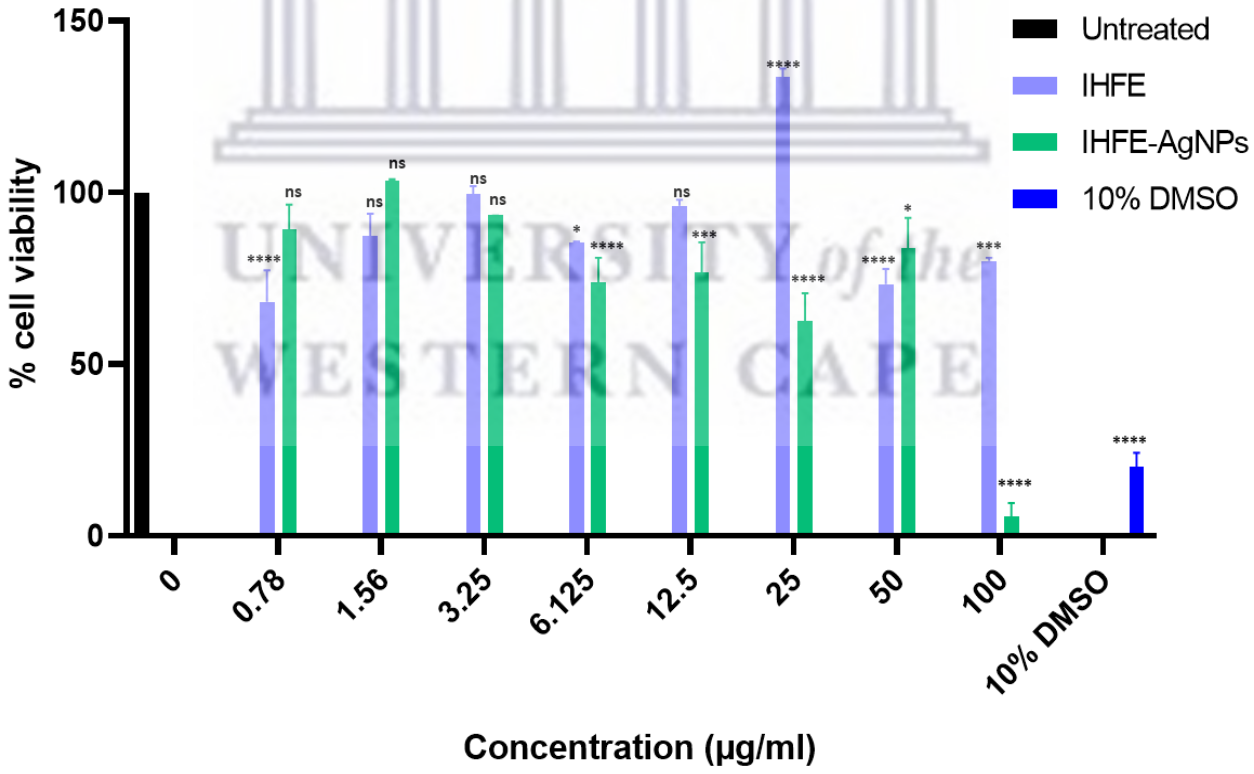

Figure 3. 17 Effect of IHFE-AgNPs on the viability of KMST-6 cells using WST-1 assay. The cells were treated with increasing concentrations of IHFE-AgNPs for 24 hours. The data is expressed in mean ± SEM (n=3). *Results represent*

the average of three independent experiments performed in triplicate. A One-Way ANOVA test was used to analyse statistical significance. Statistical significance compared to the untreated sample is non-significant indicated by ^{ns} ($p > 0.05$) and significant as indicated by * ($p < 0.05$), *** ($p < 0.001$), **** ($p < 0.0001$).

Chapter 4: Conclusion and Recommendations

The aim of the present study was to synthesise AgNPs using IHFE, investigate their antimicrobial potential against ESKAPE pathogens, and evaluate their antioxidants properties and their cytotoxicity effects. IHFE-AgNPs formation was confirmed by a change in colour followed by UV-Vis spectroscopy. DLS confirmed that the IHFE-AgNPs were monodisperse and moderately stable in colloidal solution. The spherical IHFE-AgNPs contained several functional groups that suggests involvement of polyphenols and flavonoids in their reduction and stabilization.

IHFE-AgNPs were able to inhibit the growth of both Gram-negative and Gram-positive bacteria; with Gram-negative bacteria being the most susceptible to the IHFE-AgNPs. These observations suggest that IHFE-AgNPs have a broad-spectrum antibacterial potential to be used for treatment of infections caused by AMR bacteria. Additionally, the biological activity of IHFE-AgNPs might be attributed to their antioxidant scavenging activity against free radicals such as DPPH, ABTS and TPTZ in FRAP assay. Furthermore, IHFE-AgNPs non-toxic to KMST-6 cells at concentrations below 100 µg/ml. These findings suggest that IHFE-AgNPs have the potential to be used in the biomedical application as antibacterial and antioxidant agents. However, future investigations are warranted to learn more about the antibacterial mechanism of action of the IHFE-AgNPs. Due to the antioxidant and antibacterial effects observed on IHFE-AgNPs, the application can also extend to wound-healing potential. Furthermore, based on the results observed for the antioxidant scavenging ability of the IHFE-AgNPs, anti-inflammatory study should also be evaluated. Little is known about the long-term biosafety of AgNPs, there is a higher risk that AgNPs could be absorbed through the skin and accumulated in different organs potentially causing harm. Therefore, some more research should be done to know the appropriate approaches to estimate silver ions being released from AgNPs in vivo and to perform studies on animal models looking into the different genes altered in case of longer exposure to AgNPs.

References

ABD EL-BAKY, R. M., IBRAHIM, R. A., MOHAMED, D. S., AHMED, E. F. & HASHEM, Z. S. 2020. Prevalence of Virulence Genes and Their Association with Antimicrobial Resistance Among Pathogenic E. coli Isolated from Egyptian Patients with Different Clinical Infections. *Infect Drug Resist,* 13**,** 1221-1236.

ABOYEWA, J. A., SIBUYI, N. R. S., MEYER, M. & OGUNTIBEJU, O. O. 2021. Gold Nanoparticles Synthesized Using Extracts of Cyclopia intermedia, Commonly Known as Honeybush, Amplify the Cytotoxic Effects of Doxorubicin. *Nanomaterials,* 11**,** 132.

ADZITEY, F. 2015. Antibiotic Classes and Antibiotic Susceptibility of Bacterial Isolates from Selected Poultry; A Mini Review. *World s Veterinary Journal,* 6**,** 36-36.

AHMED, S., AHMAD, M., SWAMI, B. L. & IKRAM, S. 2016. A review on plants extract mediated synthesis of silver nanoparticles for antimicrobial applications: A green expertise. *Journal of Advanced Research,* 7**,** 17-28.

AKHAVAN, O., AZIMIRAD, R., SAFA, S. & HASANI, E. 2011. CuO/Cu(OH)2 hierarchical nanostructures as bactericidal photocatalysts. *Journal of Materials Chemistry,* 21**,** 9634-9640.

AKHTAR, M. J., AHAMED, M., ALHADLAQ, H. A. & ALSHAMSAN, A. 2017. Mechanism of ROS scavenging and antioxidant signalling by redox metallic and fullerene nanomaterials: Potential implications in ROS associated degenerative disorders. *Biochimica et Biophysica Acta (BBA) - General Subjects,* 1861**,** 802-813.

AL-KADMY, I. M. S., IBRAHIM, S. A., AL-SARYI, N., AZIZ, S. N., BESINIS, A. & HETTA, H. F. 2020. Prevalence of Genes Involved in Colistin Resistance in Acinetobacter baumannii: First Report from Iraq. *Microbial Drug Resistance,* 26**,** 616-622.

ALGAMMAL, A. M., HETTA, H. F., ELKELISH, A., ALKHALIFAH, D. H. H., HOZZEIN, W. N., BATIHA, G. E.-S., EL NAHHAS, N. & MABROK, M. A. 2020. <p>Methicillin-Resistant Staphylococcus aureus (MRSA): One Health Perspective Approach to the Bacterium Epidemiology, Virulence Factors, Antibiotic-Resistance, and Zoonotic Impact</p>. *Infection and Drug Resistance,* Volume 13**,** 3255-3265.

ALIREZALU, A., AHMADI, N., SALEHI, P., SONBOLI, A., ALIREZALU, K., MOUSAVI KHANEGHAH, A., BARBA, F. J., MUNEKATA, P. E. S. & LORENZO, J. M. 2020. Physicochemical Characterization, Antioxidant Activity, and Phenolic Compounds of Hawthorn (Crataegus spp.) Fruits Species for Potential Use in Food Applications. *Foods,* 9**,** 436.

AMENDOLA, V., BAKR, O. & STELLACCI, F. 2010. A Study of the Surface Plasmon Resonance of Silver Nanoparticles by the Discrete Dipole Approximation Method: Effect of Shape, Size, Structure, and Assembly. *Plasmonics,* 5**,** 85-97.

ANANDALAKSHMI, K., VENUGOBAL, J. & RAMASAMY, V. 2015. Characterization of silver nanoparticles by green synthesis method using Pedalium murex leaf extract and their antibacterial activity. *Applied Nanoscience,* 6.

ANSAR, S., TABASSUM, H., ALADWAN, N. S. M., NAIMAN ALI, M., ALMAARIK, B., ALMAHROUQI, S., ABUDAWOOD, M., BANU, N. & ALSUBKI, R. 2020. Eco friendly silver nanoparticles synthesis by Brassica oleracea and its antibacterial, anticancer and antioxidant properties. *Scientific Reports,* 10.

AQEL, A., EL-NOUR, K. M. M. A., AMMAR, R. A. A. & AL-WARTHAN, A. 2012. Carbon nanotubes, science and technology part (I) structure, synthesis and characterisation. *Arabian Journal of Chemistry,* 5**,** 1-23.

AUNG, T., BIBAT, M. A. D., ZHAO, C.-C. & EUN, J.-B. 2020. Bioactive compounds and antioxidant activities of Quercus salicina Blume extract. *Food Science and Biotechnology,* 29**,** 449-458.

BABY, B., ANTONY, P. & VIJAYAN, R. 2018. Antioxidant and anticancer properties of berries. *Critical Reviews in Food Science and Nutrition,* 58**,** 2491-2507.

BAKOUR, M., LAAROUSSI, H., OUSAAID, D., OUMOKHTAR, B. & LYOUSSI, B. 2021. Antioxidant and Antibacterial Effects of Pollen Extracts on Human Multidrug-Resistant Pathogenic Bacteria. *Journal of Food Quality,* 2021**,** 5560182.

BALESTRI, A., CARDELLINI, J. & BERTI, D. 2023. Gold and silver nanoparticles as tools to combat multidrug-resistant pathogens. *Current Opinion in Colloid & Interface Science,* 66**,** 101710.

BALOUIRI, M., SADIKI, M. & IBNSOUDA, S. K. 2016. Methods for in vitro evaluating antimicrobial activity: A review. *J Pharm Anal,* 6**,** 71-79.

BARIŞ, Ö., GULLUCE, SAHIN, F., OZER, H., KILIC, H., OZKAN, SOKMEN, A. & OZBEK, M. 2006. Biological Activities of the Essential Oil and Methanol Extract of Achillea biebersteinii Afan. (Asteraceae). *Turkish Journal of Biology,* 30.

BECEIRO, A., TOMÁS, M. & BOU, G. 2013. Antimicrobial resistance and virulence: A successful or deleterious association in the bacterial world? *Clinical Microbiology Reviews.*

BEDLOVIČOVÁ, Z., STRAPÁČ, I., BALÁŽ, M. & SALAYOVÁ, A. 2020. A Brief Overview on Antioxidant Activity Determination of Silver Nanoparticles. *Molecules,* 25**,** 3191.

BELLANGER, X., SCHNEIDER, R., DEZANET, C., ARROUA, B., BALAN, L., BILLARD, P. & MERLIN, C. 2020. Zn2+ leakage and photo-induced reactive oxidative species do not explain the full toxicity of ZnO core Quantum Dots. *Journal of Hazardous Materials,* 396**,** 122616.

BENABDERRAHMANE, W., LORES, M., BENAISSA, O., LAMAS, J. P., DE MIGUEL, T., AMRANI, A., BENAYACHE, F. & BENAYACHE, S. 2021. Polyphenolic content and bioactivities of Crataegus oxyacantha L. (Rosaceae). *Natural Product Research,* 35**,** 627-632.

BENZIE, I. F. & STRAIN, J. J. 1996. The ferric reducing ability of plasma (FRAP) as a measure of "antioxidant power": the FRAP assay. *Anal Biochem,* 239**,** 70-6.

BHASKAR, A., KUMARI, A., SINGH, M., KUMAR, S., KUMAR, S., DABLA, A., CHATURVEDI, S., YADAV, V., CHATTOPADHYAY, D. & PRAKASH DWIVEDI, V. 2020. [6]-Gingerol exhibits potent anti-mycobacterial and immunomodulatory activity against tuberculosis. *International Immunopharmacology,* 87**,** 106809.

BHATTACHARJEE, S. 2016. DLS and zeta potential – What they are and what they are not? *Journal of Controlled Release,* 235**,** 337-351.

BLAIR, J. M., WEBBER, M. A., BAYLAY, A. J., OGBOLU, D. O. & PIDDOCK, L. J. 2015. Molecular mechanisms of antibiotic resistance. *Nat Rev Microbiol,* 13**,** 42-51.

BLECHER, K., NASIR, A. & FRIEDMAN, A. 2011. The growing role of nanotechnology in combating infectious disease. *Virulence,* 2**,** 395-401.

BOONSTRA, J. & POST, J. A. 2004. Molecular events associated with reactive oxygen species and cell cycle progression in mammalian cells. *Gene,* 337**,** 1-13.

BORAH, D., DAS, N., DAS, N., BHATTACHARJEE, A., SARMAH, P., GHOSH, K., CHANDEL, M., ROUT, J., PANDEY, P. & GHOSH, N. N. 2020. Alga-mediated facile green synthesis of silver nanoparticles: Photophysical, catalytic and antibacterial activity. *Applied Organometallic Chemistry,* 34**,** e5597.

BREIJYEH, Z., JUBEH, B. & KARAMAN, R. 2020. Resistance of Gram-Negative Bacteria to Current Antibacterial Agents and Approaches to Resolve It. *Molecules,* 25**,** 1340.

CAROLINE, M. L., MUTHUKUMAR, R. S., A, H. H. & N, N. 2023. Anticancer Effect of Plectranthus Amboinicus and Glycyrrhiza Glabra on Oral Cancer Cell Line: An Invitro Experimental Study. *Asian Pac J Cancer Prev,* 24**,** 881-887.

CHALOUPKA, K., MALAM, Y. & SEIFALIAN, A. M. 2010. Nanosilver as a new generation of nanoproduct in biomedical applications. *Trends Biotechnol,* 28**,** 580-8.

CHANDRA, H., BISHNOI, P., YADAV, A., PATNI, B., MISHRA, A. & NAUTIYAL, A. 2017. Antimicrobial Resistance and the Alternative Resources with Special Emphasis on Plant-Based Antimicrobials—A Review. *Plants,* 6**,** 16.

CHOW, J. W. & SHLAES, D. M. 1991. Imipenem resistance associated with the loss of a 40 kDa outer membrane protein in Enterobacter aerogenes. *Journal of Antimicrobial Chemotherapy,* 28**,** 499-504.

CHRISTAKI, E., MARCOU, M. & TOFARIDES, A. 2020. Antimicrobial Resistance in Bacteria: Mechanisms, Evolution, and Persistence. *J Mol Evol,* 88**,** 26-40.

CILLARD, J., CILLARD, P. & CORMIER, M. 1980. Effect of experimental factors on the prooxidant behavior of α-tocopherol. *Journal of the American Oil Chemists' Society,* 57**,** 255-261.

CLOGSTON, J. D. & PATRI, A. K. 2011. Zeta potential measurement. *Methods Mol Biol,* 697**,** 63-70.

COOKE, M. S., EVANS, M. D., DIZDAROGLU, M. & LUNEC, J. 2003. Oxidative DNA damage: mechanisms, mutation, and disease. *The FASEB Journal,* 17**,** 1195-1214.

CORNAGLIA, G., GUAN, L., FONTANA, R. & SATTA, G. 1992. Diffusion of meropenem and imipenem through the outer membrane of Escherichia coli K-12 and correlation with their antibacterial activities. *Antimicrobial agents and chemotherapy,* 36**,** 1902-1908.

CORNAGLIA, G., MAZZARIOL, A., FONTANA, R. & SATTA, G. 1996. Diffusion of carbapenems through the outer membrane of enterobacteriaceae and correlation of their activities with their periplasmic concentrations. *Microb Drug Resist,* 2**,** 273-6.

COX, G. & WRIGHT, G. D. 2013. Intrinsic antibiotic resistance: Mechanisms, origins, challenges and solutions. *International Journal of Medical Microbiology,* 303**,** 287-292.

CROES, S., STOBBERINGH, E. E., STEVENS, K. N., KNETSCH, M. L. & KOOLE, L. H. 2011. Antimicrobial and anti-thrombogenic features combined in hydrophilic surface coatings for skin-penetrating catheters. Synergy of co-embedded silver particles and heparin. *ACS Applied Materials & Interfaces,* 3**,** 2543-2550.

CUEVAS-DURÁN, R. E., MEDRANO-RODRÍGUEZ, J. C., SÁNCHEZ-AGUILAR, M., SORIA-CASTRO, E., RUBIO-RUÍZ, M. E., DEL VALLE-MONDRAGÓN, L., SÁNCHEZ-MENDOZA, A., TORRES-NARVAÉZ, J. C., PASTELÍN-HERNÁNDEZ, G. & IBARRA-LARA, L. 2017. Extracts of Crataegus oxyacantha and Rosmarinus officinalis Attenuate Ischemic Myocardial Damage by Decreasing Oxidative Stress and Regulating the Production of Cardiac Vasoactive Agents. *Int J Mol Sci,* 18.

DANKOVICH, T. A. & GRAY, D. G. 2011. Bactericidal paper impregnated with silver nanoparticles for point-of-use water treatment. *Environmental science & technology,* 45**,** 1992-1998.

DAS, P., GHOSAL, K., JANA, N. K., MUKHERJEE, A. & BASAK, P. 2019. Green synthesis and characterization of silver nanoparticles using belladonna mother tincture and its efficacy as a potential antibacterial and anti-inflammatory agent. *Materials Chemistry and Physics,* 228**,** 310-317.

DE ABREU COSTA, L., HENRIQUE FERNANDES OTTONI, M., DOS SANTOS, M., MEIRELES, A., GOMES DE ALMEIDA, V., DE FÁTIMA PEREIRA, W., ALVES DE AVELAR-FREITAS, B. & EUSTÁQUIO ALVIM BRITO-MELO, G. 2017. Dimethyl Sulfoxide (DMSO) Decreases Cell Proliferation and TNF-α, IFN-γ, and IL-2 Cytokines Production in Cultures of Peripheral Blood Lymphocytes. *Molecules,* 22**,** 1789.

DEEPAK, V., UMAMAHESHWARAN, P. S., GUHAN, K., NANTHINI, R. A., KRITHIGA, B., JAITHOON, N. M. H. & GURUNATHAN, S. 2011. Synthesis of gold and silver nanoparticles using purified URAK. *Colloids and Surfaces B: Biointerfaces,* 86**,** 353-358.

DESHMUKH, S. P., PATIL, S. M., MULLANI, S. B. & DELEKAR, S. D. 2019. Silver nanoparticles as an effective disinfectant: A review. *Materials Science and Engineering: C,* 97**,** 954-965.

DOAN, V.-D., THIEU, A. T., NGUYEN, T.-D., NGUYEN, V.-C., CAO, X.-T., NGUYEN, T. L.-H. & LE, V. T. 2020. Biosynthesis of Gold Nanoparticles Using Litsea cubeba Fruit Extract for Catalytic Reduction of 4-Nitrophenol. *Journal of Nanomaterials,* 2020**,** 4548790.

DUBE, P., MEYER, S., MADIEHE, A. & MEYER, M. 2020. Antibacterial activity of biogenic silver and gold nanoparticles synthesized from Salvia africana-lutea and Sutherlandia frutescens. *Nanotechnology,* 31**,** 505607.

DURAZZO, A., LUCARINI, M., NOVELLINO, E., SOUTO, E. B., DALIU, P. & SANTINI, A. 2018. Abelmoschus esculentus (L.): Bioactive Components' Beneficial Properties-Focused on Antidiabetic Role-For Sustainable Health Applications. *Molecules,* 24.

DUTTA, A. 2017. Chapter 4 - Fourier Transform Infrared Spectroscopy. *In:* THOMAS, S., THOMAS, R., ZACHARIAH, A. K. & MISHRA, R. K. (eds.) *Spectroscopic Methods for Nanomaterials Characterization.* Elsevier.

DUVAL, R. E., GOUYAU, J. & LAMOUROUX, E. 2019a. Limitations of Recent Studies Dealing with the Antibacterial Properties of Silver Nanoparticles: Fact and Opinion. *Nanomaterials,* 9**,** 1775.

DUVAL, R. E., GRARE, M. & DEMORÉ, B. 2019b. Fight Against Antimicrobial Resistance: We Always Need New Antibacterials but for Right Bacteria. *Molecules,* 24**,** 3152.

EL-KAZZAZ, W., METWALLY, L., YAHIA, R., AL-HARBI, N., EL-TAHER, A. & HETTA, H. F. 2020. Antibiogram, Prevalence of OXA Carbapenemase Encoding Genes, and RAPD-Genotyping of Multidrug-Resistant Acinetobacter baumannii Incriminated in Hidden Community-Acquired Infections. *Antibiotics,* 9**,** 603.

ELBAGORY, A. M., CUPIDO, C. N., MEYER, M. & HUSSEIN, A. A. 2016. Large Scale Screening of Southern African Plant Extracts for the Green Synthesis of Gold Nanoparticles Using Microtitre-Plate Method. *Molecules,* 21.

ELBAHNASAWY, M. A., SHEHABELDINE, A. M., KHATTAB, A. M., AMIN, B. H. & HASHEM, A. H. 2021. Green biosynthesis of silver nanoparticles using novel endophytic Rothia endophytica: Characterization and anticandidal activity. *Journal of Drug Delivery Science and Technology,* 62**,** 102401.

ELEMIKE, E. E., FAYEMI, O. E., EKENNIA, A. C., ONWUDIWE, D. C. & EBENSO, E. E. 2017. Silver Nanoparticles Mediated by Costus afer Leaf Extract: Synthesis, Antibacterial, Antioxidant and Electrochemical Properties. *Molecules,* 22**,** 701.

ELOFF, J. N. 2019. Avoiding pitfalls in determining antimicrobial activity of plant extracts and publishing the results. *BMC Complementary and Alternative Medicine,* 19**,** 106.

ELSUPIKHE, R. F., SHAMELI, K., AHMAD, M. B., IBRAHIM, N. A. & ZAINUDIN, N. 2015. Green sonochemical synthesis of silver nanoparticles at varying concentrations of κ-carrageenan. *Nanoscale research letters,* 10**,** 1-8.

FADAKA, A. O., MEYER, S., AHMED, O., GEERTS, G., MADIEHE, M. A., MEYER, M. & SIBUYI, N. R. S. 2022. Broad Spectrum Anti-Bacterial Activity and Non-Selective Toxicity of Gum Arabic Silver Nanoparticles. *Int J Mol Sci,* 23.

FARHAN, S. M., IBRAHIM, R. A., MAHRAN, K. M., HETTA, H. F. & ABD EL-BAKY, R. M. 2019. <p>Antimicrobial resistance pattern and molecular genetic distribution of metallo-β-lactamases producing Pseudomonas aeruginosa isolated from hospitals in Minia, Egypt</p>. *Infection and Drug Resistance,* Volume 12**,** 2125-2133.

FERNÁNDEZ, L. & HANCOCK, R. E. 2012. Adaptive and mutational resistance: role of porins and efflux pumps in drug resistance. *Clin Microbiol Rev,* 25**,** 661-81.

FERREIRA, C., PEREIRA, A., MELO, L. & SIMÕES, M. 2010. Advances in industrial biofilm control with micro-nanotechnology. *Current research, technology and education topics in applied microbiology and microbial biotechnology,* 2**,** 845-854.

FÖRSTERMANN, U. 2010. Nitric oxide and oxidative stress in vascular disease. *Pflugers Archiv European Journal of Physiology.*

FOUNOU, R. C., FOUNOU, L. L. & ESSACK, S. Y. 2017. Clinical and economic impact of antibiotic resistance in developing countries: A systematic review and meta-analysis. *PLOS ONE,* 12**,** e0189621.

FREITAS, A. R. & WERNER, G. 2023. Nosocomial Pathogens and Antimicrobial Resistance: Modern Challenges and Future Opportunities. *Microorganisms,* 11**,** 1685.
GAHLAWAT, G. & CHOUDHURY, A. R. 2019. A review on the biosynthesis of metal and metal salt nanoparticles by microbes. *RSC advances,* 9**,** 12944-12967.
GANGWAR, M. S. & AGARWAL, P. 2023. Plasmon-enhanced photoluminescence and Raman spectroscopy of silver nanoparticles grown by solid state dewetting. *Journal of Physics: Condensed Matter,* 35**,** 325301.
GECER, E. N. 2021. Green Synthesis of Silver Nanoparticles from Salvia aethiopis L. and Their Antioxidant Activity. *Journal of Inorganic and Organometallic Polymers and Materials,* 31**,** 4402-4409.
GHAFFARI-MOGHADDAM, M. & HADI-DABANLOU, R. 2014. Plant mediated green synthesis and antibacterial activity of silver nanoparticles using Crataegus douglasii fruit extract. *Journal of Industrial and Engineering Chemistry,* 20**,** 739-744.
GHAFFARI, S. 2008. Oxidative Stress in the Regulation of Normal and Neoplastic Hematopoiesis. *Antioxidants & Redox Signaling,* 10**,** 1923-1940.
GILL, M. J., SIMJEE, S., AL-HATTAWI, K., ROBERTSON, B. D., EASMON, C. S. F. & ISON, C. A. 1998. Gonococcal Resistance to β-Lactams and Tetracycline Involves Mutation in Loop 3 of the Porin Encoded at the

penB

Locus. *Antimicrobial Agents and Chemotherapy,* 42**,** 2799-2803.
GIURAZZA, R., MAZZA, M. C., ANDINI, R., SANSONE, P., PACE, M. C. & DURANTE-MANGONI, E. 2021. Emerging Treatment Options for Multi-Drug-Resistant Bacterial Infections. *Life,* 11**,** 519.
GONELIMALI, F. D., LIN, J., MIAO, W., XUAN, J., CHARLES, F., CHEN, M. & HATAB, S. R. 2018. Antimicrobial Properties and Mechanism of Action of Some Plant Extracts Against Food Pathogens and Spoilage Microorganisms. *Frontiers in Microbiology,* 9.
GRAZIO, W. S. 2021. Indian Hawthorne berries.
GURUNATHAN, S., KALISHWARALAL, K., VAIDYANATHAN, R., VENKATARAMAN, D., PANDIAN, S. R. K., MUNIYANDI, J., HARIHARAN, N. & EOM, S. H. 2009. Biosynthesis, purification and characterization of silver nanoparticles using Escherichia coli. *Colloids and Surfaces B: Biointerfaces,* 74**,** 328-335.
HAJIPOUR, M. J., FROMM, K. M., AKBAR ASHKARRAN, A., JIMENEZ DE ABERASTURI, D., LARRAMENDI, I. R. D., ROJO, T., SERPOOSHAN, V., PARAK, W. J. & MAHMOUDI, M. 2012. Antibacterial properties of nanoparticles. *Trends in Biotechnology,* 30**,** 499-511.
HALLIWELL, B. & GUTTERIDGE, J. M. C. 2015. *Free Radicals in Biology and Medicine*.
HEFLISH, A. A., BEHIRY, S. I., AL-ASKAR, A. A., SU, Y., ABDELKHALEK, A. & GABER, M. K. 2023. Rhaphiolepis indica Fruit Extracts for Control Fusarium solani and Rhizoctonia solani, the Causal Agents of Bean Root Rot. *Separations,* 10**,** 369.
HETTA, H. F., RAMADAN, Y. N., AL-HARBI, A. I., A. AHMED, E., BATTAH, B., ABD ELLAH, N. H., ZANETTI, S. & DONADU, M. G. 2023. Nanotechnology as a Promising Approach to Combat Multidrug Resistant Bacteria: A Comprehensive Review and Future Perspectives. *Biomedicines,* 11**,** 413.
HIEMER, B., ZIEBART, J., JONITZ-HEINCKE, A., GRUNERT, P. C., SU, Y., HANSMANN, D. & BADER, R. 2016. Magnetically induced electrostimulation of human osteoblasts results in enhanced cell viability and osteogenic differentiation. *Int J Mol Med,* 38**,** 57-64.
HUANG, X., JAIN, P. K., EL-SAYED, I. H. & EL-SAYED, M. A. 2007. Gold nanoparticles: interesting optical properties and recent applications in cancer diagnostics and therapy. *Nanomedicine (Lond),* 2**,** 681-93.
HUH, A. J. & KWON, Y. J. 2011. "Nanoantibiotics": A new paradigm for treating infectious diseases using nanomaterials in the antibiotics resistant era. *Journal of Controlled Release,* 156**,** 128-145.

IQBAL, M., ZAFAR, H., MAHMOOD, A., NIAZI, M. B. K. & ASLAM, M. W. 2020. Starch-capped silver nanoparticles impregnated into propylamine-substituted PVA films with improved antibacterial and mechanical properties for wound-bandage applications. *Polymers,* 12**,** 2112.

IRAVANI, S., KORBEKANDI, H., MIRMOHAMMADI, S. V. & ZOLFAGHARI, B. 2014. Synthesis of silver nanoparticles: chemical, physical and biological methods. *Research in pharmaceutical sciences,* 9**,** 385.

JAYARAMAN, R. 2009. Antibiotic resistance: An overview of mechanisms and a paradigm shift. *Current Science,* 96**,** 1475-1484.

JEREMIAH, S. S., MIYAKAWA, K., MORITA, T., YAMAOKA, Y. & RYO, A. 2020. Potent antiviral effect of silver nanoparticles on SARS-CoV-2. *Biochemical and Biophysical Research Communications,* 533**,** 195-200.

JOOST, U., JUGANSON, K., VISNAPUU, M., MORTIMER, M., KAHRU, A., NÕMMISTE, E., KATUS, U., KISAND, V. & IVASK, A. 2014. Photocatalytic antibacterial activity of nano-TiO2 (anatase)-based thin films: Effects on Escherichia coli cells and fatty acids. *Journal of photochemistry and photobiology. B, Biology,* 142C**,** 178-185.

JUBEH, B., BREIJYEH, Z. & KARAMAN, R. 2020. Resistance of Gram-Positive Bacteria to Current Antibacterial Agents and Overcoming Approaches. *Molecules,* 25**,** 2888.

KAREEM, S. M., AL-KADMY, I. M., KAZAAL, S. S., MOHAMMED ALI, A. N., AZIZ, S. N., MAKHARITA, R. R., ALGAMMAL, A. M., AL-REJAIE, S., BEHL, T., BATIHA, G. E.-S., EL-MOKHTAR, M. A. & HETTA, H. F. 2021. Detection of gyrA and parC Mutations and Prevalence of Plasmid-Mediated Quinolone Resistance Genes in Klebsiella pneumoniae. *Infection and Drug Resistance,* Volume 14**,** 555-563.

KATTA, R. & BROWN, D. N. 2015. Diet and Skin Cancer: The Potential Role of Dietary Antioxidants in Nonmelanoma Skin Cancer Prevention. *Journal of Skin Cancer,* 2015**,** 1-10.

KAUSHAL, P., VERMA, N., KAUR, K. & SIDHU, A. 2021. Green Synthesis: An Eco-friendly Route for the Synthesis of Iron Oxide Nanoparticles. *Frontiers in Nanotechnology,* 3**,** 655062.

KEHRIBAR, L., AYDıN, M., COŞKUN, H. S. & SURUCU, S. 2023. Silver Nanoparticles Enhance the Antibacterial Effect of Antibiotic-Loaded Bone Cement. *Cureus,* 15**,** e34992.

KEREN, I., WU, Y., INOCENCIO, J., MULCAHY, L. R. & LEWIS, K. 2013. Killing by Bactericidal Antibiotics Does Not Depend on Reactive Oxygen Species. *Science,* 339**,** 1213-1216.

KESHARWANI, P., JAIN, K. & JAIN, N. K. 2014. Dendrimer as nanocarrier for drug delivery. *Progress in Polymer Science,* 39**,** 268-307.

KHALIL, I., YEHYE, W. A., ETXEBERRIA, A. E., ALHADI, A. A., DEZFOOLI, S. M., JULKAPLI, N. B. M., BASIRUN, W. J. & SEYFODDIN, A. 2019. Nanoantioxidants: Recent Trends in Antioxidant Delivery Applications. *Antioxidants,* 9**,** 24.

KHAN, I., SAEED, K. & KHAN, I. 2017. Nanoparticles: Properties, applications and toxicities. *Arabian Journal of Chemistry,* 12**,** 908-931.

KHAN, M., KHAN, M., ADIL, S. F., TAHIR, M. N., TREMEL, W., ALKHATHLAN, H. Z., AL-WARTHAN, A. & SIDDIQUI, M. R. 2013. Green synthesis of silver nanoparticles mediated by Pulicaria glutinosa extract. *Int J Nanomedicine,* 8**,** 1507-16.

KHORRAMI, S., ZARRABI, A., KHALEGHI, M., DANAEI, M. & MOZAFARI, M. R. 2018. Selective cytotoxicity of green synthesized silver nanoparticles against the MCF-7 tumor cell line and their enhanced antioxidant and antimicrobial properties. *Int J Nanomedicine,* 13**,** 8013-8024.

KLAUNIG, J. E. & KAMENDULIS, L. M. 2004. The Role of Oxidative Stress in Carcinogenesis. *Annual Review of Pharmacology and Toxicology,* 44**,** 239-267.

KRCE, L., ŠPRUNG, M., RONČEVIĆ, T., MARAVIĆ, A., ČIKEŠ ČULIĆ, V., BLAŽEKA, D., KRSTULOVIĆ, N. & AVIANI, I. 2020. Probing the Mode of Antibacterial Action of Silver Nanoparticles Synthesized by Laser Ablation in Water: What Fluorescence and AFM Data Tell Us. *Nanomaterials,* 10**,** 1040.

KRUIS, F. E., FISSAN, H. & RELLINGHAUS, B. 2000. Sintering and evaporation characteristics of gas-phase synthesis of size-selected PbS nanoparticles. *Materials Science and Engineering: B,* 69**,** 329-334.
KULKARNI, N. & MUDDAPUR, U. 2014. Biosynthesis of Metal Nanoparticles: A Review. *Journal of Nanotechnology,* 2014**,** 510246.
KULSHRESTHA, S., QAYYUM, S. & KHAN, A. U. 2017. Antibiofilm efficacy of green synthesized graphene oxide-silver nanocomposite using Lagerstroemia speciosa floral extract: A comparative study on inhibition of gram-positive and gram-negative biofilms. *Microbial pathogenesis,* 103**,** 167-177.
KUMAR, A., VEMULA, P. K., AJAYAN, P. M. & JOHN, G. 2008. Silver-nanoparticle-embedded antimicrobial paints based on vegetable oil. *Nature materials,* 7**,** 236-241.
KUMAR, I., MONDAL, M. & SAKTHIVEL, N. 2019. Chapter 3 - Green synthesis of phytogenic nanoparticles. *In:* SHUKLA, A. K. & IRAVANI, S. (eds.) *Green Synthesis, Characterization and Applications of Nanoparticles.* Elsevier.
LARA, H. H., AYALA-NÚÑEZ, N. V., IXTEPAN TURRENT, L. D. C. & RODRÍGUEZ PADILLA, C. 2010. Bactericidal effect of silver nanoparticles against multidrug-resistant bacteria. *World Journal of Microbiology and Biotechnology,* 26**,** 615-621.
LAVERTY, G., GORMAN, S. & GILMORE, B. 2014. Biomolecular Mechanisms of Pseudomonas aeruginosa and Escherichia coli Biofilm Formation. *Pathogens,* 3**,** 596-632.
LESNIAK, A., SALVATI, A., SANTOS-MARTINEZ, M. J., RADOMSKI, M. W., DAWSON, K. A. & ÅBERG, C. 2013. Nanoparticle Adhesion to the Cell Membrane and Its Effect on Nanoparticle Uptake Efficiency. *Journal of the American Chemical Society,* 135**,** 1438-1444.
LEVY, P. D., LARIBI, S. & MEBAZAA, A. 2014. Vasodilators in Acute Heart Failure: Review of the Latest Studies. *Current Emergency and Hospital Medicine Reports,* 2**,** 126-132.
LI, H., CHEN, Q., ZHAO, J. & URMILA, K. 2015. Enhancing the antimicrobial activity of natural extraction using the synthetic ultrasmall metal nanoparticles. *Scientific reports,* 5**,** 11033.
LI, Y., LI, X., WANG, J.-K., KUANG, Y. & QI, M.-X. 2017. Anti-hepatitis B viral activity of Phyllanthus niruri L (Phyllanthaceae) in HepG2/C3A and SK-HEP-1 cells. *Tropical Journal of Pharmaceutical Research,* 16**,** 1873.
LIAQAT, N., JAHAN, N., KHALIL-UR-RAHMAN, ANWAR, T. & QURESHI, H. 2022. Green synthesized silver nanoparticles: Optimization, characterization, antimicrobial activity, and cytotoxicity study by hemolysis assay. *Frontiers in Chemistry,* 10.
LIN, J., ZHOU, D., STEITZ, T. A., POLIKANOV, Y. S. & GAGNON, M. G. 2018. Ribosome-Targeting Antibiotics: Modes of Action, Mechanisms of Resistance, and Implications for Drug Design. *Annu Rev Biochem,* 87**,** 451-478.
LING, J., LI, Y. F. & HUANG, C. Z. 2008. A label-free visual immunoassay on solid support with silver nanoparticles as plasmon resonance scattering indicator. *Analytical biochemistry,* 383**,** 168-173.
LIU, Y. & IMLAY, J. A. 2013. Cell Death from Antibiotics Without the Involvement of Reactive Oxygen Species. *Science,* 339**,** 1210-1213.
LIU, Z., WU, Y., GUO, Z., LIU, Y., SHEN, Y., ZHOU, P. & LU, X. 2014. Effects of Internalized Gold Nanoparticles with Respect to Cytotoxicity and Invasion Activity in Lung Cancer Cells. *PLoS ONE,* 9**,** e99175.
LUSHCHAK, O., ZAYACHKIVSKA, A. & VAISERMAN, A. 2018. Metallic nanoantioxidants as potential therapeutics for type 2 diabetes: A hypothetical background and translational perspectives. *Oxidative Medicine and Cellular Longevity.*
MADIEHE, A. M., MOABELO, K. L., MODISE, K., SIBUYI, N. R., MEYER, S., DUBE, A., ONANI, M. O. & MEYER, M. 2022. Catalytic reduction of 4-nitrophenol and methylene blue by biogenic gold nanoparticles synthesized using Carpobrotus edulis fruit (sour fig) extract. *Nanomaterials and Nanotechnology,* 12**,** 184798042211082.

MAKHARITA, R. R., EL-KHOLY, I., HETTA, H. F., ABDELAZIZ, M., HAGAGY, F., AHMED, A. & ALGAMMAL, A. M. 2020. <p>Antibiogram and Genetic Characterization of Carbapenem-Resistant Gram-Negative Pathogens Incriminated in Healthcare-Associated Infections</p&gt. *Infection and Drug Resistance,* Volume 13**,** 3991-4002.

MALIK, M. A., O'BRIEN, P. & REVAPRASADU, N. 2002. A simple route to the synthesis of core/shell nanoparticles of chalcogenides. *Chemistry of Materials,* 14**,** 2004-2010.

MALLICK, K., WITCOMB, M. & SCURRELL, M. 2004. Polymer stabilized silver nanoparticles: a photochemical synthesis route. *Journal of materials science,* 39**,** 4459-4463.

MAMMARI, N., LAMOUROUX, E., BOUDIER, A. & DUVAL, R. E. 2022. Current Knowledge on the Oxidative-Stress-Mediated Antimicrobial Properties of Metal-Based Nanoparticles. *Microorganisms,* 10**,** 437.

MARTIN, D. R., SIBUYI, N. R., DUBE, P., FADAKA, A. O., CLOETE, R., ONANI, M., MADIEHE, A. M. & MEYER, M. 2021. Aptamer-Based Diagnostic Systems for the Rapid Screening of TB at the Point-of-Care. *Diagnostics (Basel),* 11.

MARTINELLI, C., PUCCI, C. & CIOFANI, G. 2019. Nanostructured carriers as innovative tools for cancer diagnosis and therapy. *APL Bioengineering,* 3**,** 011502.

MASSIRONI, A., MORELLI, A., GRASSI, L., PUPPI, D., BRACCINI, S., MAISETTA, G., ESIN, S., BATONI, G., DELLA PINA, C. & CHIELLINI, F. 2019. Ulvan as novel reducing and stabilizing agent from renewable algal biomass: Application to green synthesis of silver nanoparticles. *Carbohydr Polym,* 203**,** 310-321.

MAURICIO, M. D., GUERRA-OJEDA, S., MARCHIO, P., VALLES, S. L., ALDASORO, M., ESCRIBANO-LOPEZ, I., HERANCE, J. R., ROCHA, M., VILA, J. M. & VICTOR, V. M. 2018. Nanoparticles in Medicine: A Focus on Vascular Oxidative Stress. *Oxidative Medicine and Cellular Longevity,* 2018**,** 1-20.

MAZZONELLO, A., VALDRAMIDIS, V., FARRUGIA, C., GRIMA, J. & GATT, R. 2017. Synthesis and characterization of silver nanoparticles. *International Journal of Engineering Research,* 7**,** 41.

MCJAJE-COMMONSWIKI. 2006. *Indian Hawthorn in bloom (Raphiolepis)* [Online]. Wikepedia. [Accessed 20 December 2023].

METWALLI, K. H., KHAN, S. A., KROM, B. P. & JABRA-RIZK, M. A. 2013. Streptococcus mutans, Candida albicans, and the human mouth: a sticky situation. *PLoS pathogens,* 9**,** e1003616.

MIRANDA, A., AKPOBOLOKEMI, T., CHUNG, E., REN, G. & RAIMI-ABRAHAM, B. T. 2022. pH Alteration in Plant-Mediated Green Synthesis and Its Resultant Impact on Antimicrobial Properties of Silver Nanoparticles (AgNPs). *Antibiotics,* 11**,** 1592.

MISBA, L., KULSHRESTHA, S. & KHAN, A. U. 2016. Antibiofilm action of a toluidine blue O-silver nanoparticle conjugate on Streptococcus mutans: a mechanism of type I photodynamic therapy. *Biofouling,* 32**,** 313-28.

MOHAMMAD, G., MISHRA, V. & PANDEY, H. 2008. Antioxidant properties of some Nanoparticle may Enhance Wound Healing in T2DM Patients. *Digest Journal of Nanomaterials and Biostructures,* 3.

MOHAMMED FAYAZ, A., BALAJI, K., GIRILAL, M., KALAICHELVAN, P. & VENKATESAN, R. 2009. Mycobased synthesis of silver nanoparticles and their incorporation into sodium alginate films for vegetable and fruit preservation. *Journal of agricultural and food chemistry,* 57**,** 6246-6252.

MOORE, T. L., RODRIGUEZ-LORENZO, L., HIRSCH, V., BALOG, S., URBAN, D., JUD, C., ROTHEN-RUTISHAUSER, B., LATTUADA, M. & PETRI-FINK, A. 2015. Nanoparticle colloidal stability in cell culture media and impact on cellular interactions. *Chemical Society Reviews,* 44**,** 6287-6305.

MOURDIKOUDIS, S., PALLARES, R. M. & THANH, N. T. K. 2018. Characterization techniques for nanoparticles: comparison and complementarity upon studying nanoparticle properties. *Nanoscale,* 10**,** 12871-12934.

MULANI, M. S., KAMBLE, E. E., KUMKAR, S. N., TAWRE, M. S. & PARDESI, K. R. 2019. Emerging Strategies to Combat ESKAPE Pathogens in the Era of Antimicrobial Resistance: A Review. *Frontiers in Microbiology,* 10.

MURRAY, C. J. L., IKUTA, K. S., SHARARA, F., SWETSCHINSKI, L., ROBLES AGUILAR, G., GRAY, A., HAN, C., BISIGNANO, C., RAO, P., WOOL, E., JOHNSON, S. C., BROWNE, A. J., CHIPETA, M. G., FELL, F., HACKETT, S., HAINES-WOODHOUSE, G., KASHEF HAMADANI, B. H., KUMARAN, E. A. P., MCMANIGAL, B., ACHALAPONG, S., AGARWAL, R., AKECH, S., ALBERTSON, S., AMUASI, J., ANDREWS, J., ARAVKIN, A., ASHLEY, E., BABIN, F.-X., BAILEY, F., BAKER, S., BASNYAT, B., BEKKER, A., BENDER, R., BERKLEY, J. A., BETHOU, A., BIELICKI, J., BOONKASIDECHA, S., BUKOSIA, J., CARVALHEIRO, C., CASTAÑEDA-ORJUELA, C., CHANSAMOUTH, V., CHAURASIA, S., CHIURCHIÙ, S., CHOWDHURY, F., CLOTAIRE DONATIEN, R., COOK, A. J., COOPER, B., CRESSEY, T. R., CRIOLLO-MORA, E., CUNNINGHAM, M., DARBOE, S., DAY, N. P. J., DE LUCA, M., DOKOVA, K., DRAMOWSKI, A., DUNACHIE, S. J., DUONG BICH, T., ECKMANNS, T., EIBACH, D., EMAMI, A., FEASEY, N., FISHER-PEARSON, N., FORREST, K., GARCIA, C., GARRETT, D., GASTMEIER, P., GIREF, A. Z., GREER, R. C., GUPTA, V., HALLER, S., HASELBECK, A., HAY, S. I., HOLM, M., HOPKINS, S., HSIA, Y., IREGBU, K. C., JACOBS, J., JAROVSKY, D., JAVANMARDI, F., JENNEY, A. W. J., KHORANA, M., KHUSUWAN, S., KISSOON, N., KOBEISSI, E., KOSTYANEV, T., KRAPP, F., KRUMKAMP, R., KUMAR, A., KYU, H. H., LIM, C., LIM, K., LIMMATHUROTSAKUL, D., LOFTUS, M. J., LUNN, M., MA, J., MANOHARAN, A., MARKS, F., MAY, J., MAYXAY, M., MTURI, N., et al. 2022. Global burden of bacterial antimicrobial resistance in 2019: a systematic analysis. *The Lancet,* 399**,** 629-655.

MUTHUKRISHNAN, L., CHELLAPPA, M. & NANDA, A. 2019. Bio-engineering and cellular imaging of silver nanoparticles as weaponry against multidrug resistant human pathogens. *Journal of Photochemistry and Photobiology B: Biology,* 194**,** 119-127.

MYERS, V. R. 2023. How to Grow and Care for Indian Hawthorn. This small, slow-growing shrub is great for warmer climates. *The spruce make your own best home* [Online]. [Accessed 17 December 2023 2023].

NAGAICH, U., GULATI, N. & CHAUHAN, S. 2016. Antioxidant and Antibacterial Potential of Silver Nanoparticles: Biogenic Synthesis Utilizing Apple Extract. *Journal of Pharmaceutics,* 2016**,** 1-8.

NAZEM, A. & MANSOORI, G. A. 2008. Nanotechnology Solutions for Alzheimer's Disease: Advances in Research Tools, Diagnostic Methods and Therapeutic Agents. *Journal of Alzheimer's Disease,* 13**,** 199-223.

NAZHAND, A., LUCARINI, M., DURAZZO, A., ZACCARDELLI, M., CRISTARELLA, S., SOUTO, S. B., SILVA, A. M., SEVERINO, P., SOUTO, E. B. & SANTINI, A. 2020. Hawthorn (Crataegus spp.): An Updated Overview on Its Beneficial Properties. *Forests,* 11**,** 564.

NDIKAU, M., NOAH, N. M., ANDALA, D. M. & MASIKA, E. 2017. Green Synthesis and Characterization of Silver Nanoparticles Using Citrullus lanatus Fruit Rind Extract. *International Journal of Analytical Chemistry,* 2017**,** 8108504.

NEGI, P. S., SINGH, R. & DWIVEDI, S. K. 2018. Evaluation of Antihypertensive Effect of Fruit Beverage of Crataegus crenulata Roxb. : A wild Shrub of Himalayan Hills. *life science journal,* 3**,** 146-150.

NGOC, P. C., LECLERCQ, L., ROSSI, J.-C., DESVIGNES, I., HERTZOG, J., FABIANO-TIXIER, A.-S., CHEMAT, F., SCHMITT-KOPPLIN, P. & COTTET, H. 2019. Optimizing Water-Based Extraction of Bioactive Principles of Hawthorn: From Experimental Laboratory Research to Homemade Preparations. *Molecules,* 24**,** 4420.

NGUNGENI, Y., J, A. A., MOABELO, K. L., SIBUYI, N. R. S., MEYER, S., ONANI, M. O., MEYER, M. & MADIEHE, A. M. 2023. Anticancer, Antioxidant, and Catalytic Activities of Green Synthesized Gold Nanoparticles Using Avocado Seed Aqueous Extract. *ACS Omega,* 8**,** 26088-26101.

NGUYEN, N. D., NGUYEN, T. V., CHU, A. D., TRAN, H. V., TRAN, L. T. & HUYNH, C. D. 2018. A label-free colorimetric sensor based on silver nanoparticles directed to hydrogen peroxide and glucose. *Arabian Journal of Chemistry,* 11**,** 1134-1143.

NGUYEN, T. M.-T., HUYNH, T. T.-T., DANG, C.-H., MAI, D.-T., NGUYEN, T. T.-N., NGUYEN, D.-T., DANG, V.-S., NGUYEN, T.-D. & NGUYEN, T.-D. 2020. Novel biogenic silver nanoparticles used for antibacterial effect and catalytic degradation of contaminants. *Research on Chemical Intermediates,* 46**,** 1975-1990.

OMER, H. F., ABID, Y. K. & MOHAMMED, F. M. 2021. THE EFFECT OF FLAVONOIDS EXTRACTS FROM HAWTHORN (CRATAGUS OXYACANTHUS) AGAINST SOME GRAM-POSITIVE AND GRAM-NEGATIVE BACTERIA SPECIES. *MMSL,* 90**,** 158-164.

PAL, G., RAI, P. & PANDEY, A. 2019. Chapter 1 - Green synthesis of nanoparticles: A greener approach for a cleaner future. *In:* SHUKLA, A. K. & IRAVANI, S. (eds.) *Green Synthesis, Characterization and Applications of Nanoparticles.* Elsevier.

PALLAVICINI, P., ARCIOLA, C. R., BERTOGLIO, F., CURTOSI, S., DACARRO, G., D'AGOSTINO, A., FERRARI, F., MERLI, D., MILANESE, C., ROSSI, S., TAGLIETTI, A., TENCI, M. & VISAI, L. 2017. Silver nanoparticles synthesized and coated with pectin: An ideal compromise for anti-bacterial and anti-biofilm action combined with wound-healing properties. *Journal of Colloid and Interface Science,* 498**,** 271-281.

PANT, H. R., PANT, B., SHARMA, R. K., AMARJARGAL, A., KIM, H. J., PARK, C. H., TIJING, L. D. & KIM, C. S. 2013. Antibacterial and photocatalytic properties of Ag/TiO2/ZnO nano-flowers prepared by facile one-pot hydrothermal process. *Ceramics International,* 39**,** 1503-1510.

PELGRIFT, R. Y. & FRIEDMAN, A. J. 2013. Nanotechnology as a therapeutic tool to combat microbial resistance. *Advanced Drug Delivery Reviews,* 65**,** 1803-1815.

PHANIENDRA, A., JESTADI, D. B. & PERIYASAMY, L. 2015. Free Radicals: Properties, Sources, Targets, and Their Implication in Various Diseases. *Indian Journal of Clinical Biochemistry,* 30**,** 11-26.

PIAO, M. J., KANG, K. A., LEE, I. K., KIM, H. S., KIM, S., CHOI, J. Y., CHOI, J. & HYUN, J. W. 2011. Silver nanoparticles induce oxidative cell damage in human liver cells through inhibition of reduced glutathione and induction of mitochondria-involved apoptosis. *Toxicology Letters,* 201**,** 92-100.

PODSCHUN, R. & ULLMANN, U. 1998. Klebsiella spp. as nosocomial pathogens: epidemiology, taxonomy, typing methods, and pathogenicity factors. *Clinical microbiology reviews,* 11**,** 589-603.

POOLE, K. 2002. Mechanisms of bacterial biocide and antibiotic resistance. *Journal of Applied Microbiology,* 92**,** 55S-64S.

PRINCY, K. F. & GOPINATH, A. 2018. Optimization of physicochemical parameters in the biofabrication of gold nanoparticles using marine macroalgae Padina tetrastromatica and its catalytic efficacy in the degradation of organic dyes. *Journal of Nanostructure in Chemistry,* 8**,** 333-342.

QAYYUM, S. & KHAN, A. U. 2016. Biofabrication of broad range antibacterial and antibiofilm silver nanoparticles. *IET Nanobiotechnol,* 10**,** 349-357.

QU, Z., LIU, P., YANG, X., WANG, F., ZHANG, W. & FEI, C. 2016. Microstructure and Characteristic of BiVO4 Prepared under Different pH Values: Photocatalytic Efficiency and Antibacterial Activity. *Materials,* 9**,** 129.

QUINTEROS, M. A., CANO ARISTIZÁBAL, V., DALMASSO, P. R., PARAJE, M. G. & PÁEZ, P. L. 2016. Oxidative stress generation of silver nanoparticles in three bacterial genera and its relationship with the antimicrobial activity. *Toxicology in Vitro,* 36**,** 216-223.

RAI, M. K., DESHMUKH, S. D., INGLE, A. P. & GADE, A. K. 2012. Silver nanoparticles: the powerful nanoweapon against multidrug-resistant bacteria. *J Appl Microbiol,* 112**,** 841-52.

RAJPUT, S., KUMAR, D. & AGRAWAL, V. 2020. Green synthesis of silver nanoparticles using Indian Belladonna extract and their potential antioxidant, anti-inflammatory, anticancer and larvicidal activities. *Plant Cell Reports,* 39**,** 921-939.

RAMIREZ, M. S. & TOLMASKY, M. E. 2010. Aminoglycoside modifying enzymes. *Drug Resistance Updates,* 13**,** 151-171.

RAVICHANDRAN, A., SUBRAMANIAN, P., MANOHARAN, V., MUTHU, T., PERIYANNAN, R., THANGAPANDI, M., PONNUCHAMY, K., PANDI, B. & MARIMUTHU, P. N. 2018. Phyto-mediated synthesis of silver nanoparticles using fucoidan isolated from Spatoglossum asperum and assessment of antibacterial activities. *Journal of Photochemistry and Photobiology B: Biology,* 185**,** 117-125.

RE, R., PELLEGRINI, N., PROTEGGENTE, A., PANNALA, A., YANG, M. & RICE-EVANS, C. 1999. Antioxidant activity applying an improved ABTS radical cation decolorization assay. *Free Radical Biology and Medicine,* 26**,** 1231-1237.

REYGAERT, W. 2009. Methicillin-resistant Staphylococcus aureus (MRSA): molecular aspects of antimicrobial resistance and virulence. *Clin Lab Sci,* 22**,** 115-9.

ROBICSEK, A., STRAHILEVITZ, J., JACOBY, G. A., MACIELAG, M., ABBANAT, D., PARK, C. H., BUSH, K. & HOOPER, D. C. 2006. Fluoroquinolone-modifying enzyme: a new adaptation of a common aminoglycoside acetyltransferase. *Nat Med,* 12**,** 83-8.

SAEB, A. T. M., ALSHAMMARI, A. S., AL-BRAHIM, H. & AL-RUBEAAN, K. A. 2014. Production of Silver Nanoparticles with Strong and Stable Antimicrobial Activity against Highly Pathogenic and Multidrug Resistant Bacteria. *The Scientific World Journal,* 2014**,** 704708.

SAHANA, R., KIRUBA DANIEL, S. C. G., SANKAR, S. G., ARCHUNAN, G., VENNISON, S. J. & SIVAKUMAR, M. 2014. Formulation of bactericidal cold cream against clinical pathogens using Cassia auriculata flower extract-synthesized Ag nanoparticles. *Green Chemistry Letters and Reviews,* 7**,** 64-72.

SALARI, S., ESMAEILZADEH BAHABADI, S., SAMZADEH-KERMANI, A. & YOSEFZAEI, F. 2019. In-vitro Evaluation of Antioxidant and Antibacterial Potential of GreenSynthesized Silver Nanoparticles Using Prosopis farcta Fruit Extract. *Iran J Pharm Res,* 18**,** 430-455.

SAMROT, A. V., RAM SINGH, S. P., DEENADHAYALAN, R., RAJESH, V. V., PADMANABAN, S. & RADHAKRISHNAN, K. 2022. Nanoparticles, a Double-Edged Sword with Oxidant as Well as Antioxidant Properties—A Review. *Oxygen,* 2**,** 591-604.

SAMUEL, M. S., RAVIKUMAR, M., JOHN J., A., SELVARAJAN, E., PATEL, H., CHANDER, P. S., SOUNDARYA, J., VUPPALA, S., BALAJI, R. & CHANDRASEKAR, N. 2022. A Review on Green Synthesis of Nanoparticles and Their Diverse Biomedical and Environmental Applications. *Catalysts,* 12**,** 459.

SAMUGGAM, S., CHINNI, S. V., MUTUSAMY, P., GOPINATH, S. C. B., ANBU, P., VENUGOPAL, V., REDDY, L. V. & ENUGUTTI, B. 2021. Green Synthesis and Characterization of Silver Nanoparticles Using Spondias mombin Extract and Their Antimicrobial Activity against Biofilm-Producing Bacteria. *Molecules,* 26.

SANTAJIT, S. & INDRAWATTANA, N. 2016. Mechanisms of Antimicrobial Resistance in ESKAPE Pathogens. *BioMed Research International,* 2016**,** 1-8.

SARANGARAJAN, R., MEERA, S., RUKKUMANI, R., SANKAR, P. & ANURADHA, G. 2017. Antioxidants: Friend or foe? *Asian Pacific Journal of Tropical Medicine,* 10**,** 1111-1116.

SARWAR, A., KATAS, H., SAMSUDIN, S. N. & ZIN, N. M. 2015. Regioselective Sequential Modification of Chitosan via Azide-Alkyne Click Reaction: Synthesis, Characterization, and Antimicrobial Activity of Chitosan Derivatives and Nanoparticles. *PLoS One,* 10**,** e0123084.

SCALLAN, E., HOEKSTRA, R. M., ANGULO, F. J., TAUXE, R. V., WIDDOWSON, M.-A., ROY, S. L., JONES, J. L. & GRIFFIN, P. M. 2011. Foodborne illness acquired in the United States—major pathogens. *Emerging infectious diseases,* 17**,** 7.

SCHWARZ, S., KEHRENBERG, C., DOUBLET, B. & CLOECKAERT, A. 2004. Molecular basis of bacterial resistance to chloramphenicol and florfenicol. *FEMS Microbiol Rev,* 28**,** 519-42.

SENA, A., LAURA & CHANDEL, S., NAVDEEP 2012. Physiological Roles of Mitochondrial Reactive Oxygen Species. *Molecular Cell,* 48**,** 158-167.

SHADEL, S., GERALD & HORVATH, L., TAMAS 2015. Mitochondrial ROS Signaling in Organismal Homeostasis. *Cell,* 163**,** 560-569.

SHAMELI, K., AHMAD, M. B., YUNUS, W. M. Z. W., IBRAHIM, N. A., GHARAYEBI, Y. & SEDAGHAT, S. 2010. Synthesis of silver/montmorillonite nanocomposites using γ-irradiation. *International journal of nanomedicine***,** 1067-1077.

SHARMA, G., RAO, S., BANSAL, A., DANG, S., GUPTA, S. & GABRANI, R. 2014. Pseudomonas aeruginosa biofilm: Potential therapeutic targets. *Biologicals,* 42**,** 1-7.

SHRIVASTAVA, S., BERA, T., SINGH, S. K., SINGH, G., RAMACHANDRARAO, P. & DASH, D. 2009. Characterization of antiplatelet properties of silver nanoparticles. *ACS nano,* 3**,** 1357-1364.

SILVA, L. P., PEREIRA, T. M. & BONATTO, C. C. 2019. Chapter 7 - Frontiers and perspectives in the green synthesis of silver nanoparticles. *In:* SHUKLA, A. K. & IRAVANI, S. (eds.) *Green Synthesis, Characterization and Applications of Nanoparticles.* Elsevier.

SIMON, S., SIBUYI, N. R. S., FADAKA, A. O., MEYER, M., MADIEHE, A. M. & DU PREEZ, M. G. 2021. The antimicrobial activity of biogenic silver nanoparticles synthesized from extracts of Red and Green European pear cultivars. *Artif Cells Nanomed Biotechnol,* 49**,** 614-625.

SIMON, S., SIBUYI, N. R. S., FADAKA, A. O., MEYER, S., JOSEPHS, J., ONANI, M. O., MEYER, M. & MADIEHE, A. M. 2022. Biomedical Applications of Plant Extract-Synthesized Silver Nanoparticles. *Biomedicines,* 10**,** 2792.

SINGH, R., NEGI, P. S., DWIVEDI, S., S.K.JOSHI & BALA, M. 2018. *The Indian Hawthorn*.

SU, J. & GROVES, J. T. 2010. Mechanisms of Peroxynitrite Interactions with Heme Proteins. *Inorganic Chemistry,* 49**,** 6317-6329.

SU, Y., ZHENG, X., CHEN, Y., LI, M. & LIU, K. 2015. Alteration of intracellular protein expressions as a key mechanism of the deterioration of bacterial denitrification caused by copper oxide nanoparticles. *Sci Rep,* 5**,** 15824.

SUN, J., DENG, Z. & YAN, A. 2014. Bacterial multidrug efflux pumps: Mechanisms, physiology and pharmacological exploitations. *Biochemical and Biophysical Research Communications,* 453**,** 254-267.

TACCONELLI, E., CARRARA, E., SAVOLDI, A., HARBARTH, S., MENDELSON, M., MONNET, D. L., PULCINI, C., KAHLMETER, G., KLUYTMANS, J. & CARMELI, Y. 2018. Discovery, research, and development of new antibiotics: the WHO priority list of antibiotic-resistant bacteria and tuberculosis. *The Lancet infectious diseases,* 18**,** 318-327.

TAO, A., SINSERMSUKSAKUL, P. & YANG, P. 2006. Polyhedral silver nanocrystals with distinct scattering signatures. *Angewandte Chemie International Edition,* 45**,** 4597-4601.

TARANNUM, N., DIVYA & GAUTAM, Y. K. 2019. Facile green synthesis and applications of silver nanoparticles: a state-of-the-art review. *RSC Advances,* 9**,** 34926-34948.

TENOVER, F. C. 2006. Mechanisms of antimicrobial resistance in bacteria. *Am J Med,* 119**,** S3-10; discussion S62-70.

THAKUR, A. & REDDY, S. G. 2017. Green Synthesis of Silver Nanoparticles Using Sodium Alginate and Lignosulphonic Acid Blends. *IOP Conference Series: Materials Science and Engineering,* 225**,** 012170.

THIOLAS, A., BORNET, C., DAVIN-RÉGLI, A., PAGÈS, J. M. & BOLLET, C. 2004. Resistance to imipenem, cefepime, and cefpirome associated with mutation in Omp36 osmoporin of Enterobacter aerogenes. *Biochemical and Biophysical Research Communications,* 317**,** 851-856.

TIEN, D., LIAO, C., HUANG, J., TSENG, K., LUNG, J., TSUNG, T., KAO, W., TSAI, T., CHENG, T. & YU, B. 2008. Novel technique for preparing a nano-silver water suspension by the arc-discharge method. *Rev. Adv. mater. sci,* 18**,** 752-758.

TITUS, D., SAMUEL, J. J. & ROOPAN, S. 2019. Nanoparticle characterization techniques.

TORRES RIVERO, K., BASTOS - ARRIETA, J., FIOL, N. & PÉREZ, A. 2021. Metal and metal oxide nanoparticles: An integrated perspective of the green synthesis methods by natural products and waste valorization: applications and challenges.

TYAVAMBIZA, C., ELBAGORY, A. M., MADIEHE, A. M., MEYER, M. & MEYER, S. 2021. The Antimicrobial and Anti-Inflammatory Effects of Silver Nanoparticles Synthesised from Cotyledon orbiculata Aqueous Extract. *Nanomaterials* [Online], 11.

TYAVAMBIZA, C., MEYER, M., WUSU, A. D., MADIEHE, A. M. & MEYER, S. 2022. The Antioxidant and In Vitro Wound Healing Activity of Cotyledon orbiculata Aqueous Extract and the Synthesized Biogenic Silver Nanoparticles. *Int J Mol Sci,* 23.

ULLAH, H. & ALI, S. 2017. Classification of Anti-Bacterial Agents and Their Functions. *Antibacterial Agents.* InTech.

VADING, M., NAUCLÉR, P., KALIN, M. & GISKE, C. G. 2018. Invasive infection caused by Klebsiella pneumoniae is a disease affecting patients with high comorbidity and associated with high long-term mortality. *PLOS ONE,* 13**,** e0195258.

VALDEZ-SALAS, B., BELTRAN-PARTIDA, E., CHENG, N., SALVADOR-CARLOS, J., VALDEZ-SALAS, E. A., CURIEL-ALVAREZ, M. & IBARRA-WILEY, R. 2021. Promotion of Surgical Masks Antimicrobial Activity by Disinfection and Impregnation with Disinfectant Silver Nanoparticles. *International Journal of Nanomedicine,* Volume 16**,** 2689-2702.

VALGIMIGLI, L., BASCHIERI, A. & AMORATI, R. 2018. Antioxidant activity of nanomaterials. *Journal of Materials Chemistry B.*

VENKATESWARAN, P. S., MILLMAN, I. & BLUMBERG, B. S. 1987. Effects of an extract from Phyllanthus niruri on hepatitis B and woodchuck hepatitis viruses: in vitro and in vivo studies. *Proc Natl Acad Sci U S A,* 84**,** 274-8.

WANDA, C. R. 2018. An overview of the antimicrobial resistance mechanisms of bacteria. *AIMS Microbiology,* 4**,** 482-501.

WHO, W. H. O. 2013. WHO Traditional Medicine Strategy 15 May 2013 ed.

WHO, W. H. O. 2015. Global action plan on antimicrobial resistance. Geneva: World Health Organization.

WHO, W. H. O. 2020. WHO calls for global action on sepsis - cause of 1 in 5 deaths worldwide. Geneva.

WHO, W. H. O. 2023. World health statistics 2023: monitoring health for the SDGs, sustainable development Goals. World health statistics 2023: monitoring health for the SDGs, Sustainable Development

Goals. Geneva: World Health Organization; 2023. .

WILEY, B., SUN, Y., MAYERS, B. & XIA, Y. 2005. Shape-controlled synthesis of metal nanostructures: the case of silver. *Chemistry–A European Journal,* 11**,** 454-463.

WILKE, M. S., LOVERING, A. L. & STRYNADKA, N. C. J. 2005. β-Lactam antibiotic resistance: a current structural perspective. *Current Opinion in Microbiology,* 8**,** 525-533.

WILSON, D. N. 2014. Ribosome-targeting antibiotics and mechanisms of bacterial resistance. *Nature Reviews Microbiology,* 12**,** 35-48.

WRIGHT, G. D. 2005. Bacterial resistance to antibiotics: Enzymatic degradation and modification. *Advanced Drug Delivery Reviews,* 57**,** 1451-1470.

YIN, Q., WU, W., QIAO, R., KE, X., HU, Y. & LI, Z. 2016. Glucose-assisted transformation of Ni-doped-ZnO@carbon to a Ni-doped-ZnO@void@SiO2 core–shell nanocomposite photocatalyst. *RSC Advances,* 6**,** 38653-38661.

ZAIDI, S., MISBA, L. & KHAN, A. U. 2017. Nano-therapeutics: A revolution in infection control in post antibiotic era. *Nanomedicine: Nanotechnology, Biology and Medicine,* 13**,** 2281-2301.

ZHANG, L., PORNPATTANANANGKUL, D., HU, C.-M. & HUANG, C.-M. 2010. Development of nanoparticles for antimicrobial drug delivery. *Current medicinal chemistry,* 17**,** 585-594.

ZHANG, S., LIANG, X., GADD, G. M. & ZHAO, Q. 2019. Advanced titanium dioxide-polytetrafluorethylene (TiO2-PTFE) nanocomposite coatings on stainless steel surfaces with antibacterial and anti-corrosion properties. *Applied Surface Science,* 490**,** 231-241.

ZHAO, L. & ASHRAF, M. 2015. Influence of silver-hydroxyapatite nanocomposite coating on biofilm formation of joint prosthesis and its mechanism. *The West Indian Medical Journal,* 64**,** 506.

ZONOOZ, N. & SALOUTI, M. 2011. Extracellular biosynthesis of silver nanoparticles using cell filtrate of Streptomyces sp. ERI-3. *Scientia Iranica,* 18**,** 1631-1635.

Appendix

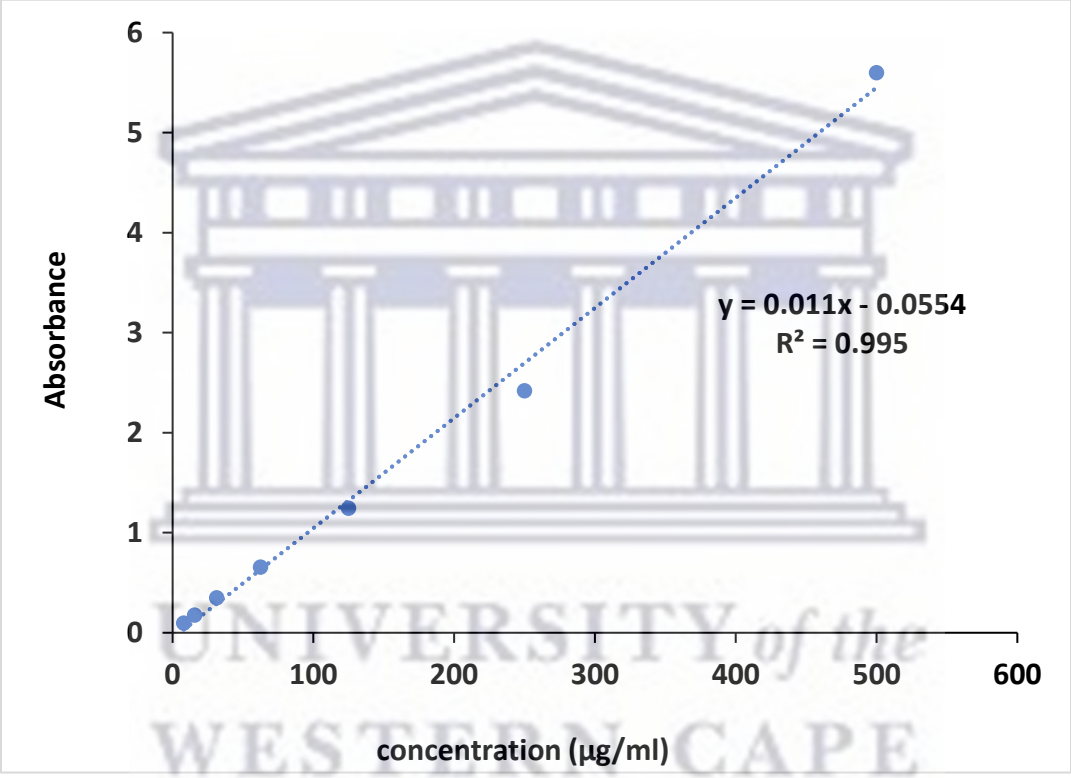

Figure 3. 18 Gallic acid calibration curve used to calculate the TPC in IHFE and the IHFE-AgNPs.